PONTIFICIA UNIVERSIDAD CATÓLICA DE CHILE
Facultad de Ciencias Biológicas
Programa de Doctorado en Ciencias Biológicas
Mención Genética Molecular y Microbiología

Evaluating the role of light and of a circadian clock in the virulence of the necrotrophic fungus *Botrytis cinerea*

Estudio de la luz y la regulación circadiana sobre la virulencia del hongo necrotrófico *Botrytis cinerea*

Tesis presentada a la Pontificia Universidad Católica de Chile como parte de los requisitos para optar al grado de Doctor en Ciencias Biológicas mención Genética Molecular y Microbiología.

Por: MONTSERRAT ALEJANDRA HEVIA HOFFMANN

Director de Tesis: Dr. Luis F. Larrondo

Comisión de Tesis: Dr. Patricio Arce
Dr. Rodrigo Gutierrez
Dr. Marcelo Yanovsky

Agosto 2015

INDEX

ACKNOCKLEDGEMENTS

I would like to express my gratitude to my advisor, Dr. Luis Fernando Larrondo Castro, for his guidance and multiple opportunities that he has offered, which allow me to advance and obtain original and publishable results.

I would like to highlight the important and critical role played by Dr. Paulo Canessa, who was always present and guided to me during all the years of my doctoral thesis. I am very grateful for the strong intellectual support, highly motivating interventions and enrichment resulting from working with him.

I would also like to thanks to the undergraduate student Hanna Müller, who extensively helped in the development of the *B. cinerea* clock story. She is the third member of the Botrytis team, together with Paulo and me.

I also thank Dr. Tudzynski and Dr. Julia Schumacher from the Molekularbiologie und Biotechnologie der Pilze, Institut für Biologie und Biotechnologie der Pflanzen, Münster, Germany, who contributed with their extensive knowledge about *B. cinerea* physiology and pathology, being critical in the development of the BcWCL1 Botrytis story.

I would also like to thank all the members of the Larrondo Lab, especially to Consuelo Olivares, Alejandro Montenegro-Montero, Felipe Muñoz and Alejandra Goity who were always provided great ideas to improve my work.
I would also like to thank to Loreto Salas and Catalina Urrejola from Dr. Rafael Vicuña´s Laboratory.

Special thanks to my husband Marcelo Potthoff, who have always been right by my side supporting and helping me in every important decision.

I would like to thank my parents, Lilian Hoffmann Willer and Edgardo Hevia Arenas, for supporting me in every moment. Special mention to my sister Constanza Hevia, who helped me with the Photoshop software: without her help I would have lost a lot of time in front of the computer.

This work would not have been possible without the financial support of CONICYT, that awarded me a 4-year Doctoral scholarship and a Doctoral thesis support scholarship and the "Vicerrectoría Adjunta de Investigación y Doctorado" at the Faculty of Biological Sciences in Pontificia Universidad Católica de Chile.

This work was funded by ICGEB CRP/ CHI09-02, FONDECYT 1090513, FONDECYT 1131030, Millennium Nucleus for Fungal Integrative and Synthetic Biology NC120043, Comisión Nacional de Investigación Científica y Tecnológica (CONICYT)-ANR-007 and CONICYT scholarship AT-24121100.

This thesis is dedicated to my parents, Lilian and Edgardo.

FIGURE INDEX

TABLE INDEX

GLOSSARY

TF: transcription factor

BcWCL1: *Botrytis cinerea* White Collar 1 Like

BcWCL2: *Botrytis cinerea* White Collar 2 Like

FRQ: frequency

TTFL: transcriptional translational feedback loop

FRC: free running conditions

DD: constant darkness conditions

LL: constant light conditions

LD: light dark cycle

ORF: open reading frame

WT: wild-type

PDA: potato dextrose agar

CM: complete medium

RT: room temperature

bp: base pair

aa: aminoacids

h: hours

hpi: hours post infection

dpi: days post infection

SUMMARY

Disease establishment and progression depends on many variable factors, being environmental signals key elements that regulate development and behavior. Recently, it has been suggested that the susceptibility of the host and the virulent potential of the hostile organism seem to differ with light-dark cycles occurring within a 24-hour day, which suggests that the outcome of the plant-pathogen interaction might be controlled by light and by an endogenous timekeeping mechanism. Circadian clocks allow organisms to anticipate predictable daily changes and a few reports in plants exemplify anticipatory mechanisms, as for example defense responses by the time when the pathogen attack is most likely to happen. Nevertheless, this concept has never been evaluated in pathogens, like fungi. Surprisingly, the only fungus in which a circadian clock has been molecularly characterized is the non-pathogenic ascomycete *Neurospora crassa*, while on the other hand, molecular mechanisms linking light sensing and virulence have never been evaluated in necrotrophic fungi. Therefore, we have studied the role of light and circadian regulation in the necrotrophic fungus *Botrytis cinerea*, which ranks as the second most important phytopathogen according to its economic and scientific importance.

In this thesis, I report how light modulates phenotypical responses and how activates changes in gene expression in *B. cinerea.* By generating a knockout strain for the putative blue light photoreceptor and transcription factor BcWCL1 we have shown that it mediates some, but not all light responses. Also, this mutant is more sensitive to oxidative stress in a light dosis-dependent manner. Using *Arabidopsis thaliana* as a host plant, we show an altered infection process for the Δ*bcwcl1* strain when light is present.

In addition, we have characterized a functional circadian clock in *B. cinerea*, demonstrating that the BcFRQ1 protein and a transcriptional complex formed by BcWCL1 and BcWCL2 are part of the circuitry of an oscillator. By generating a Δ*frq1* strain, we unveiled that this protein not only serves an important circadian role, but that it also has additional functions, impacting sexual/asexual developmental decisions.

Taking advantage of the clock mutants that we generated and of available plant arrhythmic ecotypes, we provide compelling evidence that the outcome of the plant-fungal pathogen interaction varies with the time of day, in a manner that is largely dependent on the fungal clock.

To our knowledge, these results provide the first evidence of a functional light and circadian machinery in a pathogenic fungus, confirming that components of the circadian clock (including the putative photoreceptor BcWCL1) modulate the plant-pathogen interaction from a fungal perspective. Finally, this work open up the basis for environmental and natural ways to control this major and worldwide necrotrophic fungal plant pathogen.

1. INTRODUCTION

1.1 *Botrytis cinerea*: the gray mold fungus

Botrytis cinerea Persoon: Fries [teleomorph *Botryotinia fuckeliana* (de Bary) Whetzel] is a necrotrophic fungal plant pathogen, which is responsible for the rotting of plant material causing the gray mold disease (Paul Tudzynski, 2004). The genus Botrytis comprises over 20 species, being *B. cinerea* the major representative of the genus and the second most important phytopathogen based on its scientific and economic importance (Dean et al., 2012). Whereas most Botrytis species have a narrow host range and infect monocotyledonous plants, *B. cinerea* belongs to a distinct phylogenetic clade of species infecting more than 200 different dicotyledonous plants (Staats et al., 2005, Leroch et al., 2013). This ascomyceteous fungus belongs to the class Leotiomycetes and the family Sclerotiniaceae, that also houses a closely related necrotroph, the soil-borne fungus *Sclerotinia sclerotiorum*, responsible of the white mold disease in more than 400 different plant species (Bolton et al., 2006). Despite the destructive power of the latter, it is not a good model for molecular studies because of its inability to produce conidia and therefore to develop efficient transformation protocols (Rolland et al., 2003). The genome of both fungal pathogens -strains B05.10 and T4 for *B. cinerea* and strain 1980 for *S. sclerotiorum*- were recently sequenced, so molecular and genomic information is now available to the fungal community (Amselem et al., 2011).

B. cinerea is able to kill the host cells through the production of toxins, reactive oxygen species, enzymes that break the plant tissue, and the induction of a plant produced oxidative burst, providing the means to feed on dead plant tissue. The infection process transitions through the following stages: penetration of the host surface, killing

of host tissue, formation of the primary lesion, expansion of the latter leading to secondary lesion, and tissue maceration followed by sporulation (van Kan, 2006). The fungus has also the ability to be quiescent in infected flowers for long periods of time until the fruit ripens (Williamson, 1994).

Primary hosts of *B. cinerea* are dicotyledonous plants (i.e. grape vine, strawberry, tomato, ornamental flowers) and monocots, although the latter are considered poor hosts. The parts of the plant that can be infected include stems, leaves, flowers, unripe and ripe fruits (Schumacher and Tudzynski, 2012). *B. cinerea* is a worldwide agronomical problem and particularly in Chile it produces significant losses, affecting forest nurseries (from V to X Regions), preferably plants of the *Eucalyptus globulus* and *Pinus radiata* genus (Molina, 2006) and economically relevant produce. Thus, between the most important affected Chilean fruits are apples, blueberries, peaches and wine-table grapes (Latorre et al., 2002).

The ability of *B. cinerea* to be active at temperatures as low as 0 °C (Brooks, 1917) makes it an important post-harvest pathogen of stored products that are exported, either during storage, or in transit to international markets. The optimal temperature for germination and infection is 20°C for both flowers and fruits (as tested on table grapes) and relative humidity and water is needed for infection under field conditions (Latorre and Rioja, 2002). Nonetheless, the infection process can occur from 0 to 30 °C (Latorre et al., 2002) and species of the genus *Botrytis* can be found wherever their hosts are grown, ranging from tropical and subtropical to cold areas (Elad et al., 2007).

In *B. cinerea*, macroconidia are the predominant reproductive structures (asexual spores), which can be easily propagated away from the site of production, germinating

once they reach a favorable environment, which can be a living host plant or another suitable source of food. The life cycle under laboratory conditions begins with the germination of macroconidia on primary leaves (in this example *Phaseolus Vulgaris*) within hours (Figure 1). The infective structure- named germ tube- quickly penetrates the epidermis and invades the plant tissue, causing collapse and disintegration of the plant cells. Two days after the inoculation, small necrotic spots (named primary lesions) are seen. Then, *B. cinerea* apparently overcomes the plant defense barriers and starts a massive outgrowth; hyphae are growing invasively and decompose the plant tissue very rapidly (secondary infection). After 7 days, the whole leaf is infected and becomes soft rot. At this point, conidiophores -specialized hyphal branches that produce conidia- are formed completing, thus, the asexual cycle. The conidiation process is totally dependent of the presence of light. In its absence (darkness) and after 3-4 weeks, dark melanin covered structures for survival are formed (named sclerotia). Sclerotia can germinate in three ways, by forming mycelia, conidiophores or apothecia. The latter means that sclerotia can act in the sexual cycle as female (sclerotial) parents after fertilization with microconidia from a male (spermatial) parent carrying the opposite mating type. After several weeks of incubation under diurnal illumination, apothecia can be found containing asci with eight ascospores (Schumacher and Tudzynski, 2012) (Figure 1). It is important to note that the microconidia of *B. cinerea* are not capable to infect, since they generate a short germinal tube (Jarvis, 1977).

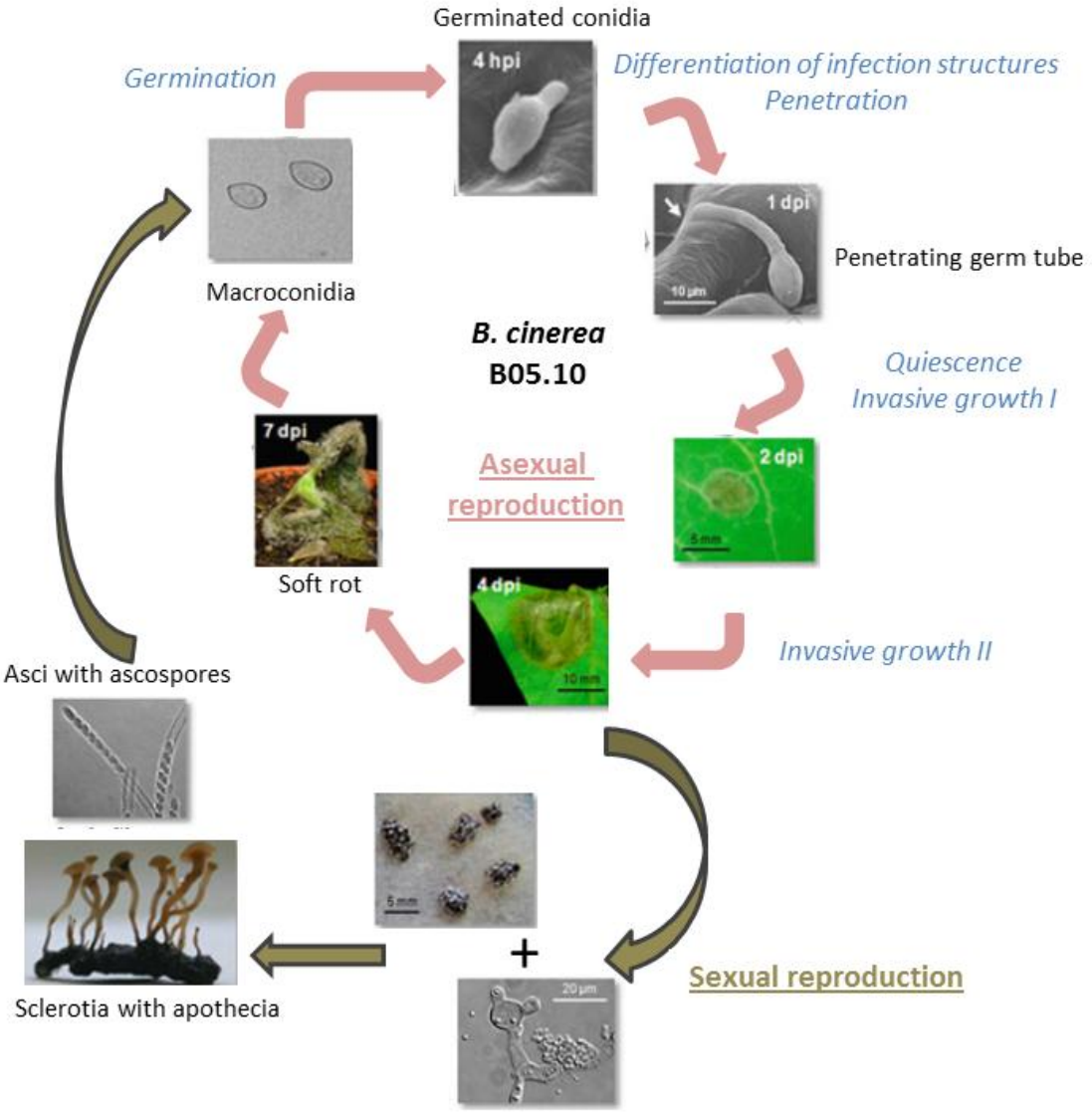

Figure 1. Life cycle of *B. cinerea* B05.10 using *Phaseolus Vulgaris* as host model. Conidia germination on bean leaves begins during the first hours and then the germ tube penetrates the epidermis. Primary lesion appears 48 hours after inoculation and after 4 days, big secondary lesions can be observed. After 7 days the plant tissue has collapsed and only gray conidiophores and conidia (soft rot) are seen. In darkness conidiation is suppressed, while sclerotia formation is promoted, which can act as female parents after fertilization if suspensions of microconidia from a male parent carrying the opposite mating type are presented. The formation of apothecia containing the asci with ascospores delayed at least two months and light must be used. Adapted from (Schumacher and Tudzynski, 2012).

The control of *B. cinerea* comprises an integrated management of cultural practices and preventive chemical control using fungicides in the most susceptible infection stages of pre-harvest and then during post-harvest mainly by utilizing anhydrous sulphurous (Esterio and Auger, 2006). However, control strategies are not entirely satisfactory. Among the main factors underpinning the development of the mold disease is the genetic variability that *Botrytis* presents, which confers resistance to fungicides with many isolates possessing resistance to up to six fungicides (Leroch et al., 2011). Quite some time ago the genetic diversity of *B. cinerea* was analyzed, discovering that different isolates contain in their genome transposable elements, which were present in multiple copies and dispersed throughout the genome. Thus, the isolates were classified according to the presence or absence of the "*Boty*" (retrotransposon) and "*Flipper*" (transposon) elements and named *transposa* (*Boty*$^{+}$/ *Flipper*$^{+}$) and *vacuma* (*Boty*$^{-}$/ *Flipper*$^{-}$) (Diolez et al., 1995, Levis et al., 1997). Later, another two isolates were detected harboring either only *Boty* (*Boty*$^{+}$/ *Flipper*$^{-}$) or only *Flipper* (*Boty*$^{-}$/ *Flipper*$^{+}$) (Giraud et al., 1997, Giraud et al., 1999). Moreover, studies based on multiloci gene genealogies, showed that *B. cinerea* is a complex of at least two phylogenetic species, called Groups I (*Botrytis pseudocinerea*) and II (*Botrytis cinerea sensu stricto*) (Fournier et al., 2003, Fournier et al., 2005). Group I consists entirely of *vacuma* isolates, whereas Group II includes *vacuma*, *transposa*, *Boty* and *Flipper* isolates (Fournier et al., 2005). In Chilean vineyards, *transposa* and *Boty* isolates are the most common, *vacuma* is in lower levels and *Flipper* has never been detected (Muñoz, 2002, Esterio et al., 2011). Interestingly, *vacuma* and *Boty* are sensitive to the fungicide iprodione (a dicarboximida), but *transposa* presents a high level of resistance, reflecting the

adaptation to chemical treatments (Esterio et al., 2011).

The genetic variability also impacts the aggressiveness that the isolates develop in different tissues, the secondary metabolites that they produce and the preferred method of reproduction (Schumacher and Tudzynski, 2012). For example, *B. cinerea* produces two families of non-host selective phytotoxic metabolites: a family of sesquiterpenoids (botryanes) and a family of polyketide derivatives named botcinolides (botcinins) (Tani et al., 2005, Tani et al., 2006, Collado et al., 2007). Despite that all isolates produce botryanes, botcinins has been only detected in more aggressive isolates (Reino, 2004) and deletion of genes involved in the botrydial biosynthetic pathway does not affect virulence in botcinins producing strains, but resulted in reduced virulence of T4 strain (which does not produce botcinins) (Siewers et al., 2005, Pinedo et al., 2008). Moreover, the *B. cinerea* T4 strain presents an "always conidia phenotype", despite the light conditions (Canessa et al., 2013). In this way, it is a very important issue to use a specific and well-characterized isolate to do phenotypic and molecular assays. Thus, *B. cinerea* B05.10 isolate, which belongs to Group II, is an aggressive strain that was isolated from *Vitis vinifera* (Buttner et al., 1994) and due to its genetic stability and high rates of homologous recombination it has become the standard recipient strain for genetic modifications (Tudzynski, 2009).

Virulence factors are effector molecules that cause damage to the host thereby enabling the pathogen to complete its disease and life cycle (Elad et al., 2007). The high efficiency of targeted gene inactivation approaches, based on fungal protoplast transformation and homologous recombination (Elad et al., 2007) has allowed a rapid functional analysis of virulence-related genes. Because the genetic variability present in

B. cinerea, the different isolates do not share a common arsenal of weapons and there are strain-specific adaptations. Here we comment on virulence genes that have been described in the *B. cinerea* B05.10 isolate, which have roles in all the stages of the virulence cycle and in different biological process: germination, penetration, fungal toxin biosynthesis, ROS generation, detoxification, plant cell wall degradation, signal transduction, light signaling, etc. The genes, function, biological process and genomic locus are summarized in Table 1.

Table 1. List of virulence factors identified in *B. cinerea* B05.10 wild-type strain

Gene	Function	Genomic locus	Biological process	References
bcpg1	Endopoligalactorunase	BC1G_11143	Plant cell wall degradation	(ten Have et al., 1998)
bcpg2	Endopoligalactorunase	BC1G_13367	Plant cell wall degradation	(Kars et al., 2005a)
bcpme1	Pectin methyl-esterase	BC1G_06840.1	Plant cell wall degradation	(Valette-Collet et al., 2003) (Kars et al., 2005b)
bcara1	Endo-arabinanase activity	BC1G_10322	Plant cell wall degradation	(Nafisi et al., 2014)
bcsod1	Superoxide dismutase	BC1G_00558	H_2O_2 generation	(Rolke Y, 2004)
bcatrb	ABC transporter	BC1G_04420.1	Detoxification	(Schoonbeek et al., 2001) (Stefanato et al., 2009)
bcnoxR	Regulatory subunit of NADPH complex	BC1G_06200	O_2^- production	(Segmuller et al., 2008)
bcnoxa	Catalytic subunit of NADPH complex	BC1G_10823	O_2^- production	(Segmuller et al., 2008)
****bcboa6***	polyketide synthase	BC1G_16086	Botcinic acid	(Dalmais et al., 2011)
bcbot2	sesquiterpene cyclase		Botrydial synthesis	
bcpic5	FKBP-type peptidyl prolyl cis-trans isomerase	BC1G_03430	Peptidyl-prolyl isomerization	(Gioti et al., 2006)
bcg1	Gα subunit of G proteins	BC1G_01681	Signal transduction	(Gronover et al., 2001)
bmp1	MAP kinase	BC1G_13966	Signal transduction	(Zheng et al., 2000) (Doehlemann et al., 2006)
bmp3	MAP kinase	BC1G_1284	Signal transduction	(Rui, 2007)
bcsak1	MAP kinase	BC1G_03001	Signal transduction	(Segmuller et al., 2007)
bac	Adenylate cyclase	BC1G_02865	Signal transduction	(Klimpel et al., 2002) (Doehlemann et al., 2006)
bcsas1	Rab/GTPase	BC1G_14039.1	Secretory pathway	(Zhang et al., 2014)
****bcpka1***	cAMP Catalytic and Regulatory subunit	BC1G_16086	Signal transduction	(Schumacher et al., 2008b)
bcpkaR				
bcvel1	Bridging protein in the putativeVELVET complex	BC1G_02977	Light dependent differentiation and secondary metabolism	(Schumacher et al., 2012)
bcwcl1	Blue light photoreceptor and GATA type TF	BC1G_13505	Light signal transduction and control of gene expression	(Canessa et al., 2013)
bctlf1	Light responsive GATA type TF	BC1G_10441	Control of gene expression	(Schumacher et al., 2014)
bcbem1	Scaffold protein in the polarity complex	BC1G_03145	Cell polarity	(Giesbert et al., 2014)
bccrz1	Calcineurin responsive Zing finger Transcription Factor	BC1G_00093	Control of gene expression	(Schumacher et al., 2008a)
bclae1	ortholog of *A. nidulans* LaeA, a interaction partner of BcVEL1	B0510_1382	Light dependent differentiation	(Schumacher et al., 2015)

1.2 The effects of light in fungi

Light is an abundant and ubiquitous signal that many organisms use to assess the status of their environment and therefore is capable of modulating major aspects of the physiology of an organism. Development, metabolism and other complex genetic programs are affected by light in filamentous fungi. Thus based on the presence or absence of this environmental cue, a variety of other fundamental processes can be triggered, including the mode (asexual/sexual) of reproduction (Corrochano, 2011). At the molecular level, these responses have been studied in detail only in a few fungal non-pathogenic models such as *Neurospora crassa*, *Aspergillus nidulans*, *Trichoderma reesei* and *Phycomyces blakesleeanus* (Purschwitz et al., 2006, Herrera-Estrella and Horwitz, 2007, Chen et al., 2010, Idnurm et al., 2010)

The molecular characterization of fungal light perception was initiated in the non- pathogenic ascomycete *N. crassa*, with the genetic isolation of the blue-light receptor *white collar-1* (*wc-1*) (Ballario et al., 1996). In this organism, blue light regulates transcriptional process, controls a circadian machinery, triggers mycelia carotenoid biosynthesis and controls sexual and asexual reproduction (formation of protoperithecia and conidiation, respectively) (Linden et al., 1997). Besides its role as a blue light photoreceptor, WC-1 is a GATA-type zinc finger transcription factor (TF) containing a DNA binding domain, two PAS (PER-ARNT-SIM) domains involved in protein-protein interaction, two putative transcriptional activation domains, a nuclear localization signal and a LOV domain (a specialized type of PAS domain) involved in environmental sensing of cues like light, oxygen and voltage. The chromophore FAD, in the LOV domain, is essential for the blue photoreceptor activity of WC-1, and for the

light-inducibility of the White Collar Complex (WCC), which is formed by WC-1 and another GATA-type TF named WC-2 (Ballario et al., 1996, He et al., 2002).

White collar-1 (WC-1) and White collar-2 (WC-2) are essential for light-mediated responses in *N. crassa*. Approximately 3% (314 genes) of the transcriptional units exhibit an early (observed after 15-30 min) or late (after 60 min and over) transcriptional response to light as part of a hierarchical transcriptional cascade initiated by the WCC (Chen et al., 2009). WCC activates the expression of early light-responsive genes upon light stimulation, while the GATA type TF SUB-1 is the key regulator of late light responses (Chen et al., 2009). Among the genes that activate the WCC, there are 24 putative TFs (Smith et al., 2010). This group of early light- WCC- dependent TFs include those regulating conidiation such as FL (*fluffy*), SAH-1 (*short aerial hyphae-1*) and CSP-1 (*conidiation separation-1*), sexual development (formation of perithecia) such as SUB-1 (*submerged protoperithecia*) and BEK-1 (*beak-1*) or both processes such as ADV-1 (*arrested development-1*) (Colot et al., 2006). In addition, the WCC is a key component of the *N. crassa* circadian clock, regulating the daily expression of the *frequency* (*frq*) gene, the central component of the oscillator (Heintzen and Liu, 2007, Lakin-Thomas et al., 2011, Montenegro-Montero and Larrondo, 2013).

Additional components capable of light-sensing such as cryptochromes (UV/ blue light receptors), opsins (putative green light receptors), red light sensors known as phytochromes and VIVID-like proteins (blue light receptors) have been identified in fungal systems (Chen et al., 2010, Idnurm and Heitman, 2010) and have been shown to modulate a lot of processes (Smith et al., 2010, Corrochano, 2011, Herrera-Estrella and Horwitz, 2007, Idnurm et al., 2010, Purschwitz et al., 2006). Interestingly, while several

filamentous fungi contain homologues of WC-1/ WC-2 TFs, the presence, number and physiological relevance of other photoreceptors vary among them, possible reflecting adaptations to different ecological niches. For example, while in *N. crassa* the small LOV domain containing protein VIVID (Heintzen et al., 2001) serves a key role in photoadapting the WCC dependent responses (Malzahn et al., 2010, Chen et al., 2010, Hunt et al., 2010), it is absent in other WCC-containing organisms like *A. nidulans*. Likewise, although red-light responses have been clearly characterized in *A. nidulans* and recently also in *A. fumigatus* (Blumenstein et al., 2005, Purschwitz et al., 2008, Rohrig et al., 2013, Fuller et al., 2013), red-light does not lead to any phenotypical or molecular change in *N. crassa* (Froehlich et al., 2005, Chen et al., 2009).

As mentioned previously, the differentiation of asexual and sexual reproductive structures in *B. cinerea* is known to be controlled by the presence or absence of light. While near-UV treatment as well as full-spectrum light induces the formation of conidiophores and macroconidia (Leach, 1962, Tan and Epton, 1973, Tan and Epton, 1974), the absence of light results in the formation of dark melanin pigmented sclerotia. Small dosages of near-UV and blue light are sufficient for inhibition of sclerotia development (Suzuki and Oda, 1979) while yellow, red and far-red light promote the formation of sclerotia (Tan and Epton, 1973). Sclerotia and microconidia are simultaneously formed during incubation in constant darkness; however, if microconidia are exclusively produced in the absence of light like the sclerotia is not clear. The formation of apothecia on the spermatized sclerotia also requires full-spectrum light in a 12 h photoperiod (Faretra, 1987). At least in the close relative *Sclerotinia sclerotiorum*, normal apothecial development is strictly dependent on near-UV light or daylight as

other qualities of light result in misshaped apothecia (Thaning and Nilsson, 2000).

In accordance with responses of *B. cinerea* to light, genes encoding potential receptors for sensing the different wavelengths could be identified in the *B. cinerea* genome (Table 2, adapted from (Schumacher and Tudzynski, 2012)). Notably, the group of fungal histidine kinases (phytochromes) representing putative red/far-red light sensors, has been expanded in *B. cinerea* and its close relative *S. sclerotiorum*; it has only one representative in *A. nidulans* and *Magnaporthe oryzae*, two in *N. crassa* but three in *B. cinerea* and *S. sclerotiorum* (Amselem et al., 2011). Potential blue light receptors are homologues of the *N. crassa* GATA TF WC1, VVD, and cryptochromes (Schumacher and Tudzynski, 2012). Several years ago, it was described a model for the regulation of light responses (conidiation) in *B. cinerea* involving a near UV/ blue receptor that closely interacts with a red/far-red photoreceptor (Tan, 1975a), nonetheless, until the development of this thesis there were no molecular reports linking the molecular effect of light in differentiation and virulence of *B. cinerea*. Recently, it was demonstrated that BcVEL1 and BcLAE1- the homologous of *A. nidulans* VELVET Vea and LaeA- interact in *B. cinerea* (Schumacher et al., 2015) and that the mutants have effect in differentiation, secondary metabolism and virulence (Schumacher et al., 2012, Schumacher et al., 2015). Nonetheless, it has not yet been described if BcVEL1 is interacting with the WCC (Canessa et al., 2013) and a putative red-light photoreceptor, as in *A. nidulans*. In the latter, the functional and physical interaction of LreA/LreB (WCC complex) with a red light sensor (phytochrome FphA) was demonstrated and FphA was shown to physically interact with the VELVET protein VeA linking thereby light signals with developmental programs and secondary metabolism (Purschwitz et al.,

2008, Bayram et al., 2008) (Table 2, adapted from (Schumacher and Tudzynski, 2012).

Table 2. The *B. cinerea* genome presents genes encoding for putative photoreceptors and related proteins

Name	Function	Gene ID *B. cinerea* B05.10 (BROAD)	Gene ID *B. cinerea* T4 (URGI)	*A. nidulans*	*N. crassa*
BcVVD1	Vivid-like 1, putative blue light sensor	BC1G_04348	BofuT4_P126250.1	-	VVD
BcCRY1	Cryptochrome 1, putative blue/ UV light sensor	BC1G_13162	BofuT4_P103490.1	CryA	NCU08626
BcCRY2	Cryptochrome 2	BC1G_08145	BofuT4_P159580.1	-	NCU00582
BcWCL1	WC1-like TF, putative blue light receptor	BC1G_13505	BofuT4_P091840.1	LreA	WC-1
BcWCL2	GATA type TF	BC1G_01840	BofuT4_P135970.1	LreB	WC-2
BOP1	Opsin 1, putative (green) light sensor	BC1G_02456	BofuT4_P110210.1	NopA	NOP-1
BOP2	Opsin 2, putative (green) light sensor	BC1G_13906	BofuT4_P163470.1	-	ORP-1
BcPHY1	Phytochrome 1, putative red/ far-red light sensor	BC1G_13369	BofuT4_P078780.1	FphA	PHY-1
BcPHY2	Phytochrome 2, putative red/ far-red light sensor	BC1G_08283	BofuT4_P014010.1	-	PHY-2
BcPHY3	Phytochrome 3, putative red/ far-red light sensor	BC1G_01106	BofuT4_P030530.1	-	-
BcVEL1	Velvet-like 1, component of the Velvet protein complex	BC1G_02976	BofuT4_P003460	VeA	VE-1
BcVEL2	Velvet-like 2, component of the Velvet complex	BC1G_11858	BofuT4_P161180	VelB	NCU02775
BcVEL3	Velvet-like 3, component of the Velvet complex	BC1G_06127	BofuT4_P017230	VosA	NCU05964
BcVEL4	Velvet-like 4, component of the Velvet complex	BC1G_11619	BofuT4_P157800	VelC	NCU07553

1.3 The effect of light in the plant- fungal interaction

Successful disease development requires that a pathogen, a susceptible host and favorable environmental conditions come together at the same time. However, the vulnerability of the susceptible host and the virulence of the attacking organism may differ with the time of the day, thus affecting the outcome of the interaction (Roden and Ingle, 2009). Only in the past years light has been recognized as an important modulator of fungal virulence (Idnurm and Crosson, 2009) and syndicated as a relevant variable with the potential to affect the outcome of the plant-pathogen interaction by modulating either plant defense responses, virulence of the pathogen or both (Roden and Ingle, 2009).

Thus, for example, it has been shown that the hypersensitive response (HR) against the Turnip Crinkle Virus in *Arabidopsis thaliana* is suppressed in darkness (Chandra-Shekara et al., 2006). Similarly, the *A. thaliana* systemic acquired response (SAR) is reduced when the plant is challenged with the avirulent pathogen *Pseudomonas syringae* in the absence of light, resulting in more bacterial growth (Zeier et al., 2004). Moreover, *A. thaliana* mutants in phytochromes *phyA* and *phyB* have compromised HR and SAR when exposed to *P. syringae* (Genoud et al., 2002, Griebel and Zeier, 2008). In addition, there is evidence that red light induces resistance to disease caused by different pathogens in rice, bean, cucumber, pepper, squash and tomato (Guo et al., 1993, Islam et al., 1998, Islam et al., 2002, Rahman et al., 2003, Wang et al., 2010). In the case of the phytopathogen *B. cinerea*, UV light increases resistance of *A. thaliana* to *B. cinerea* inoculated after the UV treatment (Demkura and Ballare, 2012), while a reduced red/ far-red light ratio sensed by a phytochrome enhances susceptibility (Cerrudo et al., 2012,

de Wit et al., 2013).

Supporting the concept that light can modulate the pathogenic potential in fungi, only putative blue light photoreceptors (WC-1 orthologues) have been implicated in modulating virulence at a molecular level, but their precise function seems to differ depending of the fungal-host system. Thus, involvement of WC-1 orthologous in virulence has been shown for the human pathogen *Cryptococcus neoformans* (Idnurm and Heitman, 2005) and in *M. oryzae*, the causal agent of the rice blast disease. In the latter case, constant light suppresses disease development, which is mediated via MGWC-1 (Kim et al., 2011b). In *Cercospora zeae-maydis*, a plant pathogen that infects leaves through stomata, WC-1 is required for stomata tropism, and for appressorium and lesion formation in maize (Kim et al., 2011a). Interestingly, in the opportunistic human pathogen *Fusarium oxysporum*, WC-1 is required for causing disease in immunocompromised mice but is dispensable for causing vascular wilt in plants (Ruiz-Roldan et al., 2008). However, none of the studies addressing virulence and light responses have included necrotrophic fungi.

Up until today, no molecular data is available regarding photoreception and virulence in *B. cinerea*. Only few reports from a phenotypical perspective have been described. For example, photo-control procedures based on the use of light of different wavelengths in greenhouses, have revealed clear effects on *B. cinerea* sporulation, while also having a positive effect on plant productivity (Kotzabasis et al., 2008). Nevertheless, it is not clear whether these different light qualities affect the fungus, the plant or both organisms. On the other hand, it has been described that the germ tube emerges on the illuminated side of the *B. cinerea* conidia, suggesting that the direction

of germination is controlled by photoreceptors sensitive to blue light (Jaffe and Etzold, 1962). Moreover, it has been shown that near UV, blue and far-red light (300-400, 400-520 and 700-810 nm, respectively) produce negative phototropism on *B. cinerea* and minimal growth of germ tubes, producing infective hyphae formation and promoting the infection in *A. thaliana*. On the other hand, positive phototropism is induced by red light (600 to 700 nm), resulting in growth of germ tubes without infective hyphae (Islam et al., 1998).

So, little is known about light and plant–pathogen interactions for filamentous fungi, in part because most research on light perception in these organisms have been done in *N. crassa*, a nonpathogenic organism. Expanding our current knowledge of light responses in plant pathogenic fungi, will surely open a fascinating research area.

1.4 Circadian clocks

Circadian clocks (from the Latin *circa diem,* or approximately a day) are endogenous cellular time-telling machineries that regulate biological rhythms in gene expression, physiology and behavior (Bell-Pedersen et al., 2005). These biological clocks have independently emerged during evolution at least three times, and its molecular description is well documented in cyanobacteria, insects, algae, plants, mammals, birds and fungi. Despite it multiple appearances during evolution, all organisms where clocks have been described display a common molecular blueprint: the core of the clock has an internal autonomous oscillator based on transcription-translation negative Feedback Loops (TTFL) (Bell-Pedersen et al., 2005).

The central oscillator brings together environmental information or inputs (i.e. light or temperature) feeding forward by controlling a large number of processes, known as outputs, in a temporal manner (Dunlap, 1999, Bell-Pedersen et al., 2005). Hence, circadian literature commonly describes that the oscillator can be synchronized along with the environment, in an "entrainment" mechanism. Sweeny (Sweeney, 1976) defined a circadian rhythm such "an oscillation in a biochemical, physiological, or behavioral function which under conditions in nature has a period of exactly 24 hours, in phase with environmental light-dark cycles, but which continues to oscillate (or free-run) with a period of approximately but usually not exactly 24 hours, in the absence of external stimuli (i.e. unchanging/constant light or darkness conditions). Moreover, the free-running period of the observed rhythm remains constant under different conditions of temperature and nutrition, reflecting a mechanism for compensation that distinguishes circadian rhythms from cell-cycle-regulated or environment driven phenomena, and other approximately 24 hour metabolic or developmental rhythms (Dunlap et al., 2007).

Studies performed in cyanobacteria, plants and mammals have shown that when the endogenous period matches the one observed in the oscillating environment, full fitness is achieved (Ouyang et al., 1998, Dodd et al., 2005, Yerushalmi and Green, 2009, Lowrey and Takahashi, 2011). Moreover, physiological/metabolic disorders and diseases have been correlated with an altered circadian regulation in mammals (Takahashi et al., 2008, Durgan and Young, 2010, Nakamura et al., 2014, Summa and Turek, 2014, Breen et al., 2014, Robinson and Reddy, 2014, Gonzalez, 2014) and the relevance of clocks on the control of immune and defense responses in mammals (Scheiermann et al., 2013, Curtis et al., 2014), flies (Lee and Edery, 2008, Kahrstrom,

2012) and plants (Sharma and Bhatt, 2014) has been described. Thus, circadian systems confer an adaptive advantage, allowing the anticipation of environmental changes or biological events that occur at predictable times of the day (McClung, 2006).

The molecular characterization of circadian clocks largely benefited from the work performed in the fungus *N. crassa* (Feldman, 1982, McClung et al., 1989), one of the main biological models for the study of chronobiology but, surprisingly, the only fungus where clocks have been molecularly characterized. In *N. crassa*, at the heart of the oscillator conforming the TTFL lays the negative element –the gene frequency (*frq*)-, whose expression is under the control of the positive element, the transcriptional complex WCC. To activate *frq* expression under constant darkness (DD), the WCC binds to a specific sequence in the *frq* promoter known as the clock-box (*c-box*), which is both necessary and sufficient for *frq* rhythmic expression (Froehlich et al., 2003). But in its role as blue light photoreceptor and TF, the WCC recognizes another sequence in the *frq* promoter, the proximal light regulatory element (PLRE), allowing acute increases in expression and the entrainment of the clock to environmental cues (Froehlich et al., 2002). So, due to the action of the WCC at the *c-box*, FRQ is produced, dimerizes and associates with a RNA-helicase known as FRH, and feeds back to block the activity of the WCC through a phosphorylation dependent mechanism, making possible a negative feedback loop. Thus, FRQ would be interacting as a scaffold protein, recruiting kinases and phosphatases to inhibit the WCC at appropriated times of the day (Mehra et al., 2009, Baker et al., 2012). At the same time, FRQ feeds forward to promote the synthesis of its activator, WC-1, making a positive feedback loop. As FRQ is progressively phosphorylated throughout the day, the repression of the WCC is relieved and FRQ

becomes proteasome-degraded, completing the transcriptional-translational negative feedback loop (TTFL) with a period of 22.5 hours (Larrondo et al., 2015). Posttranslational modifications, such as phosphorylation, are common regulatory mechanism for clock proteins trough the phyla (Gallego and Virshup, 2007, Mehra et al., 2009). *In vivo* data obtained through the use of heavy isotope labeling followed by tandem mass spectrometry, has confirmed phosphorylation in at least 85 S/T aminoacids of *N. crassa* FRQ residues (covering almost 10% of its residues) and mutations in many of these residues produce changes in the free running period of the conidiation rhythm (Baker et al., 2009, Tang et al., 2009). Recently, it has been shown that the degree of phosphorylation of FRQ (and not FRQ stability per se) is what determines the speed of the clock (Larrondo et al., 2015). In summary, the FRQ-WCC Oscillator (FWO) that is composed of positive and negative elements that form a TTFL leads to both *frq* and FRQ oscillations daily, which can be phenotypically correlated with the rhythmic pattern of conidiation or appearance of asexual spores every 22.5 h (Montenegro-Montero and Larrondo, 2013).

Several studies have demonstrated that at least 20% of the transcriptome of *N. crassa* is circadianly regulated (Bell-Pedersen et al., 1996, Zhu et al., 2001, Correa et al., 2003, Nowrousian et al., 2003, Dong et al., 2010), with genes peaking at all times of the day and controlling process such as sexual and asexual development, DNA repair, secondary metabolism, stress response, enzymatic activities, and so on (Dunlap and Loros, 2004, Vitalini et al., 2006, Lakin-Thomas et al., 2011). In addition, recent studies have indicated that up to 40% of the Neurospora genome can display rhythmic oscillations, but with high variability between replicates (Hurley et al., 2014). But, in

what way the circadian clock allows the expression of genes at different times of the day? Morning activation or night-time repression could lead to peaks during the day (*frq* is a morning-specific gene), while daytime activation and morning repression could lead to peaks during the night, which in turn will allow organisms to tune their gene expression profiles and metabolism to their environment (Montenegro-Montero and Larrondo, 2013). One example is the zinc-finger TF CSP1, which is a rhythmically expressed target of the WCC (Lambreghts et al., 2009, Smith et al., 2010) and was described as a morning repressor gene, allowing the evening expression of its targets, which oscillate in anthipase to *frq* (Sancar et al., 2011, Sancar et al., 2015).

Although *N. crassa* represents the only fungal model system in which the molecular mechanisms of circadian rhythms have been studied, there are some reports of fungi that display circadian rhythmicity at a phenotypic/behavioral level. Thus, the unicellular yeast *Saccharomyces cerevisiae* presents rhythms in cell division and aminoacid uptake, while *Schizosaccharomyces pombe* exhibits rhythms in mitosis and heat sensitivity. In both organisms, the rhythms are temperature compensated and can be entrained to light/dark cycles (Edmunds et al., 1979, Kippert, 1989, Kippert et al., 1991). In addition, metabolic rhythms, adhering to circadian principles, have been reported in *S. cerevisiae* (Eelderink-Chen et al., 2010). In the hyphomycete *Penicillium diversum* and the ascomycete plant pathogen *Sclerotinia fructigena*, conidiation persist under free-running conditions and is temperature compensated (Bourret et al., 1969, Jensen and Lysek, 1983). *Cercospora kikuchii*, an important soybean pathogen, displays circadian rhythm of hyphal melanization (Bluhm et al., 2010), while rhythms in bioluminescence have been described in forest mushroom (Oliveira et al., 2015). Rhythms in sclerotia

formation are present in the human and plant pathogen *Aspergillus flavus*, which remain under constant darkness conditions, are entrained by light cycles and also are temperature compensated (Greene et al., 2003a). *A. nidulans*, on the other hand, does not present observable circadian rhythms, but *glyceraldehyde-3-phosphate dehydrogenase* mRNA presents oscillations that are entrained by temperature (Greene et al., 2003a), although their periodicity does not fully adhere to a circadian classification.

The correct spatial and temporal regulation of gene expression that the clock achieves is what will impact the variety of biological process presents in all organisms (i.e cell growth, differentiation, etc). Despite that WC-1 acts as a blue light TF and also forms part of the TTFL of the circadian clock in *N. crassa*, the connection between light and circadian rhythms regulated pathways is not fully understood. So far, only a couple of studies have shown that the WCC activates the expression of early light-responsive genes upon a light stimuli, some of which encode for transcription factors (TFs) which are also clock controlled genes (*ccgs*) involved in the circadian rhythms of conidiation and metabolism, exemplifying a connection and overlap between both light and circadian regulatory pathways and suggesting a hierarchical arrangement of transcription factors involved in these processes (Smith et al., 2010, Sancar et al., 2015). In the case of fungi, besides Neurospora, there is no molecular information regarding how clock and light regulation may interact. Therefore, studying the connection between photo-responses and circadian regulated pathways and how these influence and confer adaptive value to relevant fungal biological processes would be of great interest, particularly in the context of fungal virulence.

1.5 The circadian clock in plant-fungal interactions

Although the idea that the outcome of a plant-pathogen interaction could be modulated by light and the circadian clock has been postulated (Roden and Ingle, 2009), there are no molecular reports about the selective advantage that circadian regulation could confer to pathogenic organisms, with the exception of phenotypic evidence laid down for an insect (Goodspeed et al., 2012) and malaria parasites (Mideo et al., 2013). In the case of fungi, *N. crassa* is the only fungus in which a circadian clock has been characterized at a molecular level, which therefore means that there are no such reports in any fungal pathogen.

Because plants are sessile organisms, they need a circadian timekeeper mechanism to anticipate cyclic and predictable environmental changes, coordinating and optimizing their physiology according to the external conditions. The circadian clock in plants control a wide variety of physiological and developmental process such as cotyledon and leaf movement (Engelmann and Johnsson, 1998), biochemical and metabolic processes (Harmer, 2009), acclimatization to abiotic and biotic stresses (Sanchez et al., 2011, Roden and Ingle, 2009) and hormone signaling (Robertson et al., 2009).

Only recently the importance of a clock has been addressed in the host plant, demonstrating that the *A. thaliana* innate immunity is controlled by a central circadian oscillator, providing an anticipation mechanism to respond before the attack of pathogens (Wang et al., 2011, Bhardwaj et al., 2011, Shin et al., 2012, Goodspeed et al., 2012, Goodspeed et al., 2013, Zhang et al., 2013). However, these studies have been done using pathogenic organisms in which no circadian regulation has been described:

oomycete pathogens (*Hyaloperonospora arabidopsidis* (*Hpa*)), virulent bacterial pathogens *(Pseudomonas syringae* pv. *tomato* DC3000 (*Pst* DC3000)) and insects (*Trichoplusia ni*). Moreover, in none of these plant pathogenic organisms the effect that light *per se* could have on virulence has not been studied.

So, considering the theoretical background of this work, it would be of great interest to understand whether a molecular clock and light-regulation modulate virulence and fitness in *B. cinerea*. Therefore, we propose to characterize a clock core component and the putative WC-1 blue light photoreceptor of this organism, evaluating the effect that both could have on its virulence.

2. HYPOTHESIS

Both light and circadian regulation modulate virulence of *Botrytis cinerea.*

General aim

To characterize part of the *B. cinerea* light and circadian regulation machinery and to determine their effect on virulence using *Arabidopsis thaliana* as a plant host model.

Specific aims

1. To characterize the presence of light and circadian regulatory components in *B. cinerea*.
2. To evaluate the effect of the putative blue light photoreceptor WC-1 in the virulence of *B. cinerea.*
3. To determine the effect of a circadian clock in the virulence of *B. cinerea.*

3. MATERIALS AND METHODS

3.1 *Botrytis cinerea* strains

Strain B05.10 of *B. cinerea* Pers. Fr. [*Botryotinia fuckeliana* (de Bary) Whetzel] originally isolated from *Vitis vinifera* (Germany) was first obtained from Fundación Ciencia&Vida (Dr. Pablo Valenzuela), and thereafter reisolated from a stock provided by the Tudzinsky laboratory (WWU, Germany). B05.10 was used in all experiments as the recipient strain for genetic modifications (Buttner et al., 1994, Quidde et al., 1998). Genome sequences of strain B05.10 (and strain T4) have been published (Amselem et al., 2011) and recently updated (Staats et al., 2005), and are available at URGI and BROAD Institute websites (http://urgi.versailles.inra.fr and http://www.broadinstitute.org/, respectively).

3.2 Culture conditions

B. cinerea strains were cultivated in Petri dishes containing one of the following solidified media: 1) **Synthetic Complete Medium** (CM: 1% Glucose, 0.2% Casein peptone, 0,1% Casaminoacids, 0,1% Yeast extract, 50 ml Salt solution (for 1L : 10.4 g KCl, 10.4 g $MgSO_4$, 30.4 g KH_2PO_4), 1 ml Vitamin solution (for 1L : 0.5 g Biotin, 50 g Nicotinamide, 16 g PABAC (*p*-aminobenzoic acid), 20 g Pyridoxine hydrochloride), 2 ml Microelement solution (for 1L : 1g $FeSO_4$ x 7 H_20, 0.15 g $CuSO_4$ x 5 H_20, 1.61 g $ZnSO_4$ x 7 H_20 , 0.1 g $MnS0_4$ x H_20, 0.1 g $(NH_4)_6Mo_7O_{24}$ x $4H_20$), pH 5.0), 2) **Potato Dextrose Agar** (PDA, AppliChem) with and without 10% homogenized bean/pea leaves, 3) **Gamborg B5** (Duchefa Biochemie) supplemented with 2% glucose (plus 70 μg/ml hygromycin B (Invitrogen) or 70 μg/ml Nourseothricine (Gold Biotechnology),

when corresponding), 4) **Synthetic Minimal Medium** (MM) (modified Czapek Dox containing 2% sucrose, 0.1% KH_2PO_4, 0.3% $NaNO_3$, 0.05% KCl, 0.05% $MgSO_4$ x 7 H_2O, 0.002% $FeSO_4$ x 7 H_2O, pH 5.0) and 5) **Malt Medium** (2% Malt Extract and 2% agar). The strains were also cultivated in PDA-containing hollow-glass tubes, known as race tubes, covered with sterile hydrophobic cotton at both ends (Montenegro-Montero and Larrondo, 2013). The strains were incubated at 20°C using Percival incubators, all equipped with cool white light fluorescent tubes (light intensity up to 100 micromoles/m2/s; wavelength 400-720 nm) in a 12:12 hours (h) light: dark regime (LD).

3.3 Light Pulse experiments

For light pulse experiments, strains were grown on PDA plates covered with cellophane and first grown in constant darkness (DD) for 48 h and then exposed to white light for the indicated periods of time.

3.4 Time Course experiments

For DD circadian experiments, strains were grown in PDA plates covered with cellophane under constant light conditions (LL) for 24 h and then transfer to DD every 4 h. For LL circadian experiments, B05.10 strain was grown in PDA plates covered with cellophane under DD for 24 h and then transfers to LL every 4 h. After 48, mycelia samples (obtained from independent PDA plates) were harvested. For the LD time course experiment, B05.10 strain was inoculated on cellophane-covered PDA Petri dishes under LD culture conditions, during 96 h. Thereafter, cultures were harvested every 2 h, during 32 h.

3.5 RNA extraction and Real-time quantitative RT-PCR (RT-qPCR)

For RNA isolation, mycelia were obtained from cellophane-covered solid media (PDA). DD cultures were harvested in a temperature-controlled darkroom equipped with low-intensity red-safety lights, and immediately frozen in liquid nitrogen. Samples from LL or light pulse culture conditions were harvested under white light, and processed accordingly. All samples were kept at -80 ºC until further purification. Frozen mycelia were ground to powder, and total RNA was isolated using TRIzol reagent (Invitrogen) as described by (Chen et al., 2009). Total RNA quantity and quality was verified using NanoDrop (Thermo Scientific) and by electrophoresis in a formaldehyde-containing agarose gel (1.2% w/v). RNA was further purified using the RQ1 RNase-free DNase (Promega), following the manufacturer's instructions. Absence of genomic DNA contaminations in the samples was confirmed by RT-minus reactions (data not shown). Thereafter, RNA samples were reverse transcribed using the MMLV reverse transcriptase (Promega), according to manufacturer's directions. One µl of cDNA was used in each RT-qPCR reaction. RT-qPCRs procedures were conducted according to the MIQE guideline (Minimum Information for Publication of Quantitative Real-Time PCR Experiments). Transcript quantification was achieved using the SensiMixPlus SYBR Green kit (12.5 µl reactions; Quantace) and the LightCycler 480 detection system (Roche) using the LightCycler 480 software (version 1.5.0.39), as described in manufacturers' manuals. Primer sequences and predicted Tm values, as well as amplicon lengths, are shown in Table 3. The RT-qPCR was performed as follows: 10 min at 95°C followed by 40 cycles of 15 s at 95°C, 15 s at 58°C, 60 °C or 62 °C (see Table 3) and 15 s at 72 °C, followed by a melting cycle from 55 to 95°C to check for amplification

specificity. Cq values were acquired during the annealing period of the RT-qPCR. Standard quantification curves with several serial 10-fold dilutions of RT-qPCR products were employed to calculate the amplification efficiency (E) of each gene, according to the equation $E = [10^{(1/slope)}]-1$. The obtained E values are also shown in Table 3. These values were used to obtain a more accurate ratio between the gene of interest (GOI) and the expression of the reference genes (*actin* and *elongation factor 1 beta*; BC1G_08198 and BC1G_03337, respectively) employed for normalization. Accurate normalization of RT-qPCR data was achieved by geometric averaging of two internal reference genes (NF: normalization factor; (Vandesompele et al., 2002)). In all experiments, expression values are referred to the first culture grown in DD.

Table 3. Oligonucleotides employed in RT-qPCR analysis

Gene	Primers 5'-3'	Primer's name	Amplicon size (bp)	Cp lower level	Cp higher level	Efficiencies (%)	Efficiency curve Rsq	Efficiency curve order of magnitude
bc actin BC1G_08198	AGCGTGAAATCGTCCGTGAT(FW) GACTGGCGGTTTGGATTTCTT(RC)	oL93 oL94	81	14.51	38.23	99.7	0.999	8
bc tubulin BC1G_05600	GCCGGGTTGCCGATAATT(FW) AGAAGAGCACCGAAACCAGATC(RC)	oL95 oL96	91	14.59	35.72	95.3	0.998	8
bcef1b BC1G_03337	GGCTACCTTGAACCCAGCAA(FW) AGCCTCCGCATCTTCTTCCT(RC)	oL297 oL298	100	11.73	24.19	106.6	0.997	5
bcwcl1 BC1G_13505	TCAATCAGTTCGTCCCCAAG(FW) CACCTGGTTGCGTGATAGGT(RC)	oL245 oL246	92	18.36	35.39	102.6	0.994	6
bcwcl2 BC1G_01840	TCCGAACCATCCTGATTTCC(FW) GATTCGCTTTCGTCAACGTG(RC)	oL325 oL326	80	11.84	32.29	95.88	0.999	7
bcfrq1 BC1G_13940	ACCCAGGAGGAAAGGTACGAA(FW) GGGAGCGGAAGGACAGATTT(RC)	oL97 oL98	86	15.98	35.69	98.4	0.996	7
BC1G_03545	GGAAGCTTCGTCTGCAGGTC(FW) GCTCTTTGTGCGGGAATGTT(RC)	oL291 oL292	120	11.96	25.65	95.8	0.999	5
bcltf1 BC1G_10441	ATGCGAAACTTACCCGCAAA(FW) CTCCGAAGATTTGGGTCGAA(RC)	oL287 oL288	80	14.69	35.41	94.1	0.999	7
bccsp1 BC1G_04022	TGCCTGCCAGAGTACAAAAG(FW) GAATGGAGGGATATCGGATG(RC)	oL1157 oL1158	104	8.91	31.48	96.8	0.992	8
*bcadv1** BC1G_05192	TCGATTCGACGATTCCCTAC(FW) AGGTCATGCGATTCGGTAAC(RC)	oL1493 oL1494	111	13.43	33.82	96.62	0.998	7
*bcvad3** Bc1G_03744	GGTGGTTTCGACAAAGATCC(FW) TACCATCTCTTTCGGCATGG(RC)	oL1497 oL1498	108	13.79	34.18	96.43	0.999	7
*bcsah1** Bc1G_08188	ACGATGTACGATTCCGATGC(FW) ACCGAACCGAAACTGCTATG(RC)	oL1487 oL1488	77	13.11	33.36	96.97	0.999	7
bcvvd1 BC1G_04348	CTTTGATTATCTCGGCAATGCA(FW) AGCGCGTTTCGAATGGTTAA(RC)	oL99 oL100	96	15.88	36.96	91.2	0.998	7
bop1 BC1G_02456	GTCTGGGGTATTGGTGATGG(FW) TACCGTCATGAGCGAACAAG(RC)	oL1171 oL1172	124	10.14	34.69	95.0	0.983	8
bccry1 BC1G_13162	TGATCGTCGGCTCTTTTCTC(FW) CATCCCCCGTTATTACTTGC(RC)	oL1153 oL1154	112	11.17	35.00	93.0	0.987	8
*bcccg1** Bc1G_11685	ATCCAAGGTGCCACTGCTAC(FW) ACATCAGCCTTGGTGTTGTG(RC)	oL1482 oL1483	149	11.38	32.14	94.06	0.999	7
bcfer1 BC1G_16428	TCCAGTCTTCATCCAAGCAC(FW) CAGCGCATTTCTCACTCTTG(RC)	oL1285 oL1286	116	12.34	31.41	83.3	0.919	6
*bcfrq1 endogenous locus***	ACCCAGGAGGAAAGGTACGAA(FW) TCAGCTCCAAATCCTATAAATGT (RC)	oL97 oL1874	129	12.32	33.61	91.8	0.998	7

An annealing temperature of 60°C and 62°C was employed for *primers and **primers, respectively.

3.6 Cloning of *bcwcl1* replacement cassettes

Two *bcwcl1* replacement cassettes were assembled using yeast recombinational cloning as described previously (Oldenburg et al., 1997). These cassettes are referred herein as replacement cassette A and B (Figure 5). Thus, the 5′- and 3′-non-coding regions of *bcwcl1* were amplified from genomic DNA of *B. cinerea* B05.10 using the primer pairs indicated in Table 4. The hygromycin (*hph*) resistance cassette was amplified from vector pLOB1 (Patel et al., 2008) (Δ*bcwcl1*, mutant 1, replacement cassette A) or pCSN44 (obtained from the Fungal Genetics Stock Center (Staben et al., 1989) as template (Δ*bcwcl1*, mutant 2 and 3; replacement cassette B). Primers employed for these PCR reactions contained 30-bp-overlapping regions, thus allowing homologous recombination. Detailed descriptions of the vectors containing the *bcwcl1* replacement cassettes are indicated in Figure 5. Fragments were co-transformed with the linearized pRS426 vector (Christianson et al., 1992) into uracil-auxotrophic *Saccharomyces cerevisiae* strain FY834 (Winston et al., 1995) for assembly. After yeast transformation, the plasmid containing the construct was recovered from yeast by *Escherichia coli* transformation. Junctions were sequenced to confirm the absence of mutations (data not shown). Thereafter, the replacement cassettes were amplified using universal primers flanking the recombination region chosen in pRS426 (Table 4) and the Expand High Fidelity (Roche), KAPA HiFi (Kapa Biosystem) or Phusion High-Fidelity (Thermo Scientific) DNA polymerases and used for transformation of *B. cinerea*.

3.7 Cloning of *bcwcl1* complementation cassette

The open reading frame (ORF) of *bcwcl1* was amplified from genomic DNA using

the primer pair *bcwcl1*-P*oli*CF/ T*gluc*-R (Table 4) and assembled with the NcoI/NotI-digested plasmid pNDN-OGG (Schumacher, 2012) by YRC, yielding pNDN-bcwcl1. This vector contains *bcwcl1* under control of the *oli*C promoter from *A. nidulans* (PoliC) and the glucanase terminator of *B. cinerea* (T*gluc*), a nourseothricin resistance cassette (*nat1*) (Gold Biotechnology) and flanking sequences for facilitating the targeted integration at the *bcniaD* locus (nitrate reductase).

3.8 Cloning of BcFRQ1-LUC translational reporter

The translational fusion was created using the firefly *luciferase* gene, which was fully codon optimized for expression in *N. crassa* (Gooch et al., 2008). 572 base pairs before the *bcfrq1* stop codon were used as 5´flank and the 3´ flank was obtained from the 3′-non-coding (downstream) region of *bcfrq1,* all amplified from genomic DNA of *B. cinerea* B05.10 using the primer pairs indicated in Table 5. The *oluc* CDS was obtain from pLL07 vector (Gooch et al., 2008) and the hygromycin (*hph*) resistance cassette was amplified from vector pLOB1 (Patel et al., 2008) (primer pairs in Table 5). Detailed description of the vector containing the BcFRQ1-LUC replacement cassettes are indicated in Figure 17. Fragments were assembled with pRS426 vector (Christianson et al., 1992) by YRC (Winston et al., 1995) and the plasmid was recovered from yeast by *E. coli* transformation. Junctions were sequenced to confirm the absence of mutations (data not shown) and the construct was amplified as described in 3.6.

3.9 Cloning of *bcfrq1* replacement cassette

The upstream and downstream-non-coding regions of *bcfrq1* were amplified from

genomic DNA of *B. cinerea* B05.10 using the primer pairs indicated in Table 6. The hygromycin (*hph*) resistance cassette was amplified from vector pLOB1 (Patel et al., 2008) (primer pairs in Table 6). Detailed description of the vector containing the *bcfrq1* replacement cassette is indicated in Figure 19. Fragments were co-transformed with the linearized pRS426 vector (Christianson et al., 1992) and assembled by YRC (Winston et al., 1995). The plasmid containing the construct was recovered from yeast by *E. coli* transformation and amplified as described in 3.6. Junctions were sequenced to confirm the absence of mutations (data not shown).

3.10 Cloning of *bcfrq1* complementation cassette

The open reading frame (ORF) of *bcfrq1* was amplified from B05.10 genomic DNA using the primer pair described in Table 7 and assembled in pRS426 (Christianson et al., 1992) by YRC (Winston et al., 1995) and then recovered from yeast by *E. coli*. This vector contains *bcfrq1*, the nourseothricin resistance cassette (*nat1*) obtained from vector pNR1 and flanking sequences to facilitate the targeted integration at the *bcfrq1* endogenous locus, in such way that the complemented *bcfrq1* is under control of its own promoter. Construct was amplified as described in 3.6. Junctions were sequenced to confirm the absence of mutations (data not shown).

3.11 Cloning of OE::*bcfrq1* replacement cassette

A construct was made in which expression of the BcFRQ1 open reading frame was dependent on the actin promoter. The cassette integration was targeted to the *bcku70* locus, since deletion of this gene does not affect *B. cinerea* growth *in vitro* or *in*

planta (Choquer et al., 2008). The *bcku70* upstream and downstream -non-coding regions, the actin promoter and *bcfrq1* ORF were amplified from genomic DNA of B05.10 wild-type strain using the primer pairs indicated in Table 8. The hygromycin (*hph*) resistance cassette was amplified from vector pCNS44 (Staben et al., 1989) (primer pairs in Table 8). Detailed description of the vector containing the OE::*bcfrq1* replacement cassette is indicated in Figure 28. Fragments were co-transformed with pRS426 (Christianson et al., 1992) and assembled by YRC (Winston et al., 1995). The plasmid containing the construct was recovered from yeast by *E. coli* transformation and amplified as described in 3.6. Junctions were sequenced to confirm the absence of mutations (data not shown).

3.12 Transformation of *B. cinerea*

B. cinerea transformation was carried out using protoplasts mediated transformation. Spore suspension was inoculated from well-sporulated one-week old Botrytis PDA plate (supplemented with 10% homogenized bean/pea leaves) in one flask containing 100 ml maltose medium 1.5% (0.5% glucose, 1.5% malt extract, 0.1% peptone, 0.1% casaminoacids, 0.1% yeast extract and 0.02% Ribonucleic acid sodium salt) during 18 hours at 20 °C and 120 rpm. The one- day old culture was filtrated using Nytex and washed with KC buffer (for 400 ml: 17.9 g KCl, 2.95 g $CaCl_2x2H_20$). 1.5 g of half-wet mycelium was collected and transferred to a flask in order to prepare protoplasts as follow: 50 mg Novozyme 234+ 100 mg Lysing Enzyme 116K1254 (Sigma)+ 5 mg Yatalase (Takara), in 11 ml of KC buffer. Protoplasts were incubated during 2 hours at 28 °C and 95 rpm. Then, protoplasts were filtrated using Nytex,

washed with KC buffer and centrifuged at 4000 rpm for 5 minutes at 4 °C (twice). Protoplasts were quantified using a Thomas chamber, using $1x10^7$ protoplasts per transformation. For each transformation, 150 µl of PCR product of the desired construction were precipitated and resuspended in 30 µl TE Buffer. 100 µl of protoplasts were mixed with the 30 µl purified PCR product, to which were added: 70 µl KC buffer (5 minutes in ice), 100 µl PEG (for 10 ml: 500 µl $CaCl_2$ 1M, 2.5 g PEG- 6000, 100 µl Tris-HCl 1M pH 7.5) (20 minutes at RT), 500 µl PEG (10 minutes in ice) and 200 µl KC. Finally, 500 µl of protoplasts were added to 50 ml SH agar (for 600 ml: 123.2 g sacarose, 0.363 g Tris pH 6.5, 0.079 g $(NH_4)_2HP0_4^-$, 0.6 g yeast extract and 7.2 g agar 1.2%), transferring 10 ml to each plate. The plates were incubated for 20 hours at 20 °C and they were overlaid with SH agar containing 70 µg/ml hygromycin B (Invitrogen) or 70 µg/ml nourseothricine (Gold Biotechnology). The homokaryotic derivates were obtained subjecting the transformants to at least four rounds of single-spore isolation (using the selection marker). Following DNA extraction (Cenis, 1992), transformants that have undergone homologous integration were confirmed by PCR using locus-specific primers with those binding in the resistant cassette or in the site corresponding to a determined construction (see Tables 4, 5, 6, 7 and 8 for more details). Absence of wild-type alleles was confirmed by using primers described in Tables 4, 5, 6, 7 and 8.

3.13 Southern Blot

PCR-verified mutants for Δ*bcwcl1 and* Δ*bcfrq1* were further analyzed by means of Southern blot hybridization employing the DIG Easy Hyb Hybridization solution (Roche) and the PCR DIG Probe Synthesis Kit (Roche) following manufacturer's

instructions.

3.14 Assessment of rhythmic luminescence

The luciferase reporter BcFRQ1-LUC (two biological replicates) was analyzed using a 1024B PIXIS-CCD camera (Princeton Instruments) at 20 °C, using petri plates fill with Gamborg B5-2% glucose, as previously described (Gooch et al., 2008). Before being transferred to DD, plates were entrained for 3 days in LD. The reporter strain was also monitored under temperature entrainment conditions using steps from 22°C to 27°C under DD conditions (12:12) and by using 22°C to 27°C temperature cycles of varying period length (16, 20 and 24 T). Bioluminescence traces were acquired using the WinView software, and analyzed in more detail using a costume-made ImageJ macro.

3.15 Fluorescence microscopy

Conidia from two-week-old culture were collected by glass wool filtration, diluted in water to 10^8 conidia/ml and then pelleted by centrifugation (3000 RPM for 20 min). Thereafter, conidia were stained with a dilution of 1 mg/ml of Hoechst 33342 (Life Technologies) for 15 minutes in darkness, and then rinsed twice with phosphate-buffered saline 1X. Conidia were mounted in 30% glycerol. Fluorescence microscopy was performed with a Nikon Eclipse C2 confocal microscope and Cytation 3 Cell Imaging Multi-Mode Reader (Biotek). Photos were obtained using NIS-Elements Microscope Imaging Software (Nikon) and Gen5 Data Analysis Software (Biotek).

3.16 *Phaseolus vulgaris* and *A. thaliana* growth

P. vulgaris cv. 90598 was obtained from the Tudzynski laboratory (WWU, Germany). *Arabidopsis thaliana* accession Columbia 0 (Col-0) and the Constitutive Expression of the *CIRCADIAN CLOCK ASSOCIATED 1* (CCA1ox) mutant line were a generous gift from the Dr. Rob McClung (Dartmouth College, USA), while the triple mutant of PSEUDO-RESPONSE REGULATORS, PRR9, PRR7 and PRR5 (*d975*) was a kind gift of Dr. Eva Farre (Michigan State University, USA). *P. vulgaris* was grown at 20°C in a 12:12 photoperiod (LD) for 14 days using Percival incubators. Arabidopsis seedlings were germinated in soil, then transferred to and grown at 22 °C for 14 days under LL and then for other two weeks at 20 °C under LD using Percival incubators. CCA1ox and *d975* plants are arrhythmic with respect to circadian outputs in LL, DD and LD (Wang and Tobin, 1998, Nakamichi et al., 2005, Nakamichi et al., 2009, Bhardwaj et al., 2011).

3.17 Virulence assays

Prior to infection, *A. thaliana* and *B. cinerea* were grown under LD conditions for two weeks at 20°C. Then, leaves of approximately one-month-old *A. thaliana* or 14 days old *P. vulgaris* plants were used to inoculate with *B. cinerea* spores, which were obtained essentially as described previously (Canessa et al., 2013). Briefly, a plug of the indicated *B. cinerea* strain was resuspended in Gamborg B5 and agitated vigorously for 15 seconds. Spores were obtained after filtration using eppendorf tubes and 1000 µl tips filled with glass wool at the tip inside the mentioned tube. The filtrated spores were quantified in a Thomas chamber and adjusted to a final concentration of $2x10^5$ spores/ml

in Gamborg B5 and 10 mM KH_2PO_4/K_2HPO4 (pH 6.4) and incubated during one hour at RT. Seven µl of conidial suspensions were used to inoculate wounded or unwounded leaves, when corresponding. Infections were done at dawn or dusk, accordingly to the photoperiod of the plant growth chamber (Percival incubator). All inoculated plants were kept inside plastic boxes at 20°C under humid environment, in LL, LD or DD conditions for 72 hours and then immediately analyzed (3 dpi). Since the different *A. thaliana* ecotypes have different leaves size, lesions on *A. thaliana* leaves -at least 180 infected leaves per *B. cinerea* strain and condition- were measured semi-automatically using the ImageJ software using an external calibration scale. The lesion area was calculated by measuring the total and infected area of the leaf, being the total area 100%. Therefore, measurements in the graphs are expressed as percentage. Lesions on beans leaves -at least 10 infected leaves per *B. cinerea* strain and condition- were also measured semi-automatically using the ImageJ software using an external calibration scale, but measurements are expressed in cm^2.

3.18 Trypan blue staining

For detection of *B. cinerea* hyphae in infected plant tissues, detached *A. thaliana* leaves were washed for 1 h with gentle agitation in absolute ethanol at 60°C to remove chlorophyll. Thereafter, leaves were incubated for 30 min in lactophenol trypan blue solution (water: glycerol: lactic acid (1:1:1) +10 ml of trypan blue solution 25 mg/ml (Sigma-Aldrich, Germany)). Finally, stained leaves were incubated for 20 min with gentle agitation in a destained solution (water: glycerol: lactic acid (1:1:1) and

transferred into 50% glycerol solution for microscopy using a Nikon Eclipse 80*i* microscope attached to a digital camera.

3.19 DAB staining

H_2O_2 levels *in planta* were determined employing 3,3'-diaminobenzidine (DAB) (Sigma) staining as described (Carvalho et al., 2008). Briefly, detached leaves were incubated in a 2 mM EDTA solution pH 5.5, and subsequently incubated in a 5 mM DAB solution pH 3.8, for 2 hours. Leaves were destained in ethanol. Thereafter, images were acquired using a Nikon Eclipse 80*i* microscope attached to a digital camera.

Table 4. Oligonucleotides employed for the generation of Δ*bcwcl1* and Δ*bcwcl1*+ Δ*bcwcl1* complementation strains

Amplification target	Primers 5'-3'	Primer name	Strain
bcwcl1 upstream non-coding region	GCGGATAACAATTTCACACAGGAAACAGC ACCAGCTGTGGAAGTGTCTG (FW)	LC-256	Δ*bcwcl1* mutant 1
bcwcl1 upstream non-coding region	CGAATCGGGAATGCGGCTCCACAGCTGCA GGGTATTTGAGCGGAGGCAGG (RC)	LC-276	Δ*bcwcl1* mutant 1
bcwcl1 downstream non-coding region	TTAATGATGATTACTAACAGATATCAAGC TTTGTCATGTTGTTATAGTCTCGG (FW)	LC-277	Δ*bcwcl1* mutant 1
bcwcl1 downstream non-coding region	GTAACGCCAGGGTTTTCCCAGTCACGACG ATCTGTATCGGGGTTGTGTTT (RC)	LC-278	Δ*bcwcl1* mutant 1
hph resistance cassette (from pLOB1 vector)	CTGCAGCTGTGGAGCCGCATT(FW)	LC-269	Δ*bcwcl1* mutant 1
hph resistance cassette (from pLOB1 vector)	AAGCTTGATATCTGTTAGTAA(RC)	LC-270	Δ*bcwcl1* mutant 1
bcwcl1 upstream non-coding region	GCGGATAACAATTTCACACAGGAAACAGC AGGATATACCGAGGGACGAG (FW)	oligo1	Δ*bcwcl1* mutants 2 & 3
bcwcl1 upstream non-coding region	GACCGGGATCCACTTAACGTTACTGAAAT CATTGAAGAAATTACTCATGATA (RC)	oligo2	Δ*bcwcl1* mutants 2 & 3
bcwcl1 downstream non-coding region	CAAAAATGCTCCTTCAATATCATCTTCTGT CTTGGCAGGGTTCTCCTGGAT (FW)	oligo3	Δ*bcwcl1* mutants 2 & 3
bcwcl1 downstream non-coding region	GTAACGCCAGGGTTTTCCCAGTCACGACG GTTGAATTGGAAAACTTGGA (RC)	oligo4	Δ*bcwcl1* mutants 2 & 3
hph resistance cassette (from pCSN44 vector)	GACAGAAGATGATATTGAAGGAGC (FW)	oL768	Δ*bcwcl1* mutants 2 & 3
hph resistance cassette (from pCSN44 vector)	GATTTCAGTAACGTTAAGTGG (RC)	oL687	Δ*bcwcl1* mutants 2 & 3
Amplification of genetic constructs (from pRS426)	GGCAGTGAGCGCAACGCAAT (FW)	oL83	-
Amplification of genetic constructs (from pRS426)	ATTCAGGCTGCGCAACTGTT (RC)	oL84	-
Amplification of *bcwcl1*, to be fused to P*oliC* promoter	TCCATCACATCACAATCGATCCAACCATG CCAATGACCCAAGCAGACTTG (FW)	*bcwcl1*-P*oliC*-F	Δ*bcwcl1 +bcwcl1*
Amplification of *bcwcl1*, to be fused to T*gluc* terminator	AATCATACATCTTATCTACATACGCTAAC CCTCCTTGAAAATCTCATTA (RC)	*bcwcl1*-T*gluc*-R	Δ*bcwcl1 +bcwcl1*
5' integration, at *bcwcl1* locus; diagnostic PCR	GAGAGACAGGATGGTACAAATGAG (FW)	oL588	Δ*bcwcl1*mutant 1, 2 & 3
3' integration, at *bcwcl1* locus; diagnostic PCR	ACACTTGTGCTTGTGCTTGC (RC)	oL589	Δ*bcwcl1*mutant 1, 2 & 3
5' integration, at P*oliC* promoter; diagnostic PCR	GGTACTGCCCCACTTAGTGGCAGCTCGCG (RC)	oL585	Δ*bcwcl1* mutant 1
3' integration, at "*tubA*" terminator; diagnostic PCR	GGTCCTCGGAGTGCAGATGGG (FW)	oL584	Δ*bcwcl1* mutant 1
5' integration, at *hph* CDS; diagnostic PCR	ATGGCTGTGTAGAAGTACTC (FW)	oL32	Δ*bcwcl1* mutants 2 & 3
3' integration, at *hph* CDS; diagnostic PCR	TCGCCCTCCGAGAGCTGCAT (RC)	oL29	Δ*bcwcl1* mutants 2 & 3
bcwcl1 ORF, diagnostic PCR	GTATCAACCCCCACGGCTCTCA (FW)	oL586	-
bcwcl1 ORF, diagnostic PCR	CGGCGAATGCGGAATACCA (RC)	oL587	-
bcwcl1 5' integration at *bcniaD* locus, diagnostic PCR	GGCATCTCTTGGAGGAAGAA (FW)	oL1226	Δ*bcwcl1 +bcwcl1*
5' integration at *bcniaD* locus, diagnostic PCR	CGCATATCAGCATATCGAGATGTCC (FW)	oL1716	Δ*bcwcl1 +bcwcl1*

Table 5. Oligonucleotides employed for the generation of BcFRQ1-LUC translational reporter

Amplification target	Primers 5'-3'	Primer name	Strain
572 pb before *bcfrq1* stop codon	GCGGATAACAATTTCACACAGGAAAC AGCTGCACACAATTTCACAGTCT (FW)	LC-267	BcFRQ1-LUC
572 pb before *bcfrq1* stop codon	GGGGCCCTTCTTGATGTTCTTGGCGTC CTCAAGCTCCACCTCATCGCTCT (RC)	LC-229	BcFRQ1-LUC
oLuc CDS	GAGGACGCCAAGAACATCAA (FW)	LF-125	BcFRQ1-LUC
oLuc CDS	TCAGAGCTTGGACTTGCCGC (RC)	LF-126	BcFRQ1-LUC
bcfrq1 3´UTR	GCCAAGAAGGGCGGCAAGTCCAAGC TCTGAATGTTGTAAACATTTATAGGA (FW)	LC-230	BcFRQ1-LUC
bcfrq1 3´UTR	CGAATCGGGAATGCGGCTCCACAGCT GCAGTGCATTTTCCATTCCATCGTACA (RC)	LC-268	BcFRQ1-LUC
bcfrq1 downstream non-coding region	TTAATGATGATTACTAACAGATATCA AGCTTAAATTAGGTTACTCAGCGTTA (FW)	LC-271	BcFRQ1-LUC
bcfrq1 downstream non-coding region	GTAACGCCAGGGTTTTCCCAGTCACG ACGCGTCATAGATGGTGACATAG (RC)	LC-272	BcFRQ1-LUC
hph resistance cassette (from pLOB1 vector)	CTGCAGCTGTGGAGCCGCATT (FW)	LC-269	BcFRQ1-LUC
hph resistance cassette (from pLOB1 vector)	AAGCTTGATATCTGTTAGTAA (RC)	LC-270	BcFRQ1-LUC
Amplification of genetic constructs (from pRS426)	GGCAGTGAGCGCAACGCAAT (FW)	oL83	-
Amplification of genetic constructs (from pRS426)	ATTCAGGCTGCGCAACTGTT (RC)	oL84	-
upstream integration, at *bcfrq1* locus; diagnostic PCR	GTACATACACGATGGGCGACGA (FW)	oligoB_ FRQluc	BcFRQ1-LUC
upstream integration, at *bcfrq1* locus; diagnostic PCR	TCGGTCTGTGAGAATGAGAT (RC)	LL30	BcFRQ1-LUC
downstream integration, at the carboxyl terminal *bcfrq1* region; diagnostic PCR	GATCTTGACACCATAACGGCTT (FW)	tubA_out	BcFRQ1-LUC
downstream integration, at the carboxyl terminal *bcfrq1* region; diagnostic PCR	ATAACAATAAAATCGCAACCCCAGA (RC)	oligoA_ FRQluc	BcFRQ1-LUC

Table 6. Oligonucleotides employed for the generation of Δ*bcfrq1* strains

Amplification target	Primers 5'-3'	Primer name	Strain
bcfrq1 upstream non-coding region	GCGGATAACAATTTCACACAGGAAACAGCGAG TAGAGGTACATTGGACGGGA (FW)	LC-242	Δ*bcfrq1*
bcfrq1 upstream non-coding region	CGAATCGGGAATGCGGCTCCACAGCTGCAGTA AGGAAGGTGTGATGAAGG (RC)	LC-273	Δ*bcfrq1*
bcfrq1 downstream non-coding region	TTAATGATGATTACTAACAGATATCAAGCTTGA TCTAGATATAGGAATGTA (FW)	LC-274	Δ*bcfrq1*
bcfrq1 downstream non-coding region	GTAACGCCAGGGTTTTCCCAGTCACGACGGCA GGTCCAAGAGCAGAGCA (RC)	LC-275	Δ*bcfrq1*
hph resistance cassette (from pLOB1 vector)	CTGCAGCTGTGGAGCCGCATT (FW)	LC-269	Δ*bcfrq1*
hph resistance cassette (from pLOB1 vector)	AAGCTTGATATCTGTTAGTAA (RC)	LC-270	Δ*bcfrq1*
Amplification of genetic constructs (from pRS426)	GGCAGTGAGCGCAACGCAAT (FW)	oL83	-
Amplification of genetic constructs (from pRS426)	ATTCAGGCTGCGCAACTGTT (RC)	oL84	-
downstream integration, at *bcfrq1* locus; diagnostic PCR	AGCATGGGGATCAACTCTTG (RC)	oL686	Δ*bcfrq1*
upstream integration, at *bcfrq1* locus; diagnostic PCR	CGTTGATTGGAACAATGCAG (FW)	F1_new	Δ*bcfrq1*
downstream integration, at *hph* CDS; diagnostic PCR	ATGGCTGTGTAGAAGTACTC (FW)	oL32	Δ*bcfrq1*
upstream integration, at *hph* CDS; diagnostic PCR	GTCCGATAAAATGGTACTGCC (RC)	oliC_out	Δ*bcfrq1*
bcfrq1 ORF, diagnostic PCR	TCGCAGGTGACCCGCCATACT (FW)	frqFW_inner	-
bcfrq1 ORF, diagnostic PCR	TCTAGACGCCGAACAACCATCCTT (RC)	frqRC_inner	-

Table 7. Oligonucleotides employed for the generation of the *Δbcfrq1+bcfrq1* complementation strain

Amplification target	Primers 5'-3'	Primer name	Strain
bcfrq1 upstream non-coding region	GCGGATAACAATTTCACACAGGAAACAGC GAGTAGAGGTACATTGGACGGGA (FW)	LC-242	Δ*bcfrq1+bcfrq1*
bcfrq1 upstream non-coding region	GACCGGGATCCACTTAACGTTACTGAAATC TCAAAGCTCCACCTCATCGC (RC)	oL1520	Δ*bcfrq1+bcfrq1*
bcfrq1 downstream non-coding region	GCTCCTTCAATATCATCTTCTGTCGATCTAG ATATAGGAATGTATATATATATA (FW)	oL1521	Δ*bcfrq1+bcfrq1*
bcfrq1 downstream non-coding region	GTAACGCCAGGGTTTTCCCAGTCACGACGG CAGGTCCAAGAGCAGAGCAGGGCA (RC)	LC-241	Δ*bcfrq1+bcfrq1*
nat1 resistance cassette (from pNR1 vector)	GATTTCAGTAACGTTAAGTGGATCCCGGTC GACCAGGAGTTTCATAACATCCACGG (FW)	oL1559	Δ*bcfrq1+bcfrq1*
nat1 resistance cassette (from pNR1 vector)	GACAGAAGATGATATTGAAGGAGCATTTTT GCCGGATTGGTCAAGATTTGCGTCCG (RC)	oL1560	Δ*bcfrq1+bcfrq1*
Amplification of genetic constructs (from pRS426)	GGCAGTGAGCGCAACGCAAT (FW)	oL83	-
Amplification of genetic constructs (from pRS426)	ATTCAGGCTGCGCAACTGTT (RC)	oL84	-
upstream integration, at *bcfrq1* locus; diagnostic PCR	CGTTGATTGGAACAATGCAG (FW)	oligoF1_new	Δ*bcfrq1+bcfrq1*
upstream integration, at *bcfrq1*; diagnostic PCR	CTCGGAGGGGTAACTCTTTGCT (RC)	oL167	Δ*bcfrq1+bcfrq1*
downstream integration, at *bcfrq1* locus; diagnostic PCR	AGCATGGGGATCAACTCTTG (FW)	oL686	Δ*bcfrq1+bcfrq1*
downstream integration, at *nat* CDS; diagnostic PCR	GGTACTGCCCCACTTAGTGGCAGCTCGCG (RC)	oL585	Δ*bcfrq1+bcfrq1*
bcfrq1 ORF, diagnostic PCR	TCGCAGGTGACCCGCCATACT (FW)	frqFW_inner	-Δ*bcfrq1+bcfrq1*
bcfrq1 ORF, diagnostic PCR	TCTAGACGCCGAACAACCATCCTT (RC)	frqRC_inner	Δ*bcfrq1+bcfrq1*

Table 8. Oligonucleotides employed for the generation of OE::*bcfrq1* strain

Amplification target	Primers 5'-3'	Primer name	Strain
bcku70 upstream non-coding region	GCGGATAACAATTTCACACAGGAAACAGC AGCGGAGATATATTATTATC (FW)	oL20	OE::*bcfrq1*
bcku70 upstream non-coding region	GACCGGGATCCACTTAACGTTACTGAAATC GCTTGTTTATCTTGTTCGAA (RC)	oL770	OE::*bcfrq1*
bcku70 downstream non-coding region	TTGGAGGAGAGCGATGAGGTGGAGCTTTGA TCGCTCGTTAAAAAGGTGAC (FW)	oL1523	OE::*bcfrq1*
bcku70 downstream non-coding region	GTAACGCCAGGGTTTTCCCAGTCACGACGA GATCTGCAACAATCTGTGA (RC)	oL27	OE::*bcfrq1*
actin promoter	AAAAATGCTCCTTCAATATCATCTTCTGTCT CTAACGCGCGTCTGATGGT (FW)	oL771	OE::*bcfrq1*
actin promoter	AACCATGGATGGATCCGATTCCGAATTCAT GGTTGATAAATTAAGACGTT (RC)	oL1522	OE::*bcfrq1*
bcfrq1 at ATG	ATGAATTCGGAATCGGATCCATCC (FW)	oL1524	OE::*bcfrq1*
bcfrq1 at STOP codon	TCAAAGCTCCACCTCATCGCT (RC)	oL1525	OE::*bcfrq1*
hph resistance cassette (from pCNS44 vector)	GATTTCAGTAACGTTAAGTGG (FW)	oL687	OE::*bcfrq1*
hph resistance cassette (from pCNS44 vector)	GACAGAAGATGATATTGAAGGAGC (RC)	oL768	OE::*bcfrq1*
Amplification of genetic constructs (from pRS426)	GGCAGTGAGCGCAACGCAAT (FW)	OL83	-
Amplification of genetic constructs (from pRS426)	ATTCAGGCTGCGCAACTGTT (RC)	OL84	-
upstream integration, at *bcku70*locus; diagnostic PCR	CTTCTTCCCGTCGCATCTT (FW)	oL867	OE::*bcfrq1*
upstream integration, at *hph* CDS; diagnostic PCR	ATGGCTGTGTAGAAGTACTC (RC)	oL32	OE::*bcfrq1*
downstream integration, at *bcfrq1*; diagnostic PCR	GCACCGACCGTATGAGAGTT (FW)	oL241	OE::*bcfrq1*
downstream integration, at *bcku70* locus; diagnostic PCR	GGAATTGGCACTGGGTTATC (RC)	oL868	OE::*bcfrq1*
bcku70 ORF, diagnostic PCR	CGTGACCATGAGTTTGATCG (FW)	oL871	-
bcku70 ORF, diagnostic PCR	TTGGGTAGTTCCTTGGATCG (RC)	oL872	-

4. RESULTS

4.1 Characterization of a putative light-sensing component in *B. cinerea* and its role in virulence

4.1.1 Light leads to phenotypical changes influencing the mode of reproduction, growth rates and pigment accumulation in *B. cinerea* B05.10

In order to confirm that B05.10 behaves like the *B. cinerea* strains used by Tan and colleagues in the 1970's to study light responses (Tan and Epton, 1973, Tan and Epton, 1974, Tan, 1974, Tan, 1975a, Tan, 1975b, Suzuki et al., 1977, Honda and Yunoki, 1978, Suzuki and Oda, 1979), cultures were exposed to different light wavelengths covering blue, green, yellow and red spectra. In agreement with the previous findings on light-responsive strains, B05.10 predominantly forms conidia under short-wavelength light (blue, green light) and sclerotia under long-wavelength light (yellow, red light) when applied in a LD photoperiod (Figure 2A). Nevertheless, exposure to blue light negatively affects conidia production while enhancing aerial (sterile) hyphae formation (Figure 2A, LD versus BL). This is in agreement with old reports describing the capacity of blue light to inhibit conidiation and to cause the "de-differentiation" of already developing conidiophore and sclerotial to sterile hyphae (Tan, 1974, Suzuki et al., 1977, Suzuki and Oda, 1979). Together with the finding that already small dosages of white light suppress sclerotia development, it can be concluded that under DD and long-wave (red) light sclerotia formation is promoted (Figure 2A, YL and RL).

In order to closely mimic environmental oscillations, in addition to constant light LL and DD conditions, 12:12 LD cycles were assayed to compare growth rates and colony morphology of B05.10 cultures. As *B. cinerea* grows very fast reaching the edge of a

Petri dish within a short period of time, PDA-containing hollow glass tube, also know as race tubes (Montenegro-Montero and Larrondo, 2013) were used since they allow monitoring growth for longer periods of time (3 to 4 weeks). As noted in Figure 2B and 2C, significant differences in the average daily growth rates were observed depending of the lightening conditions. Thus, light negatively affects growth rates yielding 61% (LL) and 82% (LD) of the recorded daily growth rate observed in DD. This result indicates that light -especially when applied in excess (LL)- represents a stress factor for *B. cinerea*. Interestingly, the growth retardation in LL was accompanied by the accumulation of a dark pigment. During incubation in LD conditions, B05.10 forms a regular "banding" pattern, hence, gray "bands" due to conidiation in the light are followed by white "bands" due to the absence of conidiation in the dark (Figure 2B). This growth pattern is also visible during LD incubation in Petri dishes where daily growth rates have been artificially decreased by the addition of SDS (Figure 2D) and does not appear during incubation in LL and DD (Figure 2B).

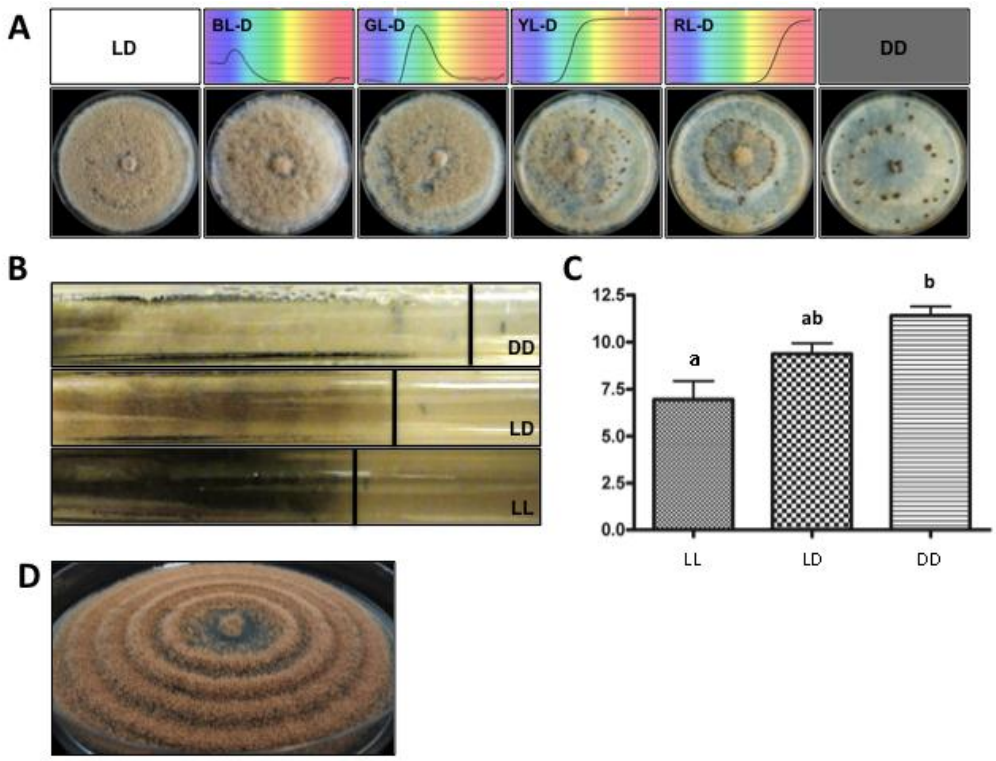

Figure 2. Light controls differentiation and growth in *B. cinerea* B05.10 strain. **(A)** Response of *B. cinerea* B05.10 to different wavelengths of light. B05.10 was incubated during 10 days on solid CM in DD and LD employing light of different wavelengths. Transmitted light wavelengths were controlled using Petri dish chambers covered with Roscolux polyester filters. Thus, illumination with white light yields blue (BL), green (GL), yellow (YL) or red (RL) light, as it can be observed from the filter transmission spectra for the used filters (#381 Baldassari Blue, #389 Chroma Green, #312 Canary and #27 Med Red) indicated on top of each plate. **(B)** Linear growth rates of *B. cinerea* B05.10 grown under different light conditions. The strain was incubated in race tubes containing PDA medium under LL, LD and DD conditions. After 7 days, race tubes were taken out and pictures were acquired from the top section of each tube. The vertical black lines indicate the growth fronts. **(C)** Quantification of linear growth rates observed in (B). The plot represents mean (± SEM) corresponding to the first 7 days of growth in race tubes. Letters indicate significant differences ($p<0.001$). **(D)** ‘‘Banding’’ phenotype of *B. cinerea* B05.10. The strain was incubated for 7 days in LD on solid CM supplemented with 0.02% SDS to reduce the daily growth rates (approx. 50% of radial growth on CM). The colony reached the edge of the Petri dish after 5 days of incubation. Each ring of conidia corresponds to one day (first ring was formed 2 days after inoculation).

4.1.2 The genome of *B. cinerea* presents light- responsive genes, whose transcript levels increase in response to light

As described previously, *B. cinerea* possesses genes encoding for putative cryptochromes -with potential for UV/ blue light sensing (*bccry1*, *bccry2*)- red light sensing phytochromes (*bcphy1*, *bcphy2*, *bcphy3*), opsins (*bop1*, *bop2*), and putative blue light receptors such as VIVID- and WC1-like proteins (*bcvvd1*, *bcwcl1*) (Schumacher and Tudzynski, 2012). Moreover, genes encoding homologues of the *N. crassa* circadian clock component FRQ (*bcfrq1*), and WC-2 (*bcwcl2*), as well as putative light-responsive TFs can be identified in its genome database. These include SUB-1 (*bcltf1*), SAH-1 (*bcsah1*), VAD-3 (*bcvad3*) and CSP-1 (*bccsp1*). Young undifferentiated mycelium was selected to monitor the expression of some putative light-responsive candidate genes, based on the knowledge gathered in *N. crassa*. This type of tissue, when grown in the absence of light, is fully developmentally competent and able to bear conidia or sclerotia depending on the following illumination event. Thus, strain B05.10 was cultivated for 2 days in DD on solid medium (PDA) covered with a cellophane overlay (see methods). Then, DD-grown cultures were further kept in the dark or exposed to white light pulses for periods of 5, 15, 30, 60 or 180 min. RNA was subjected to RT-qPCR, evaluating the transcript levels of *bcwcl1*, *bcwcl2*, *bcfrq1*, *bcltf1* and *bcvvd1* (Figure 3). Short light pulses (5 min) were sufficient to induce the expression of *bcfrq1* (5-fold), *bcvvd1* (15-fold) and *bcltf1* (5-fold), though transcript abundance of the latter gene further increased by prolonged exposure to light (approx. 15-fold). Expression of *bcwcl1* and *bcwcl2* was not significantly affected by short-term light treatments, but a two-fold increment of transcript levels was observed for *bcwcl1* during incubation in LL ($P<0.05$, T-test).

Likewise, transcript levels of the other genes in analysis were elevated in LL compared to DD. As a negative control, we chose the homologue of *acon-3*/*medA*, a transcriptional regulator that is not light induced and that controls conidiation in *N. crassa* (Chung et al., 2011). As its homologue in the latter organism, the gene *bcmedA* (BC1G_03545) was not expressed in a light-dependent fashion (Figure 3). Moreover, additional RT-qPCR experiments (see below) showed a light-dependent increase in the mRNA levels of additional genes encoding for putative photoreceptors (*bop1*, *bccry1*) and TFs (*bccsp1*, *bcsah1*). In aggregate, these findings demonstrate that there is an increase in the mRNA levels of different genes in response to light, like in *N. crassa.*

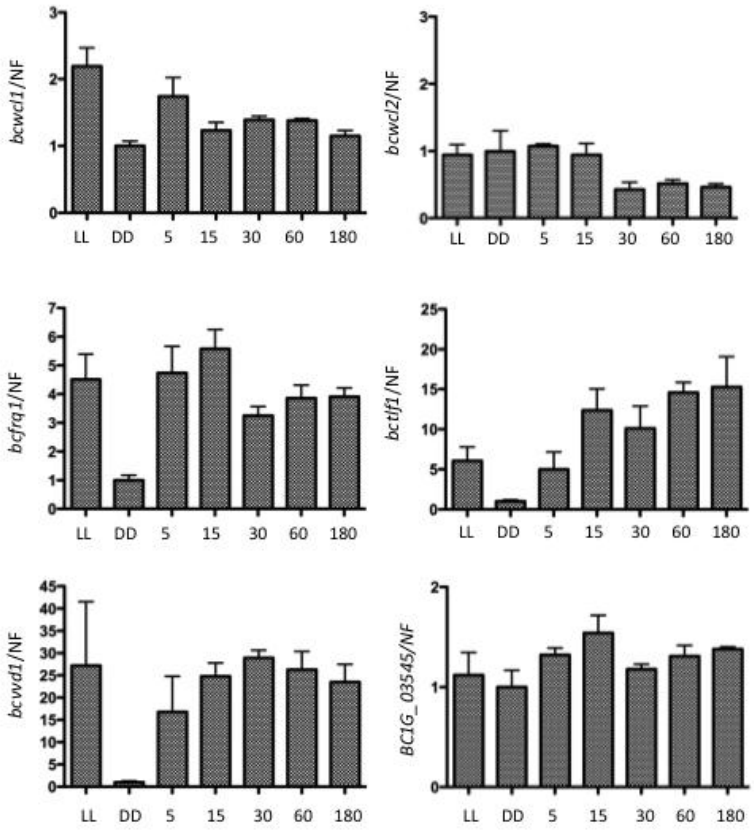

Figure 3. White light leads to a fast increase in transcript levels of key selected genes in *B. cinerea*. Transcript levels, for selected genes, were analyzed by RT-qPCR as described in methods. Values are referred to the DD culture (control = 1). Bars represent the mean ± SEM. A normalization factor (NF) was calculated for gene expression normalization (see methods). Values were calculated from 2 biological independent experiments (2 technical replicates each). Primer pairs employed for RT-qPCR amplification are indicated in Table 3. Bc1G_03545 encodes the homologue of ACON-3, a transcriptional regulator that controls conidiation in *N. crassa.*

4.1.3 The BcWCL1 and BcWCL2 proteins in *B. cinerea*

Since the putative TFs associated with light-responsiveness exhibit significant conservation among filamentous fungi, we focused our study in the White Collar Complex (WCC), specifically in the putative blue light photoreceptor/TF BcWCL1. It is important to note that the WC-1 and WC-2 proteins in *B. cinerea* were named as "like" proteins (BcWC**L**1 and BcWC**L**2, respectively), since it has not been demonstrated that they are *per se* TFs and since we do not know if BcWCL1 is a blue light photoreceptor (Schumacher, 2012). Nonetheless, bimolecular fluorescence complementation (BIFC) assays demonstrated that BcWCL1 and BcWCL2 interact in the nuclei of vegetative hyphae of *B. cinerea* confirming the existence of a BcWCL1/ BcWCL2 complex (WCC) in this organism, like in *N. crassa* (Schumacher, 2012). Moreover, both proteins present the classical domains described for WC-1 and WC-2 orthologous in other filamentous fungi (see below).

The open reading frame (ORF) of *bcwcl1* (*white collar 1*-like) comprises 3,765 bp, is interrupted by a single intron of 351 bp located towards the 3'-end of the gene and encodes a protein of 1,137 aa. Like its counterparts in other fungi, BcWCL1 contains a LOV (light-oxygen-voltage) domain, two PAS domains, a putative nuclear localization signal (NLS, ^{922}RKKRKRRK^{929}) and a GATA-type zinc-finger DNA-binding domain at the C terminus (Figure 4). BlastP analyses revealed overall amino acid identities of BcWCL1 to proteins of *S. sclerotiorum* (SWC1; 1,146 aa), *N. crassa* (WC-1; 1,167 aa) and *A. nidulans* (LreA; 837 aa) of 75, 46 and 41%, respectively (Figure 4).

The 509-aa long BcWCL2 is encoded by an ORF of 1,723 bp with two introns (128 and 65 bp) and contains a single PAS domain, a putative NLS (^{422}KKKK^{445}) and a

GATA-type DNA binding domain. BcWCL2 shares higher and lower degrees of similarity with the homologous proteins from *N. crassa* (53% aa identity with WC-2) and *A. nidulans* (35% aa identity with LreB), respectively (Figure 4).

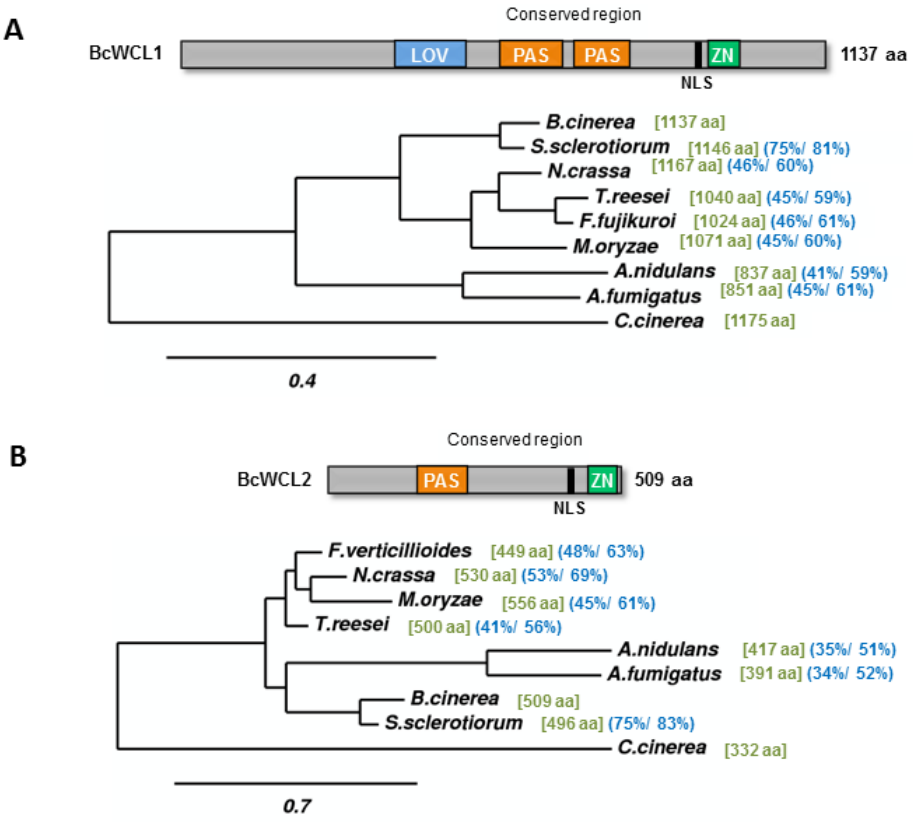
A
Conserved region
BcWCL1
LOV
PAS
PAS
ZN
1137 aa
NLS
B.cinerea [1137 aa]
S.sclerotiorum [1146 aa] (75%/ 81%)
N.crassa [1167 aa] (46%/ 60%)
T.reesei [1040 aa] (45%/ 59%)
F.fujikuroi [1024 aa] (46%/ 61%)
M.oryzae [1071 aa] (45%/ 60%)
A.nidulans [837 aa] (41%/ 59%)
A.fumigatus [851 aa] (45%/ 61%)
C.cinerea [1175 aa]
0.4
B
Conserved region
BcWCL2
PAS
ZN
509 aa
NLS
F.verticillioides [449 aa] (48%/ 63%)
N.crassa [530 aa] (53%/ 69%)
M.oryzae [556 aa] (45%/ 61%)
T.reesei [500 aa] (41%/ 56%)
A.nidulans [417 aa] (35%/ 51%)
A.fumigatus [391 aa] (34%/ 52%)
B.cinerea [509 aa]
S.sclerotiorum [496 aa] (75%/ 83%)
C.cinerea [332 aa]
0.7

Figure 4. Phylogenetic trees of *white collar like* (BcWCL1 and BcWCL2) transcription factors identified in the *B. cinerea* B05.10 genome database. (A) White Collar 1 phylogenetic reconstruction. Schematic representation (top) of the BcWCL1 protein from *B. cinerea*. Protein domains and the nuclear localization signal (NLS) were predicted by a Pfam (http://pfam.sanger.ac.uk) and WoLF PSORT search (http://wolfpsort.org), respectively. LOV: light-oxygen-voltage domain; PAS: PER-ARNT-SIM domain; ZN: GATA-type zinc finger DNA-binding domain. Sequence alignments and tree constructions (bottom) were performed using the "One Click" method and standard parameters at Phylogeny.fr (http://www.phylogeny.fr). The White Collar *1* homologue from the basidiomycete *Coprinopsis cinerea* was employed as outgroup. Each protein size is indicated next to the tree in square brackets. After BlastP at NCBI (http://www.ncbi.nlm.nih.gov) using the *B. cinerea* BcWCL1 sequence, the percent amino acid sequence identity and positive substitutions were recorded (indicated in round brackets next to the tree, respectively). Protein accession numbers: *B. cinerea* BcWCL1 (BC1G_13505), *S. sclerotiorum* (SS1G_11953, SS1G_11954, revised annotation), *N. crassa* WC-1 (NCU02356.7), *Trichoderma reesei* (AAV80185.1), *Fusarium fujikuroi* WcoA (CAO85915.1), *Magnaporthe oryzae* MgWC1 (MGG_03538.5), *A. nidulans* LreA (CBF82714.1), *A. fumigatus* LreA (EAL92988.1) and *C. cinerea* DST1 (BAD99145.1). **(B)** White Collar *2* phylogenetic reconstruction. Schematic representation (top) of the BcWCL2 protein from *B. cinerea*. Protein accession numbers (included in the tree; bottom) include: *B. cinerea* BcWCL2 (BC1G_01840), *S. sclerotiorum* (SS1G_12238), *N. crassa* WC-2 (NCU00902.7), *T. reesei* (AAV80186.1), *Fusarium verticillioides* (ADG85115.1), *M. oryzae* (MGG_04521), *A. nidulans* LreB (AAP47576.1), *A. fumigatus* LreB (XP_751563.1) and *C. cinerea* (BAK82128.1).

4.1.4 BcWCL1 mediates some- but no all- light responses in *B. cinerea*

To elucidate the function of BcWCL1 in *B. cinerea*, we generated three independent deletion mutants for *bcwcl1* (Δ*bcwcl1*-1 to -3) in the B05.10 genomic background by homologous recombination (for details, see Material and Methods, (Figure 5). As the three analyzed mutants exhibited the same phenotype, usually the results for one arbitrarily chosen deletion mutant are presented. At a first glance, when wild-type and Δ*bcwcl1* strains were cultivated in Petri dishes, both strains exhibited comparable growth rates in all tested light conditions (data not shown). However, long-term growth assays performed in race tubes demonstrated that Δ*bcwcl1* mutants exhibited wild-type-like growth rates in DD, but reduced daily growth rates under LL conditions when compared to the wild-type strain. As shown in Figure 6A, a significantly reduced accumulative growth after 14 days of incubation under LL was observed for Δ*bcwcl1* (75% of the growth determined for the wild-type in the same conditions (right panel)). Importantly, Δ*bcwcl1* as well as the wild-type displayed a sustained and marked reduction in their accumulative growth rates in LL (20% and 27% of the growth observed in DD, respectively) (right panel). However, light applied as LD decreased growth rates of both strains in a similar manner (65 and 63% of the growth observed in DD, respectively) (right panel). It is worth to mention that while the DD data shown in Figure 2 was acquired daily using low-intensity red-safety lights, the DD cultures from Figure 6 were never subjected to any light source until the end of the experiment, when the growth front was measured. Notably, the characteristic regular ‘‘banding’’ pattern shown in Figure 2 for B05.10 wild-type strain under LD conditions, was still observed in the Δ*bcwcl1* deletion mutant (and it is even more pronounced),

suggesting that other photoreceptors could be involved in the light phenotypical responses to regular photoperiod. Bottom or lateral views of the race tubes allow an evident visualization of this phenotype (Figure 6B and C).

To establish a connection between the increase in transcript levels of different genes in response to light and BcWCL1 function, wild-type B05.10 and the Δ*bcwcl1* mutant were incubated in the dark and then exposed to light for 30 and 60 min (Figure 7). Expression levels of all chosen genes encoding predicted photoreceptors (*bcvvd1*, *bccry1, bop1*) were strongly induced by light in the wild-type but not in the Δ*bcwcl1* mutant (no significant differences were observed). On the other hand, those genes encoding for putative TFs showed contrasting results. While *bccsp1* was significantly induced upon light stimulation in the wild-type but not in the Δ*bcwcl1* mutant, both *bcltf1* and *bcsah1* showed a clear light-dependent induction in both strains (i.e. 24- and 10-fold for *bcltf1* in the wild-type and Δ*bcwcl1*, respectively). On the other hand, putative light-responsive TFs encoding genes *bcadv1* and *bcvad3* were not light-induced. Other known *N. crassa* WCC targets such as *bcfrq1*, *bcfer1* (the latter gene encoding for a putative ferroquelatase) and *bcvvd1* were induced by light only in the wild-type strain, but *bcccg1* (which encodes for the ortholog of the *clock-control gene 1* of *N. crassa*) showed light-inducibility in both wild-type and Δ*bcwcl1* strains. These results suggest that in addition to BcWCL1, other photoreceptors could be participating in controlling the light-dependent expression of some light inducible genes, contrary to what has been shown in *N. crassa.*

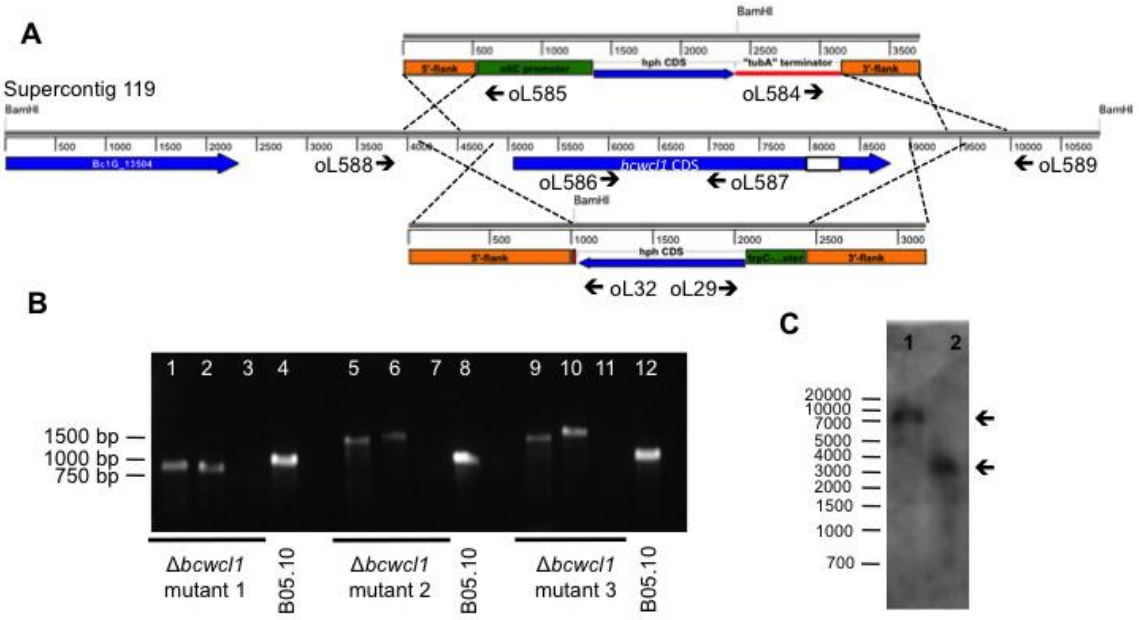

D

Amplicon	Primer pair	Sequence (5´-3´)	Clon	Lane in (B)	Expected size (bp)
upstream integration	oL588 oL585	GAGAGACAGGATGGTACAAATGAG GGTACTGCCCCACTTAGTGGCAGCTCGCG	1	1	846
downstream integration	oL589 oL584	ACACTTGTGCTTGTGCTTGC GGTCCTCGGAGTGCAGATGGG	1	2	802
upstream integration	oL588 oL32	GAGAGACAGGATGGTACAAATGAG ATGGCTGTGTAGAAGTACTC	2,3	5,9	1411
downstream integration	oL589 oL29	ACACTTGTGCTTGTGCTTGC TCGCCCTCCGAGAGCTGCAT	2,3	6,10	1588
bcwcl1	oL586 oL587	GTATCAACCCCCACGGCTCTCA CGGCGAATGCGGAATACCA	--	3-4, 7-8 11-12	950

Figure 5. Generation of Δ*bcwcl1* strains. (A) Replacement strategy scheme showing the expected *in-locus* insertion of the replacement constructs, as well as each replacement cassette employed in this work. Schematic representation of a 10.5 kb genomic region (between *Bam*HI restriction sites) of the *bcwcl1* locus, located in Supercontig 119 of the B05.10 strain genome database. The *bcwcl1* gene and its transcriptional orientation (3,765bp; Bc1G_13505, genomic coordinates 27645-31409) are represented as a blue arrow. A single intron, located towards the 3'-end of the gene, is indicated in a white box. Gene model Bc1G_13504 is shown as a reference. The gene replacements cassettes employed to obtain Δ*bcwcl1* (mutant 1) and Δ*bcwcl1* (mutants 2 and 3) strains are shown above (replacement cassette A) and below (replacement cassette B) the *bcwcl1* gene model. In both cases, the position of the genomic regions employed for the homologous recombination (orange boxes) and KO generation are shown (to scale) next to *bcwcl1*. Gene model Bc1G_13506 (located downstream the 3'-flank) has been omitted from the scheme. Black arrows show primers used for diagnostic PCRs, indicating their respective position and orientation. **(B)** Diagnostic PCRs showing *in-locus* integration. Homologous integration at 5'- (lanes 1, 5 and 9) and 3'- region (lanes 2, 6 and 10) are shown for each analyzed mutant. No wild-type locus was observed for each Δ*bcwcl1* mutant after single-spore isolation (see methods) (lanes 3, 7 and 11) in comparison with the B05.10 wild-type strain (lanes 4, 8 and 12). **(C)** Southern blot hybridization. Ten µg of genomic DNA was digested with *Bam*HI, and hybridized with the full-length *hph* CDS used as probe (expected sizes: mutant 1, 6321bp; mutants 2 and 3, 3344bp). To simplify the figure, only the hybridizations of mutants 1 and 2 are shown (lanes 1 and 2, respectively). **(D)** Primer pairs used in diagnostic PCRs. Their respective position and orientation is depicted in (A) (with respect to the gene transcriptional orientation) and Table 4.

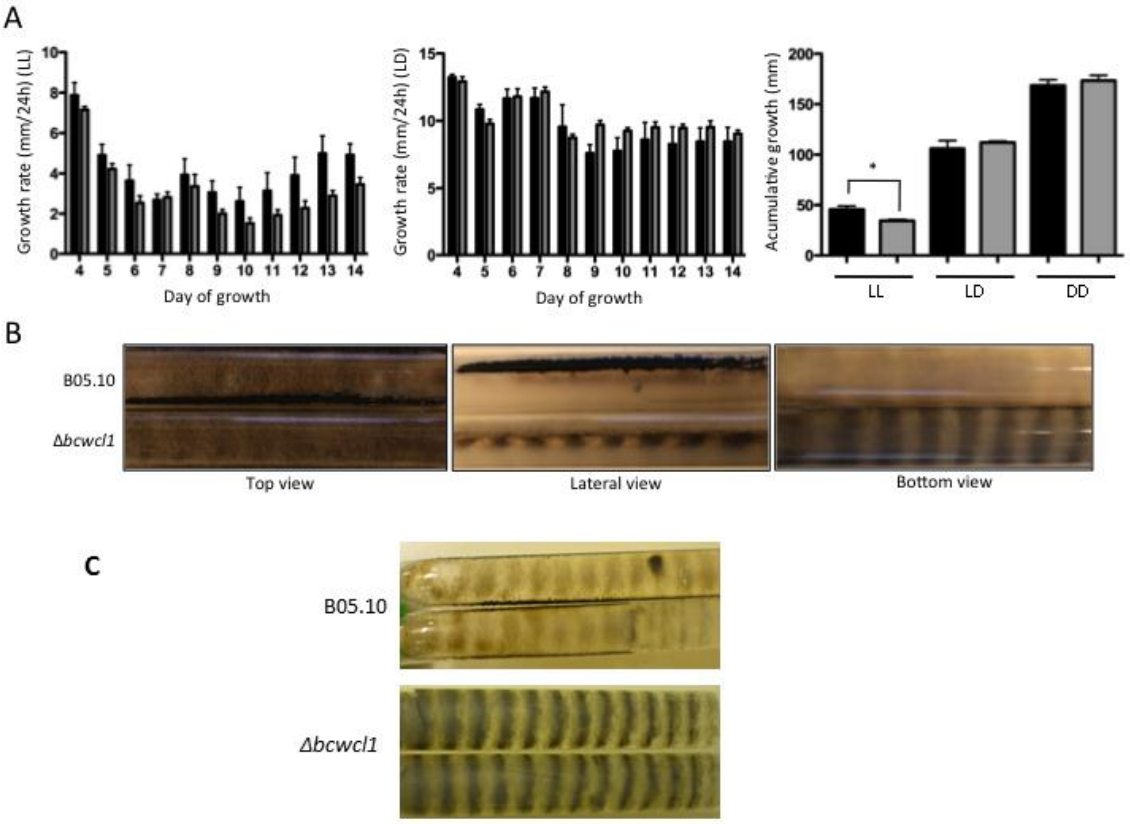

Figure 6. Light negatively affects *B. cinerea* linear growth rates. **(A)** Linear growth rates of wild-type (black bars) and Δ*bcwcl1* (grey bars) strains were measured in race tubes assays. For LL and LD conditions, growth rates were determined daily (left and central panel). The accumulative growth (right panel) was determined for LL, LD and DD conditions after 14 days of incubation. Each bar represents the mean ± SEM of three independent Δ*bcwcl1* mutants (four technical replicates each). Statistical differences ($p < 0.05$) are indicated with asterisks. **(B)** Phenotypic characterization of the Δ*bcwcl1* mutant (clone 1) grown for 7 days in race tubes under LD conditions. **(C)** Enlarged bottom view of B05.10 and Δ*bcwcl1* strains grown under LD conditions.

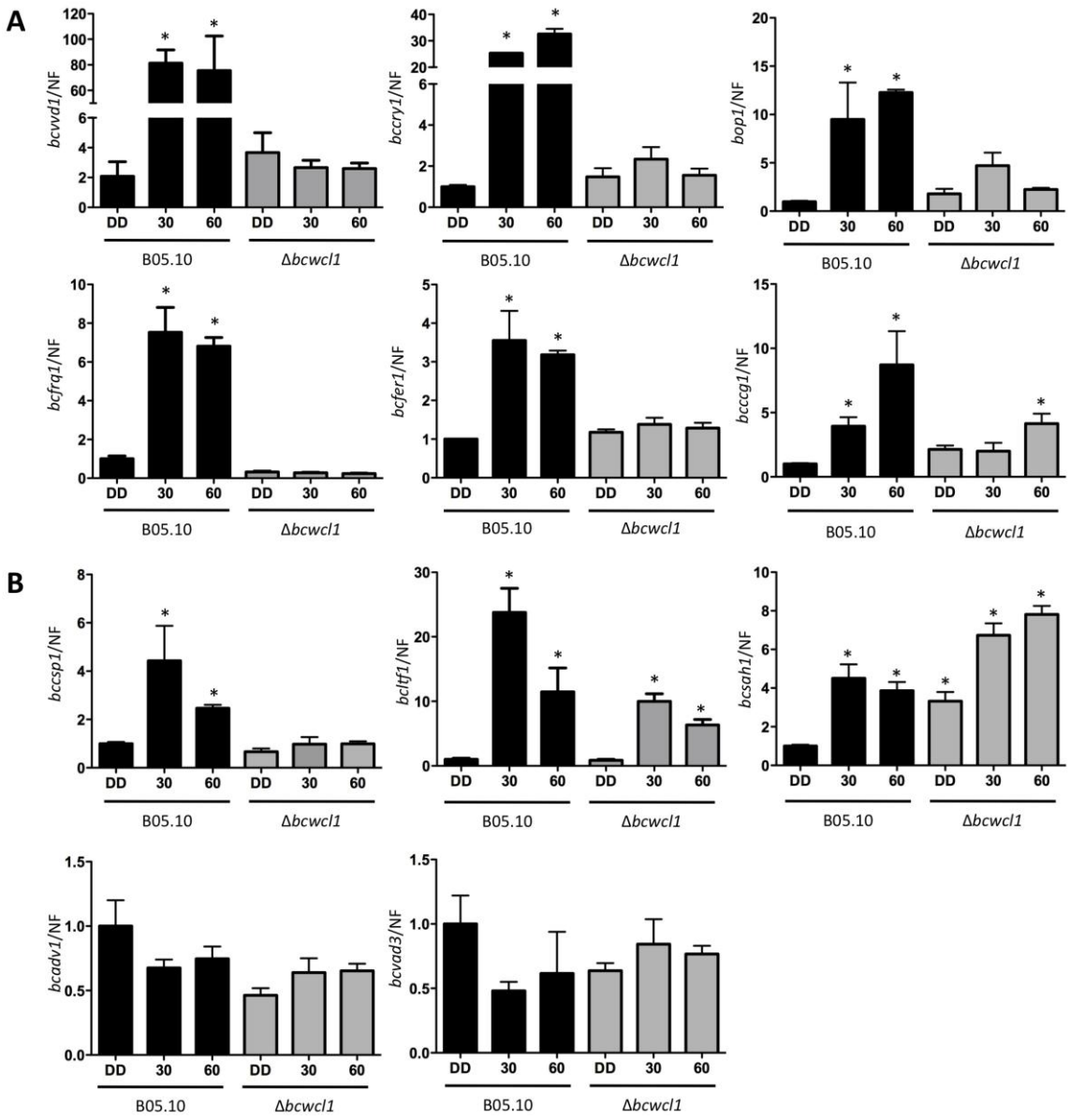

Figure 7. BcWCL1 mediates some – but not all – light dependent changes in gene expression in *B. cinerea*. Several light-responsive genes non-coding (A) and coding for TFs (B) increase their transcript levels in response to (white) light pulses (30 and 60 min) in wild-type B05.10 and the Δ*bcwcl1* mutant. Values are referred to B05.10 grown in DD (control). Bars represent mean ± SEM. A normalization factor (NF) was calculated to normalize gene expression data (see methods). Values were calculated from three biological replicates with two technical replicates.

4.1.5 The *bcwcl1* gene complements the *bcwcl1* deletion mutant in *B. cinerea*

Three independent deletion mutants for *bcwcl1* (Δ*bcwcl1*-1 to 3) having single integration of the replacement cassettes (Figure 5, Table 4) were generated and confirmed to exhibit the same phenotype. Strain Δ*bcwcl1*-1 was arbitrary chosen as recipient for genetic complementation to fully establish that the deletion of *bcwcl1* can explain the observed light-dependent phenotypes. As shown in Figure 8A, *bcwcl1* was targeted to the *bcniaD* locus by homologous recombination yielding Δ*bcwcl1+bcwcl1*. As expected, in the absence of light, strain B05.10 formed sclerotia in contrast to Δ*bcwcl1* which persisted in conidiating, while the expression of *bcwcl1* in the Δ*bcwcl1* background restored sclerotia formation (Figure 8B). In addition, light-inducibility in the complemented strain was analyzed by RT-qPCR. As observed in Figure 8C, light induction of both *bcfrq1* and *bcvvd1* were recovered in Δ*bcwcl1+bcwcl1* to similar levels when compared to strain B05.10. In aggregate, these results confirm that the hyperconidiation phenotype accompanied by the loss of sclerotial development and the absence of an increase in gene expression in response to light observed for the Δ*bcwcl1* mutant are due to the deletion of *bcwcl1*.

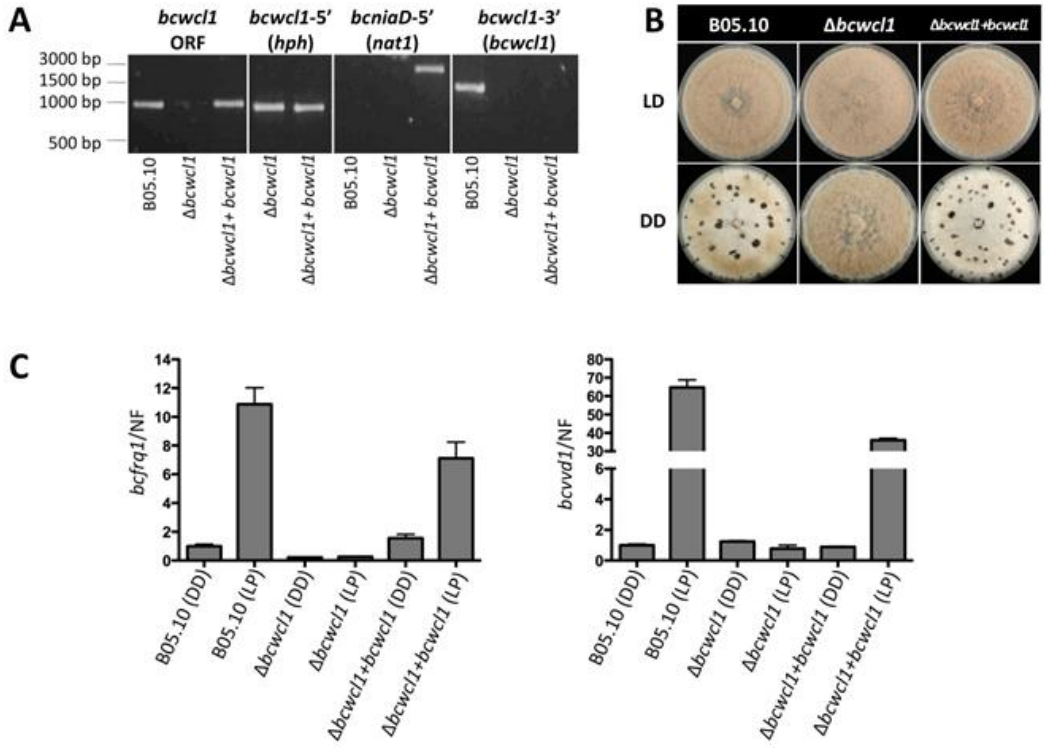

Figure 8. Complementation of the *bcwcl1* deletion mutant. (A) Genotypification of the Δ*bcwcl1* complemented strain (Δ*bcwcl1*+*bcwcl1*) showing the amplification of *bcwcl1* (*bcwcl1*-ORF; oL586+ oL587) inserted at the *bcniaD* locus (*bcniaD*-5′(*nat1*); oL1226+ oL1716) and not at the *bcwcl1* locus (*bcwcl1*-3′; oL1226+ oL589), which contains the *hph* cassette used for *bcwcl1* deletion (*bcwcl1*-5′ (*hph*); oL588+ oL585). Primer pairs details are indicated in Table 4. **(B)** Phenotypic characterization of a representative Δ*bcwcl1*+*bcwcl1* complemented strain demonstrated the restoration of sclerotia formation under DD culture conditions. (**C**) RT-qPCR of the Δ*bcwcl1*+*bcwcl1* mutant showing restoration of light-inducibility of gene expression (DD: constant darkness; LP: 60 min light pulse). Values are referred to the B05.10 strain grown under DD conditions (control = 1). Bars represent mean values ± SEM. *bcfrq1* and *bcvvd1* were chosen since no light-induction is observed in the Δ*bcwcl1* strain.

4.1.6 The BcWCL1 is involved in oxidative stress response

Light -especially when applied in excess (LL)- exerts detrimental effects on growth rates of *B. cinerea* wild-type and Δ*bcwcl1* strains (Figure 2 and 6), which could be in part due to perturbation in the homeostasis of cellular ROS (Reactive Oxygen Species) levels. To evaluate a possible connection between light sensitivity and ROS, we exposed both strains to hydrogen peroxide (H_2O_2) under different illumination conditions (Figure 9A). The wild-type strain fails in coping with H_2O_2 in LL, LD and DD, if we compare with the growth rate in the absence of the stressor agent. On the other hand, the Δ*bcwcl1* mutant displayed an increased sensitivity when H_2O_2 is present, especially when light was applied in excess (LL). Given that exogenously applied H_2O_2 enhances light's negative effect on growth in Δ*bcwcl1* strains, we wanted to know whether the toxic effect of light itself can be ameliorated by increasing antioxidant potential, restoring thus, cellular ROS homeostasis. For this, we monitored radial growth rates of wild-type and Δ*bcwcl1* strains cultivated on minimal medium (MM) with and without an antioxidant (5 g/l ascorbic acid) (Figure 9B). On minimal medium, light sensitivity (measured as colony diameter) of Δ*bcwcl1* was already detectable in LD and became more pronounced in LL (63% and 39% of the growth observed in DD, respectively), whereas the wild-type exhibited comparable growth rates in DD and LD and slightly reduced growth rates in LL (75% of the growth observed in DD). Notably, the addition of ascorbic acid rescued the light dependent reduction in growth observed for Δ*bcwcl1* to wild-type levels, indicating that light can generate oxidative stress and that the action of the BcWCL1 is needed to cope with this strong environmental variable.

It has been suggested that in *N. crassa* the WCC may sense not only light but also the redox potential of the cell through one of the PAS domains presented in WC-1 and/or WC-2 (Crosthwaite et al., 1997, Linden et al., 1997, Yoshida and Hasunuma, 2004, Vitalini et al., 2006) and that higher ROS concentration enhances conidiation banding (Belden et al., 2007, Yoshida et al., 2011). In this way, we wanted to know if the stable banding pattern phenotype seen in the Δ*bcwcl1* strain (Figure 6B and C) is due to the presence of ROS. Race tubes were filled with PDA, PDA plus the antioxidant N-acetyl-L-cysteine and PDA plus N-acetyl-glycine, molecule that has no effect on ROS production. As depicted in Figure 10, Δ*bcwcl1* loses the enhanced banding phenotype when grown under a LD cycle and in the presence of the N-acetyl-L-cysteine antioxidant, if we compared with the cyclic banding observed when race tube are only fill with PDA or N-acetyl-glycine, reinforcing the idea that BcWCL1 is indispensable to cope with ROS.

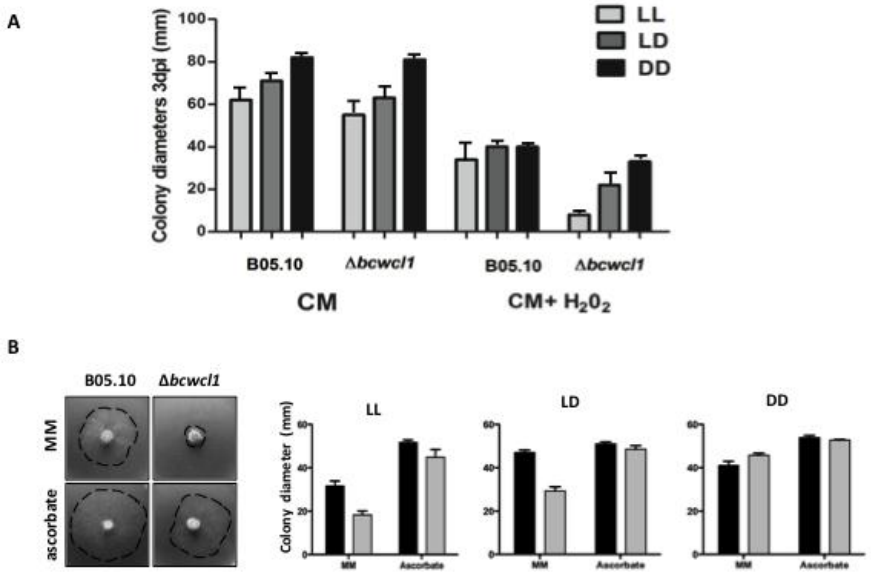

Figure 9. Deletion of *bcwcl1* affects the response to oxidative stress. (A) Strains B05.10 and Δ*bcwcl1* were grown for 3 days under DD, LD and LL (black, grey and light grey bars, respectively) on solid CM in the absence of stressors agents (control) and in the presence of 7.5 mM H_2O_2. Mean values ± SEM were calculated from five colonies per strain grown in each condition. **(B)** Ascorbate increases growth rates of the wild-type B05.10 (black bars) and Δ*bcwcl1* (grey bars) strains in the presence of light (LD and LL). Both strains were incubated for 3 days on MM (minimal medium) supplemented with 5 g/l ascorbate. Mean values ± SEM were calculated from five colonies per strain in each condition.

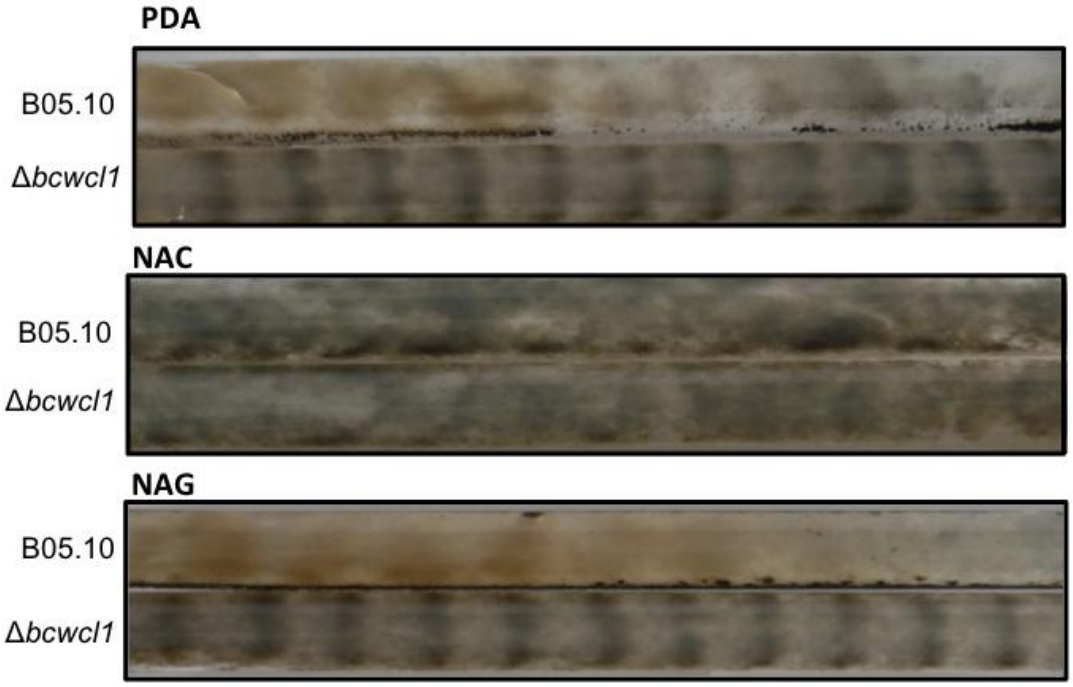

Figure 10. The Δ*bcwcl1* knockout strain loses the banding pattern phenotype when is grown in presence of an antioxidant. The Δ*bcwcl1* strain was grown in the presence of 5 mM N-acetyl-L-cysteine (antioxidant), 5 Mm N-acetyl-glycine (no effect on ROS production) and PDA (control) for 14 days under LD conditions. The pictures are representative of three independent assays.

4.1.7 BcWCL1 is required for full virulence in the presence of light

To gain insight into the relevance of light and BcWCL1 in the *B. cinerea*-plant interaction, we assayed virulence of the Δ*bcwcl1* deletion mutant on French bean (*P. vulgaris*) and *A. thaliana* Col-0 plants representing highly and moderately susceptible hosts of *B. cinerea*, respectively. Reduced lesion sizes were observed on *P. vulgaris* plants that were incubated for 3 days in LD but not for those incubated in DD (Figure 11A). However, from 4 dpi and over, no further differences between the wild-type and the Δ*bcwcl1* strain were detected as both strains finally proceeded to colonize the plant tissue, ending in soft rot and conidiation (Figure 11B).

The impact of light on the plant-pathogen interaction was more precisely analyzed using *A. thaliana* as a host. First, plants were normally grown using 12:12 h LD photoperiod, and thereafter incubated in LL, LD and DD. Remarkably, we observed that light conditions already severely affected the infection of plants by the wild-type strain. Thus, and in comparison with the DD culture condition, 65% (LL) and 19% (LD) reductions in the lesion areas on *A. thaliana* leaves were observed for the wild-type strain (Figure 12A and C). Importantly, further reductions of lesion areas were observed for the Δ*bcwcl1* mutant in a light-dependent manner (in comparison with the DD culture condition, 85% (LL) and 53% (LD) reductions). Reduced proliferation of fungal material on the host was furthermore confirmed by trypan blue staining (Figure 12B). Since plant responses to abiotic and biotic stress conditions are characterized by an oxidative burst, and that Δ*bcwcl1* mutants are hypersensitive to H_2O_2 under LL conditions, we evaluated the accumulation of H_2O_2 in infected plant tissues by using 3,3'- diaminobenzidine (DAB). However, no differences between the B05.10 wild-type

strain and the deletion mutant in any light condition were observed, suggesting that the Δ*bcwcl1* mutant has problems to cope with ROS and that BcWCL1 is necessary to achieve and efficient infection process when light is present (Figure 13).

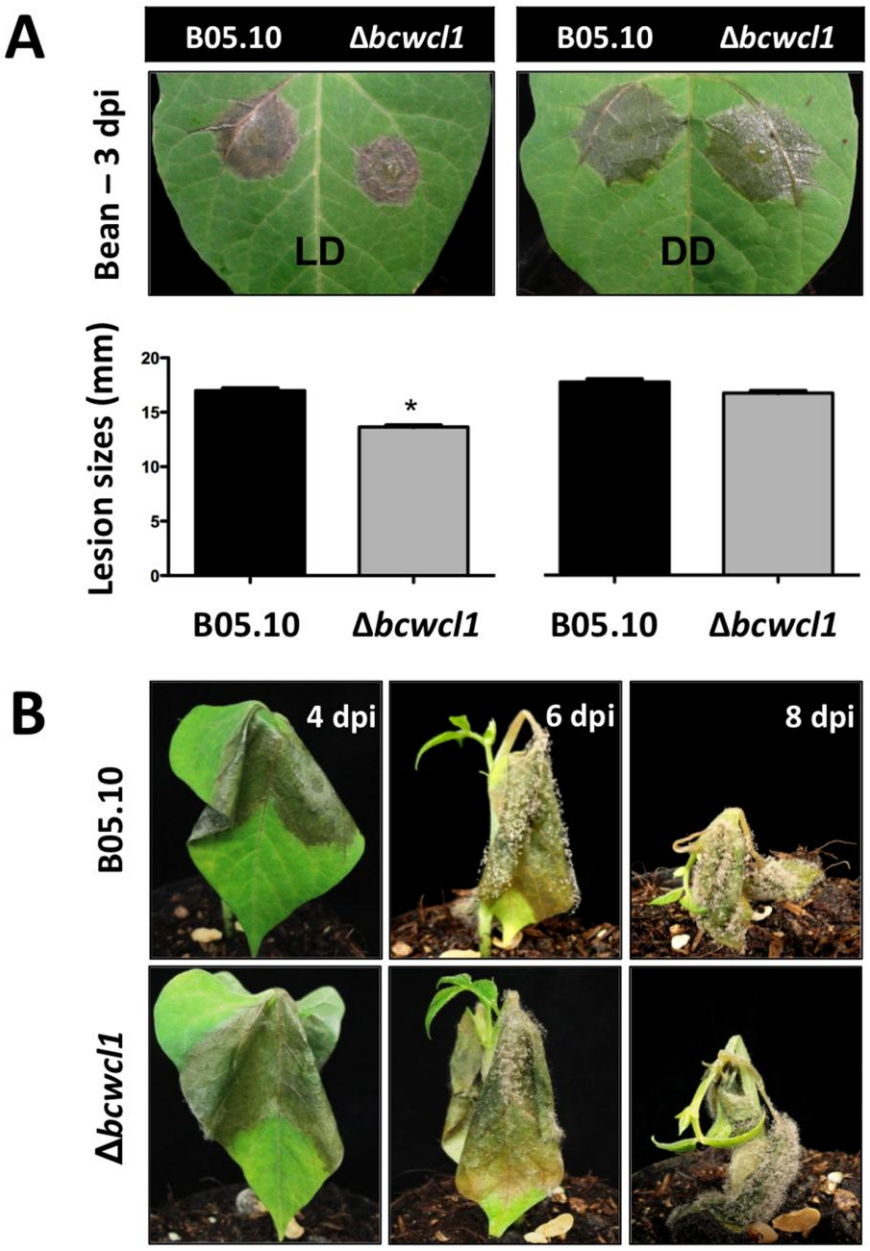

Figure 11. Virulence of Δ*bcwcl1* mutants is impaired in a light-dependent fashion. **(A)** Lesion spreading of Δ*bcwcl1* mutants is slightly affected in LD but not in DD. Primary leaves of *P. vulgaris* plants were inoculated with conidial suspensions and incubated for 3 days in humid conditions under LD or DD conditions. Mean values ± SEM of lesion diameters were calculated from 22 lesions per strain and light condition, with two measurements per lesion. Statistical differences ($p<0.05$) are indicated with asterisks. **(B)** Soft rot formation and conidiation are not affected by the deletion of *bcwcl1*. No significant differences were observed when inoculated plants were incubated in LD or DD after 4 dpi and over. Plants incubated in LD are shown.

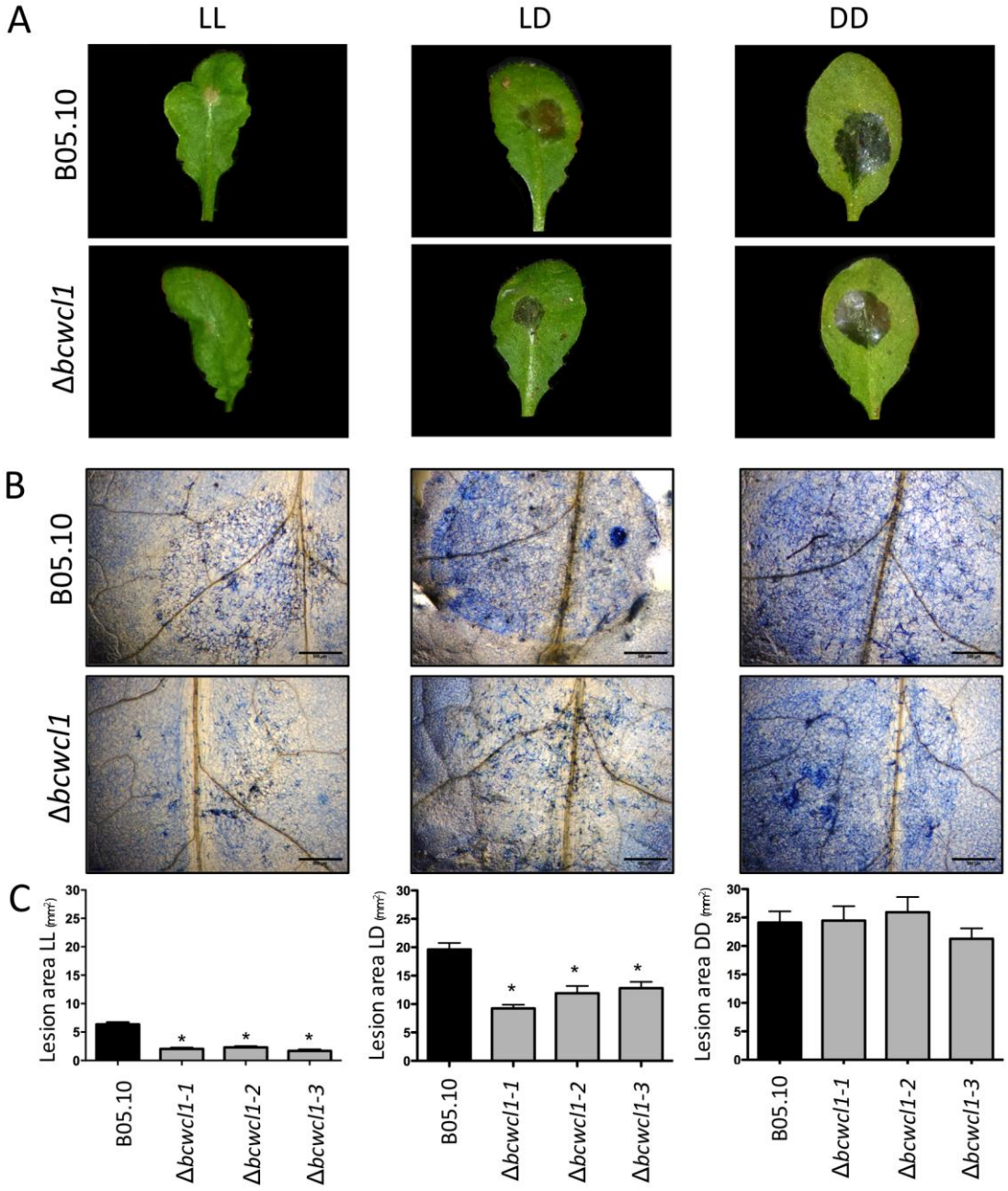
A
LL
LD
DD
B05.10
Δbcwcl1
B
B05.10
Δbcwcl1
C
Lesion area LL (mm²)
Lesion area LD (mm²)
Lesion area DD (mm²)
0
5
10
15
20
25
30
*
B05.10
Δbcwcl1-1
Δbcwcl1-2
Δbcwcl1-3

Figure 12. BcWCL1 is required to achieve full virulence in the presence of light. **(A)** Conidia ($2x10^5$ /ml, 7µl) from the B05.10 wild-type strain (top) and a representative Δ*bcwcl1* mutant (bottom) were inoculated at dawn on approximately 1 month-old *A. thaliana* (Col-0) plants, grown at 20 °C under LD (12:12 h) conditions. After spore inoculation, plants were grown for 3 days under LL, LD or DD conditions. Pictures were acquired after 3 dpi. Representative leaves for each culture condition are shown. **(B)** Trypan blue staining showing fungal growth in plants at 3 dpi. Fungal growth is visible as thread-like stained structures (black scale bars represent 500 µm). **(C)** Quantification of the lesion area obtained from at least four independent virulence assays for each Δ*bcwcl1* mutant. Bars represent the mean ± SEM. Significant differences in comparison with the lesion observed for the B05.10 wild-type strain are indicated with asterisks ($p<0.05$).

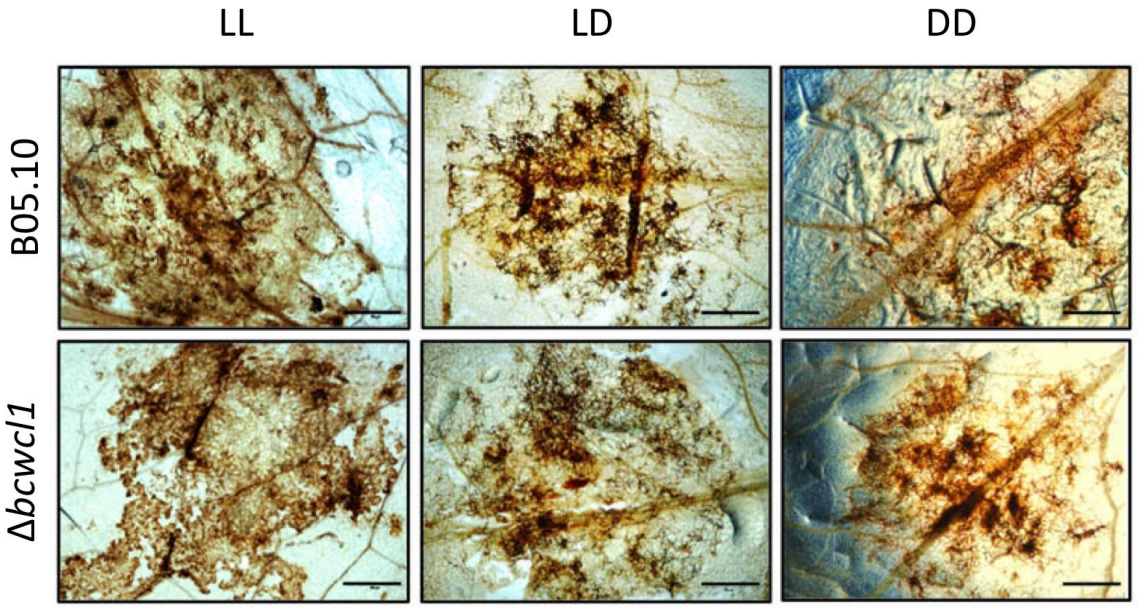

Figure 13. No differences were observed for H_2O_2 accumulation in B05.10 and Δ*bcwcl1* infected plant tissues. *A. thaliana* Col-0 plants were inoculated with conidial suspensions of the indicated strains and incubated in LL, LD or DD conditions. After 3 days, leaves were detached and subjected to 3,3′-diaminobenzidine (DAB) staining. A brown precipitate, indicative for H_2O_2 accumulation, was observed in infected but not in non-inoculated plant tissues (data not shown). Scale bars represent 500 µm.

4.2 Characterization of a circadian clock in *B. cinerea* and its role in virulence

4.2.1 The *B. cinerea* genome encodes for proteins that could be involved in a circadian clock, including the core-oscillator component *frequency*

As previously described, the genes encoding for the putative TF/blue-light photoreceptor White Collar-1 (BcWCL1), the TF White Collar-2 (BcWCL2) and Frequency (BcFRQ1) were identified in the *B. cinerea* genome database (Canessa et al., 2013), which are known as key central components of the circadian clock in *N. crassa* (Montenegro-Montero and Larrondo, 2013). BcWCL1 and BcWCL2 interact with each other forming the WCC (Schumacher, 2012) and *bcfrq1* mRNA levels respond to light in a WCC-dependent manner (Canessa et al., 2013). Moreover, a putative gene model encoding for FRH (termed BcFRH1; BC1G_14187), a FRQ-interacting RNA helicase that participates in circadian regulation in *N. crassa* (Cheng et al., 2005), can be also identified in the Botrytis genome. In this context, we proposed to characterize a functional circadian clock in *B. cinerea*.

The *bcfrq1* ORF comprises 2,958 bp, is interrupted by an intron of 54 bp located towards the 5' end of the gene and encodes for a 967 aa protein. For comparative purposes, the diversity of FRQ-like proteins in a large group of fungal species obtained from the non-redundant NCBI protein database, including *B. cinerea* and *N. crassa*, is depicted (Figure 14A). Multiple sequence alignments showed overall aa identities of BcFRQ1 to proteins of *S. sclerotiorum* (973 aa), *S. borealis* (960 aa), *F. fujikuroi* (960 aa), *N. crassa* (989 aa), *T. reesei* (1,014 aa) and *M. oryzae* (995 aa) of 77.2, 65.4, 32.5, 31.3, 31.0 and 29.2%, respectively.

Close examination of the protein alignments allowed the identification of several domains (Figure 14B). Like its *N. crassa* ortholog, BcFRQ1 contains a coiled-coiled domain to allow the FRQ-FRQ interaction (CC; located at the N terminus), a nuclear localization signal (NLS), two FRQ-CKI interaction domains (FCD1 and 2), a FRQ-FRH interaction domain (FFD), two PEST domains (PEST-1 and PEST-2) that are important for FRQ turnover and stabilization, respectively (Baker et al., 2009) and the presence of several phosphorylation sites spread along the BcFRQ1 protein. Among these are S67, S76, T236, S510, S512 and S521, which have been shown to increase the free running period when mutated to alanine in *N. crassa* (equivalent to S72, S76, S240, S538, S540 and S548 in *N. crassa*) (Baker et al., 2009). On the other hand, residues that when mutated in *N. crassa* decrease the free running period include –in *B. cinerea*- S888, S895 and S896 (S900, T915 and T917 in *N. crassa*).

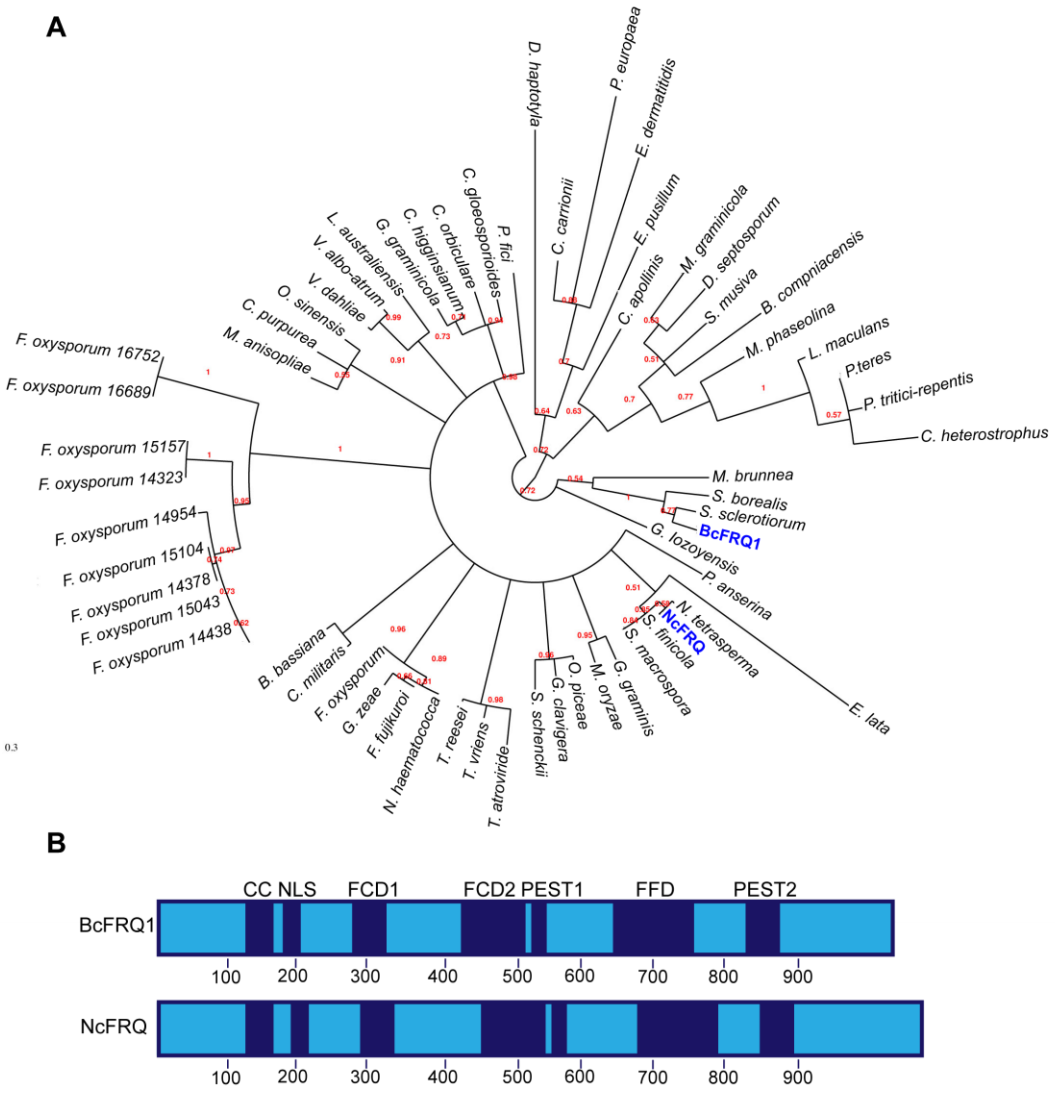
A
D. haptotyla
P. europaea
E. dermatitidis
C. carrionii
E. pusillum
C. apollinis
M. graminicola
D. septosporum
S. musiva
B. compniacensis
M. phaseolina
L. maculans
P.teres
P. tritici-repentis
C. heterostrophus
C. gloeosporioides
P. fici
C. orbiculare
C. higginsianum
G. graminicola
L. australiensis
V. albo-atrum
V. dahliae
O. sinensis
C. purpurea
M. anisopliae
F. oxysporum 16752
F. oxysporum 16689
F. oxysporum 15157
F. oxysporum 14323
F. oxysporum 14954
F. oxysporum 15104
F. oxysporum 14378
F. oxysporum 15043
F. oxysporum 14438
M. brunnea
S. borealis
S. sclerotiorum
BcFRQ1
G. lozoyensis
P. anserina
N. tetrasperma
NcFRQ
S. fimicola
S. macrospora
G. graminis
M. oryzae
O. piceae
G. clavigera
S. schenckii
T. atroviride
T. vriens
T. reesei
N. haematococca
F. fujikuroi
G. zeae
F. oxysporum
C. militaris
B. bassiana
E. lata
0.3
B
CC NLS
FCD1
FCD2 PEST1
FFD
PEST2
BcFRQ1
NcFRQ
100
200
300
400
500
600
700
800
900

Figure 14. Characterization of BcFRQ1 from *B. cinerea*. (A) Phylogenetic reconstruction of FRQ-like fungal proteins. FRQ proteins (60) from *B. cinerea* (BcFRQ1) and *N. crassa* (NcFRQ) are indicated in blue. FRQ-like proteins include (NCBI protein accession numbers within brackets): *B. cinerea* BcFRQ1 [154294335], *N. crassa* NcFRQ [P19970], *N. tetrasperma* [336467537], *S. fimicola* [6016053], *S. macrospora* [336273286], *P. anserina* [171679583], *G. zeae* [46123353], *N. haematococca* [302916523], *T. virens* [358386587], *T. reesei* [340518956], *L. australiensis* [6016052], *T. atroviride* [358394546], *F. fujikuroi* [517315082], *O. sinensis* [531860335], *G. graminicola* [310791992], *V. dahliae* [346973720], *V. albo-atrum* [302415673], *C. gloeosporioides* [530462205], *C. orbiculare* [477524733], *C. higginsianum* [380494367], *M. anisopliae* [322708167], *B. bassiana* [400601938], *C. militaris* [573976580], *P. fici* [573064331], *C. purpurea* [399171881], *G. graminis* [402080287], *M. oryzae* [440475186], *G. clavigera* [320588478], *S. schenckii* [550810796], *S. sclerotiorum* [156039415], *M. brunnea* [406861981], *E. lata* [471570736], *G. lozoyensis* [512205333], *S. borealis* [563296614], *M. phaseolina* [407924717], *C. apollinis* [494826879], *P. tritici-repentis* [189211261], *M. graminicola* [398396682], *L. maculans* [396498772], *P. teres* [330929727], *S. musiva* [453084522], *D. septosporum* [452840537], *B. compniacensis* [449299600], *O. piceae* [512186601], *C. heterostrophus* [452002440], *C. carrionii* [565935815], *P. europaea* [568120504], *E. pusillum* [539437374], *E. dermatitidis* [378731978], *D. haptotyla* [526204507] and *F. oxysporum* FOXG_16752, FOXG_16689, FOXG_15157, FOXG_15104, FOXG_15043, FOXG_14954, FOXG_14438, FOXG_14378, FOXG_14323 and FOXG_07759 (obtained from the BROAD Institute). **(B)** Schematic representation of BcFRQ1 and NcFRQ showing the position of the translational start and stop codons, domain structure and their respective positions. Previously defined functional domains (blue) include: CC, coiled-coiled domain; NLS, nuclear localization signal; FCD1 and FCD2, FRQ-CKI interacting domains; FFD, FRQ-FRH interacting domain; PEST1 and PEST2 (proline (P), glutamate (E), serine (S) and threonine (T) rich sequence) domains. Protein domains were inferred from multiple sequence alignments of the FRQ-like proteins employed in (A).

4.2.2 *B. cinerea* possesses a functional circadian clock

To assess whether the B05.10 WT strain has an active circadian clock and an associated circadian phenotype, we analyzed if the regular "conidiation banding pattern" previously described under a LD regime (Figure 2B and D) (Canessa et al., 2013), is maintained under free running conditions (FRC; constant darkness, DD). As shown in Figure 15, the B05.10 strain does not present a circadian phenotype under DD, at least under the culture conditions tested, indicating that the banding phenotype is a direct result of the LD cycle.

Since FRQ has a central role in the TTFL that give rise to the *N. crassa* circadian oscillator (Aronson et al., 1994a), we characterized *bcfrq1* mRNA expression levels under different culture conditions, looking for molecular evidence of circadian control. As shown in Figure 16A, *bcfrq1* mRNA levels oscillate under LD culture conditions, remaining high during the lights-on period in contrast to the lower levels observed during the lights-off phase. Notably, and showing a key characteristic of circadian behavior (Dunlap, 1999), *bcfrq1* transcript levels anticipate the transition from darkness to light, observed as a gradual increment in the mRNA levels (from LD=14 to LD=22) during the light-off period, in advance to the lights-on stage. In order to test whether these oscillations persist under FRC -in the absence of environmental oscillations- *bcfrq1* mRNA levels were also analyzed under DD culture conditions. As observed in Figure 16B, *bcfrq1* mRNA levels exhibit a robust oscillatory expression pattern under DD. In contrast, under LL culture conditions, highly induced and non-oscillatory expression levels of *bcfrq1* were observed (Figure 16C) as it has been described in *N. crassa* (Crosthwaite et al., 1995). Finally, employing the Δ*bcwcl1* deletion mutant

(Canessa et al., 2013), we confirmed that *bcfrq1* circadian oscillations under DD are lost in this knockout strain (Figure 16D), as it has been shown in *N. crassa* (Lee et al., 2003). Taken together, these results confirm the functional and genetic relationship between these two well characterized clock proteins encoding genes, under both entrainment (LD) as well as circadian (DD and LL) culture conditions.

In order to study circadian rhythms *in vivo*, we established a real-time luciferase reporter system in *B. cinerea*, an approach previously employed to track *in vivo* FRQ levels in Neurospora (Larrondo et al., 2012). Here, the *oluc* sequence (Gooch et al., 2008) was fused to the ORF of BcFRQ1 (BcFRQ1-LUC) (Figure 17) at the endogenous *bcfrq1* locus by a *knock in* strategy (Larrondo et al., 2009), allowing to follow directly BcFRQ1 levels. The results depicted in Figure 18A showed the quantification of BcFRQ1-LUC expression levels in Gamborg B5 solid cultures, showing rhythms in luminescence with a period close to 24 hours. Using temperature steps from 22 to 27 °C during 12:12 hours and under DD conditions, the translational bioluminescent reporter can be entrained by temperature cycles, exhibiting an anticipatory behavior (Figure 18B). Pregueiro (Pregueiro et al., 2005) described a phase angle experiment to show if a strain is entrained rather than being driven by temperature cycles with different period length (T). If the strain is entrained by temperature, there is a dynamic phase change, which can be visualized as a slope line (as a function of the different period length), while the line is vertical in an arrhythmic strain. So, to provide additional proof of the functionality of the Botrytis oscillator, we confirmed the existence of changes in phase angle of the peaks of BcFRQ1-LUC expression when subjected to temperature entrainment cycles with different T (Figure 18C). In aggregate, the results depicted in

Figure 16 and 18 confirm that *bcwcl1*, *bcfrq1* and BcFRQ1 are part of the circuitry of the *B. cinerea* TTFL circadian oscillator.

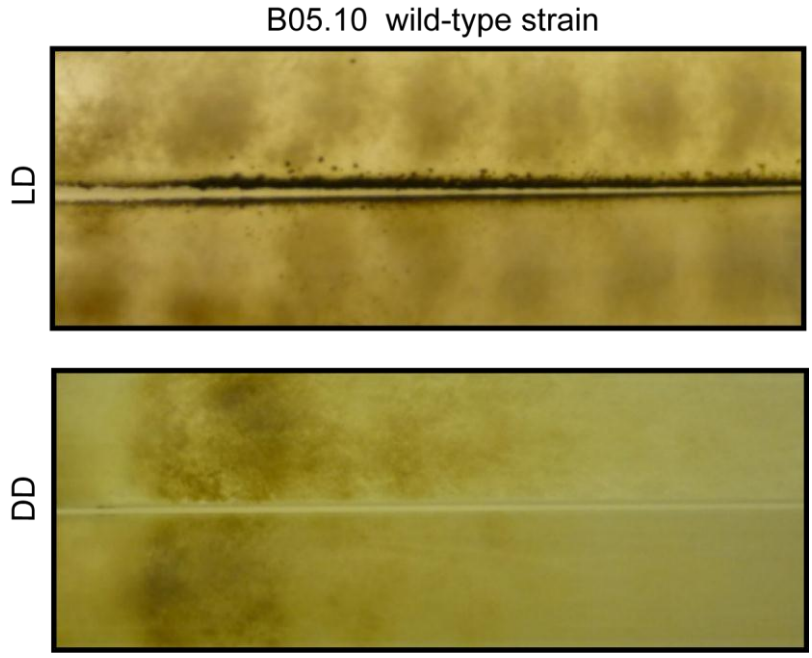

Figure 15. B05.10 WT strain does not present a conidiation banding pattern under FRC. *B. cinerea* spores ($2x10^5$/ml, 7µl) were inoculated in race tubes containing PDA medium under LD and DD at 25 °C. After 3 weeks, pictures were acquired from the top section of each tube. The picture shows two race tubes for each culture condition and is a representative example of three independent assays.

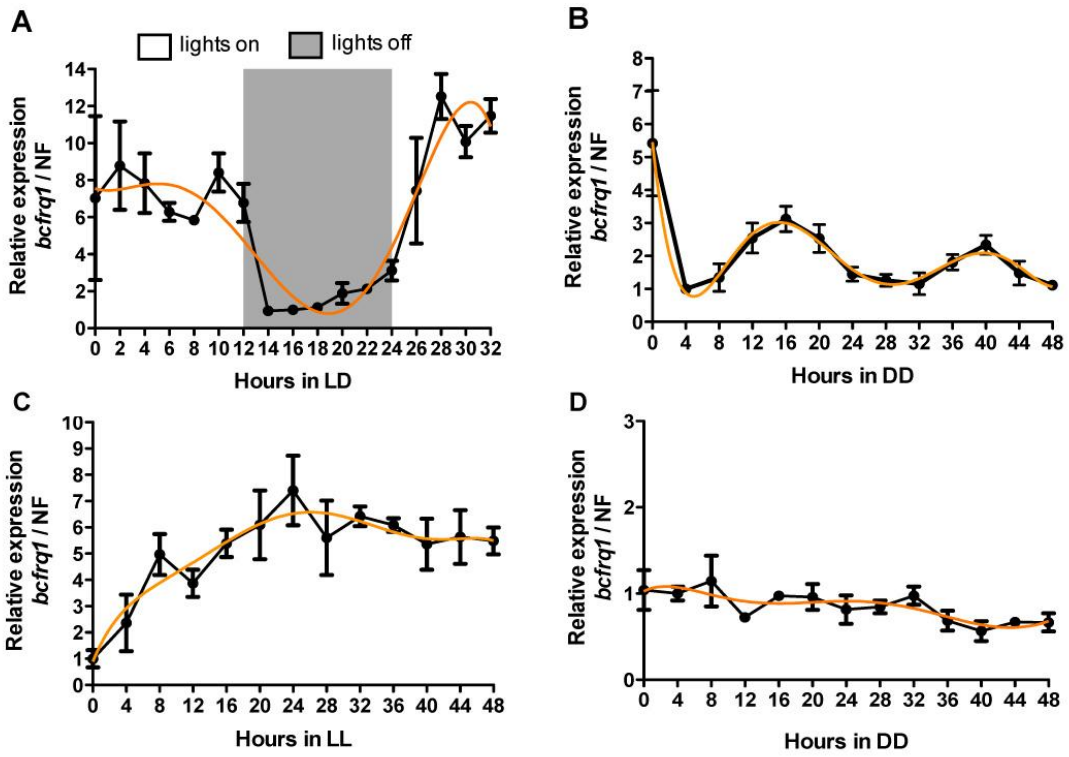

Figure 16. The *bcfrq1* transcript levels present daily oscillations that are lost in the Δ*bcwcl1* strain and under constant light conditions. (A) The *B. cinerea* B05.10 WT strain was inoculated on cellophane-covered PDA Petri dishes under LD culture conditions, during 96 h. Thereafter, cultures were harvested every 2 h, during 32 h. Subsequently, gene expression was analyzed by RT-qPCR as described in methods. The lights-on and off periods are denoted in white and grey backgrounds, respectively. Expression values are referred to the culture grown 4 h in the dark (1 = LD16). **(B)** The B05.10 strain was first incubated under LL during 24 h and subsequently transferred to DD culture conditions every 4 h, during 48 h. Expression values are referred to the culture grown 4 h in the dark (1 = DD4) **(C)** The WT strain was first grown under DD conditions during 24 h. Thereafter, cultures were transferred from DD to LL every 4 h, during 48 h. Expression values are referred to the cultures obtained in the dark (1 = LL0). **(D)** Transcript levels of *bcfrq1* were analyzed in the Δ*bcwcl1* mutant strain (Canessa et al., 2013) grown as mentioned in (B). Expression values are referred to the culture grown 4 h in the dark (1 = DD4). The plot for Fig. 1A, C and D represents two biological with two technical replicates each and for Fig. 1B represents four biological with three technical replicates each. Each point (in black) represents mean values ± SEM, while a trend line is depicted in orange. A normalization factor (NF) was calculated for gene expression normalization (see methods). Primer pairs employed for RT-qPCR amplification are indicated in Table 3.

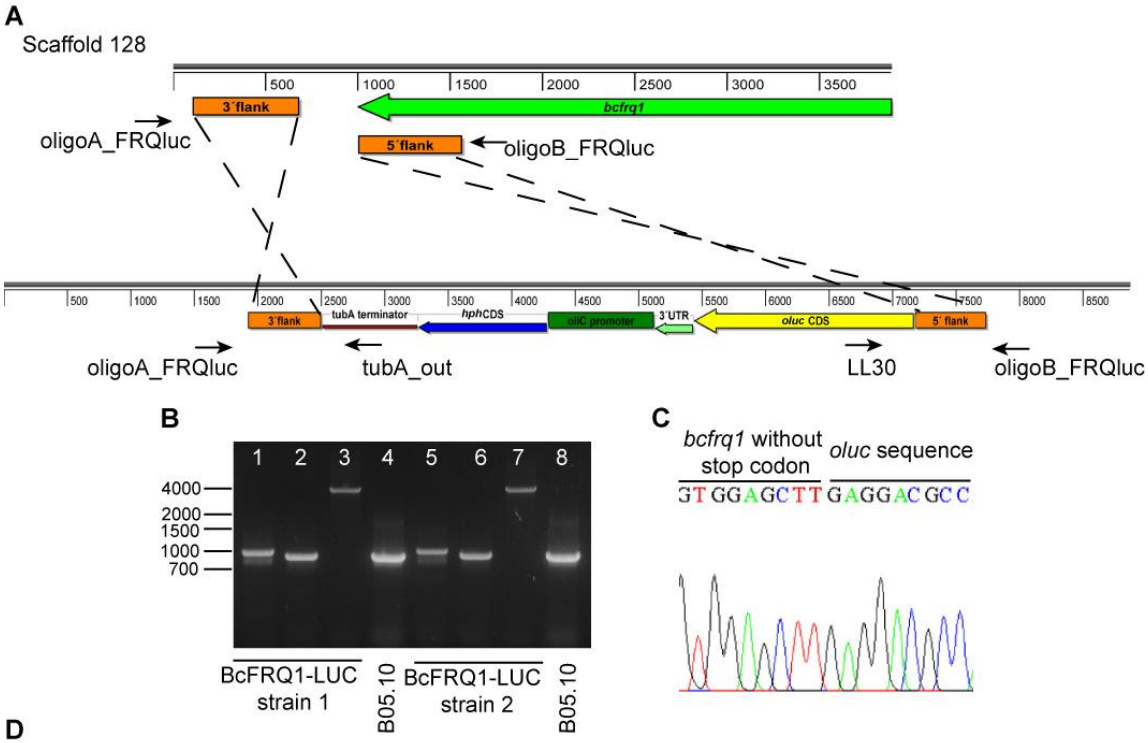

D

Amplicon	Primer pair	Sequence (5´-3´)	Lane in (B)	Expected size (bp)
downstream integration,at *bcfrq1* locus	oligoA_FRQluc tubA_out	ATAACAATAAAATCGCAACCCCAGA GATCTTGACACCATAACGGCTT	1,5	948
upstream integration, at the *bcfrq1* carboxyl terminal region	oligoB_FRQluc LL30	GTACATACACGATGGGCGACGA TCGGTCTGTGAGAATGAGAT	2,6	755
to check homo/heterokaryon status	LC-272 oL1554	TCGCAGGTGACCCGCCATACT TCTAGACGCCGAACAACCATCCTT	3,7/4,8	3,491/851

Figure 17. Generation of BcFRQ1-LUC strains. (A) Replacement strategy scheme showing the expected *in-locus* insertion of the replacement construct. Schematic representation of the *bcfrq1* locus, located in Supercontig 128 of the B05.10 strain genome database. The *bcfrq1* gene and its transcriptional orientation (2,958bp; Bc1G_13940, genomic coordinates 37815-40772) are represented as a green arrow. Additional gene models were omitted to simplify the figure. The gene replacement cassette employed to obtain the BcFRQ1-LUC strain is shown bellow the *bcfrq1* gene model. The position of the genomic regions employed for the homologous recombination (orange boxes) are shown. Black arrows show primers used for diagnostic PCRs, indicating their respective position and orientation. **(B)** Diagnostic PCRs showing *in-locus* integration. Homologous integration at the carboxyl terminal region of *bcfrq1* and downstream region of *bcfrq1* are shown for the two BcFRQ1-LUC strains. **(C)** Sequence chromatogram showing the junction of *bcfrq1* and *oluc*. **(D)** Primer pairs used in diagnostic PCRs. Their respective position and orientation is depicted in (A) (with respect to the gene transcriptional orientation) and Table 5.

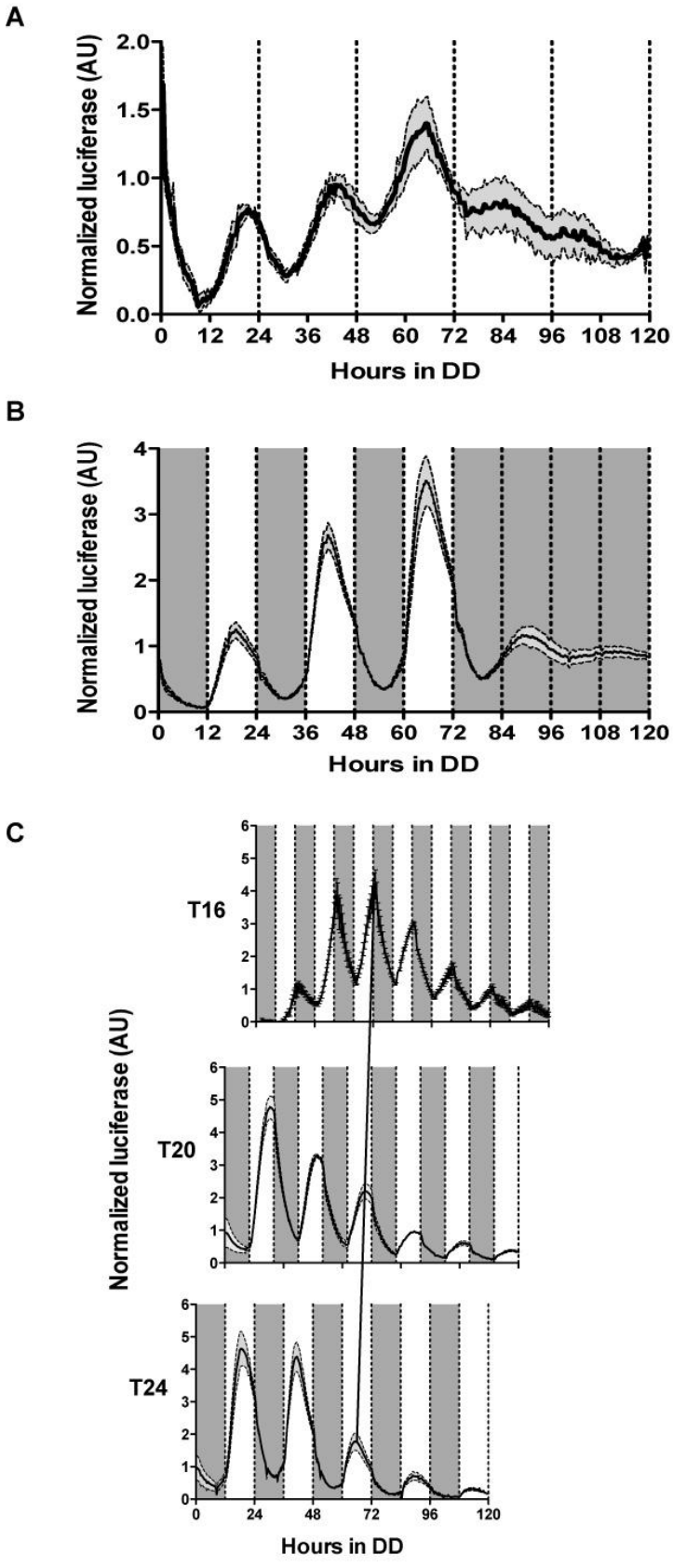
A
Normalized luciferase (AU)
2.0
1.5
1.0
0.5
0.0
0 12 24 36 48 60 72 84 96 108 120
Hours in DD
B
Normalized luciferase (AU)
4
3
2
1
0
0 12 24 36 48 60 72 84 96 108 120
Hours in DD
C
Normalized luciferase (AU)
T16
T20
T24
0 24 48 72 96 120
Hours in DD

Figure 18. The BcFRQ1-LUC translational reporter oscillates under free running conditions and temperature cycles of different T. (A) The translational reporter strains were entrained for 3 days under LD (12:12) conditions at 20 °C. Thereafter, LUC activity was monitored under DD at 20 °C. **(B)** BcFRQ1-LUC was monitored under temperature cycles using steps from 22 °C (grey) to 27 °C (white) under DD conditions. After 72 h, strains were subjected to temperature free running conditions of 22°C. **(C)** For phase angle experiments, 22/27 °C temperature cycles (grey and white, respectively) of varying period length (indicated at left) were used. In all cases, strains were pre-grown for 3 days under LD (12:12). Bioluminescence traces were acquired using the WinView software, and analyzed in more detail using a costume-made ImageJ macro. The plots represent the mean of two biological with two technical replicates each. Mean values are plotted as a black line, while SEM is represented as grey-filled area.

4.2.3 The Δ*bcfrq1* mutant displays impaired macroconidiation and increased sclerotia production, phenotype that is dependent on media composition

Once we were able to show that *B. cinerea* has a functional circadian oscillator, we wanted to assess whether it is capable of modulating virulence. For this purpose, four independent *bcfrq1* deletion mutants were generated (Δ*bcfrq1*, 1 to 4), having single integration of the replacement cassette (Figure 19).

When we grew the Δ*bcfrq1* strain in Potato Dextrose Agar (PDA), the knockout strain showed a developmentally altered phenotype, dramatically differing from the wild-type strain (Figure 20). Thus, while the B05.10 strain normally develops sclerotia in the absence of light (Rodriguez-Romero et al., 2010, Canessa et al., 2013) and produces conidia in its presence (LD), the Δ*bcfrq1* strain showed abundant sclerotia formation and almost a null conidia production in the presence of this environmental cue (Figure 20A). In order to deepen this observation, tissue was obtained from LD cultures of the Δ*bcfrq1* strain, and compared to those from the B05.10 and Δ*bcwcl1* strains. Conidia were stained with Hoechst 33342 (nuclear staining) and visualized by fluorescence microscopy. As shown in Figure 20B, the Δ*bcfrq1* strain presents mainly mononucleated conidia, consistent with the size and morphology of microconidia (sexual conidia). In contrast, both WT and Δ*bcwcl1* strains showed the characteristic macroconidia (asexual conidia) with three to five nuclei, as previously described (Urbasch, 1985, Schumacher and Tudzynski, 2012).

Since the Δ*bcfrq1* knockout strain show different developmental phenotypes, we assessed the growth under different culture media composition. Surprisingly, when we used a complete defined media (CM), the Δ*bcfrq1* strain phenotype is similar of that of

B05.10 WT strain, producing macroconidia under LD (Figure 21A and B). Nonetheless, when cultivated under the same LD conditions, but on PDA, Gamborg B5 or Malt media, Δ*bcfrq1* forms sclerotia and produces microconidia, consistent with what has been observed for the B05.10 only under DD conditions (Figure 21A and B) and suggesting an alteration in the crossroads of light/clock and nutrient sensing machineries.

A

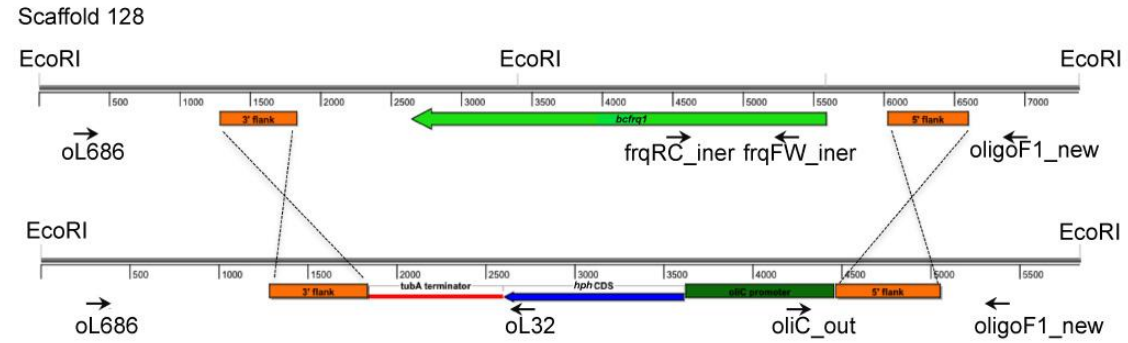

B

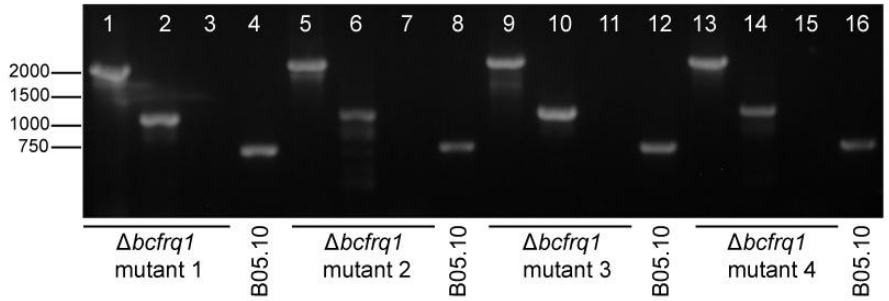

C

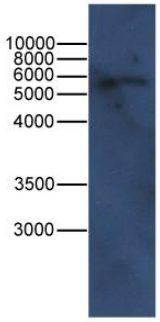

D

Amplicon	Primer pair	Sequence (5´-3´)	Lane in (B)	Expected size (bp)
downstream integration, at *bcfrq1* locus	oL686 oL32	AGCATGGGGATCAACTCTTG ATGGCTGTGTAGAAGTACTC	1, 5, 9, 13	2,350
upstream integration, at *bcfrq1* locus	oligoF1_new oliC_out	CGTTGATTGGAACAATGCAG GTCCGATAAAATGGTACTGCC	2, 6, 10, 14	1,065
bcfrq1	frqFW_iner frqRC_iner	TCGCAGGTGACCCGCCATACT TCTAGACGCCGAACAACCATCCTT	3-4, 7-8, 11-12, 15-16	710

Figure 19. Generation of the Δ*bcfrq1* mutants. (A) Schematic representation of the Δ*bcfrq1* locus depicting the *in-locus* insertion of the gene replacement cassette employed for mutant generation (bottom). Orange boxes denote the genomic regions employed for homologous recombination of the replacement cassette, while black arrows show primers used for diagnostic PCRs, indicating their relative position and orientation. **(B)** Diagnostic PCRs showing *in locus* integration. Homologous integration at downstream (lanes 1, 5, 9 and 13) and upstream of *bcfrq1* locus (lanes 2, 6, 10 and 14) are shown for each analyzed mutant. No wild-type locus was observed for each Δ*bcfrq1* mutant after single-spore isolation (see methods) (lanes 3, 7, 11 and 15) in comparison with the B05.10 wild-type strain (lanes 4, 8, 12 and 16). **(C)** Southern blot hybridization. Ten μg of genomic DNA was digested with EcoRI, and hybridized with the full-length *hph* CDS used as probe (expected size: 5,845 bp). To simplify the figure, only the hybridization of mutant 1 is shown. **(D)** Primer pairs used in diagnostic PCRs. Their respective position and orientation is depicted in (A) (with respect to the gene transcriptional orientation) and Table 6.

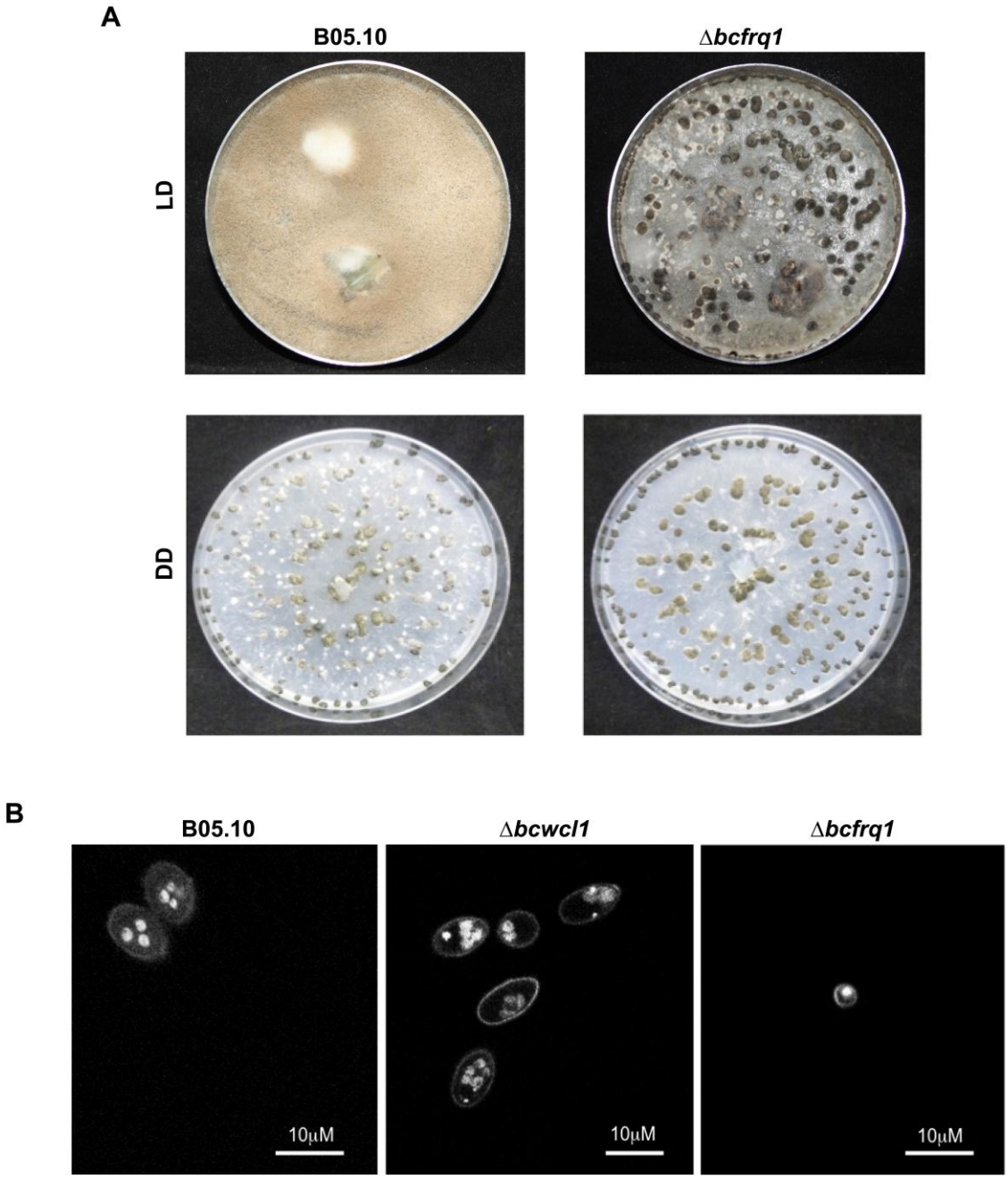

Figure 20. The Δ*bcfrq1* strain presents an altered differentiation phenotype when is grown on PDA. (A) B05.10 WT and Δ*bcfrq1* strains were incubated on PDA plates for 14 days in LD and DD culture conditions. Δ*bcfrq1* produces sclerotia in LD, in contrast to what is described for the B05.10 strain, which produces sclerotia only in DD. Also, a null conidia formation phenotype was observed in Δ*bcfrq1* strain under both conditions. **(B)** Spores of WT, Δ*bcwcl1* and Δ*bcfrq1* strains were incubated with the blue fluorochrome stain Hoechst and visualized by fluorescence microscopy using the Nikon Eclipse C2 confocal microscope. Δ*bcfrq1* strain presents only one nucleus when compared with the B0.510 wild-type and Δ*bcwcl1* strains, indicating that-at least in this case- *bcfrq1* gene is required for macroconidia production. Scale bars represents 10 um.

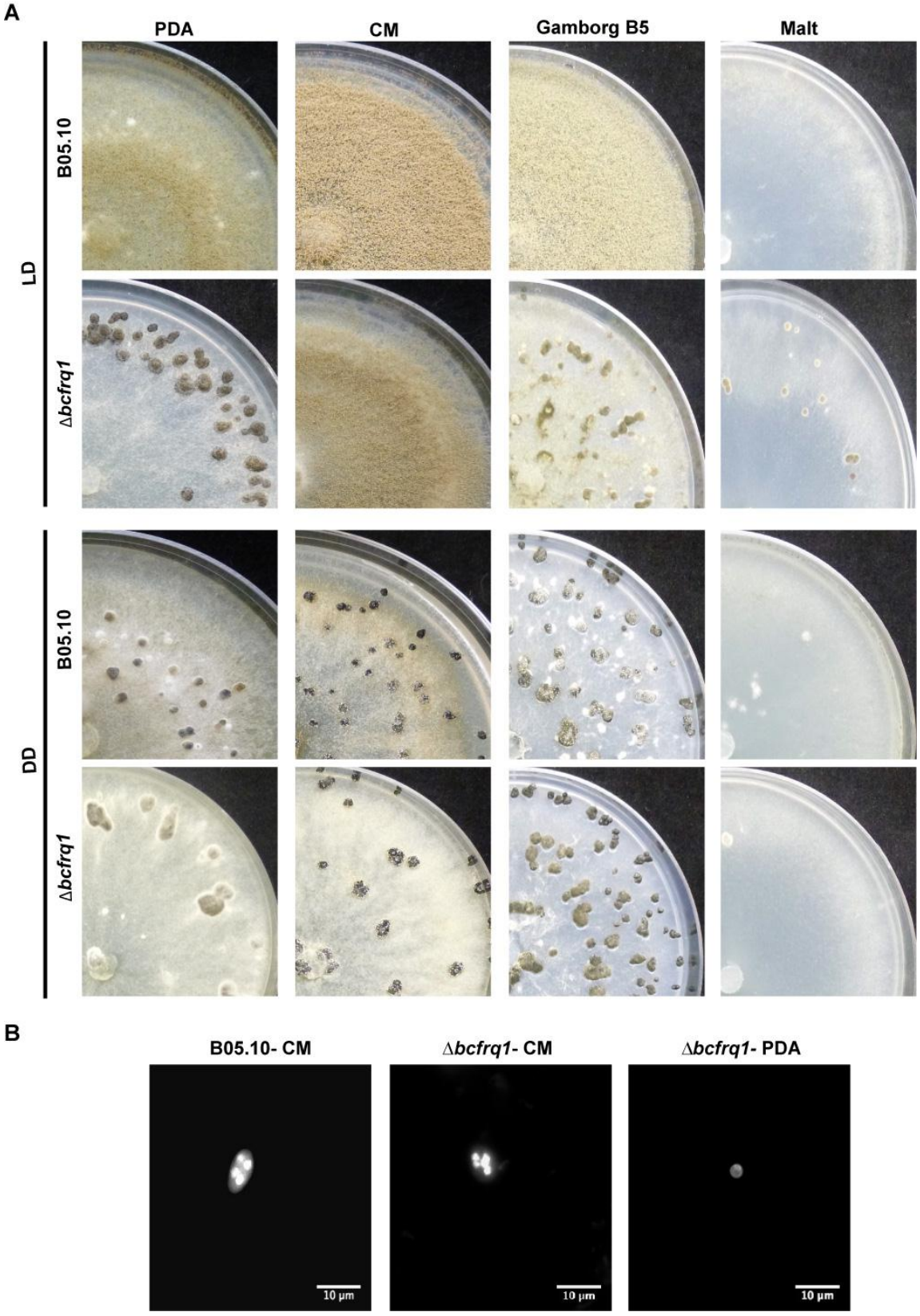
A
PDA
CM
Gamborg B5
Malt
LD
B05.10
Δbcfrq1
DD
B05.10
Δbcfrq1
B
B05.10- CM
Δbcfrq1- CM
Δbcfrq1- PDA
10 µm
10 µm
10 µm

Figure 21. The Δ*bcfrq1* strain is able to form macroconidia when is grown on Complete Medium (CM). (A) B05.10 wild-type and Δ*bcfrq1* strains were incubated on PDA, CM, Gamborg B5 and Malt media for 14 days in LD and DD culture conditions. **(B)** Spores of 14 day olds of B05.10 WT and Δ*bcfrq1* strains were incubated with the blue fluorochrome stain Hoechst and visualized by fluorescence microscopy using the Cytation 3 Cell Imaging Multi-Mode Reader.

4.2.4 Variation in nitrogen sources in complete medium produce a reversal of the Δ*bcfrq1* developmental phenotype

As recently explained, under certain media conditions the Δ*bcfrq1* strain displays severe developmental phenotype, producing survival structures named sclerotia. This led us hypothesize that a certain nutritional restriction may be driving a morphological development of the knockout strain. To address this point, different versions of the synthetic CM were prepared, in order to determine the specific compound(s) responsible for the phenotypic switch of the mutant strain to asexual development (macroconidia production). Seven different media were tested; each of one lacked one of the components of the original medium (Pontecorvo et al., 1953): glucose, Casaminoacids, casein peptone, yeast extract, salt solution, vitamin solution or microelement solution. Plates were inoculated with B05.10 WT or Δ*bcfrq1* strain and grew for two weeks in Light-Dark 12:12 cycles at 20º C. As observed in Figure 22, absence of glucose, yeast extract or any of the solutions do not drive back the mutant strain into the sexual cycle, continuing on producing macroconidia under these conditions. On the contrary, when Casaminoacids and casein peptone are excluded from the preparation, suppression of macroconidiation is observed while sclerotia formation starts, consistent with the phenotype obtained when the mutant strain grows in PDA, Gamborg B5 and Malt media (Figure 21). The B05.10 WT strain and complemented strain (data not shown) do not change the way they grow under the modifications afore mentioned, attributing the phenotype directly to an altered pathway in the Δ*bcfrq1* strain.

In order to determine if the sexual phenotype of Δ*bcfrq1* strain is a response to the inability to use the nitrogen sources in any form, we probe selectivity to primary

(glutamine, glutamate and ammonium) or secondary (nitrate and nitrite, the rest of amino acids and nitrogenous bases) nitrogen sources. We observed that in the presence of primary sources (ammonium sulfate, $(NH_4)_2SO_4$) the knockout strain is able to form macroconidia, but in the presence of secondary sources (sodium nitrate, $NaNO_3$) the Δ*bcfrq1* mutant starts sclerotia and microconidia production, which suggests that our deletion mutant has problems in metabolizing secondary nitrogen sources (data not shown).

It is noteworthy to mention that when removing the yeast extract, the Δ*bcfrq1* strain still is able to form macroconidia. One possible explanation is that the nitrogen sources in the yeast extract are low, in such way that when we remove this component, the asexual phenotype is maintained. On the other hand, Δ*bcfrq1* strain is not capable of sensing, acquire and / or use primary nitrogen sources in PDA. Although all amino acids are present in the potato extract, including primary sources as glutamine and glutamate, the mutant strain maintains it sexual phenotype. One explanation is that the aminoacids are not free in the medium, while there are forming large peptides that the knockout strain is not capable to digest, which does not happen when the aminoacids are freely supplemented to the culture medium. This suggests that in addition to the inability of using secondary nitrogen sources, exists incapacity to degrade extracellular proteins, which could be related to an inability to efficiently secrete proteases.

The experiments described above, related to nitrogen, are part of the undergraduate thesis of Hanna Müller.

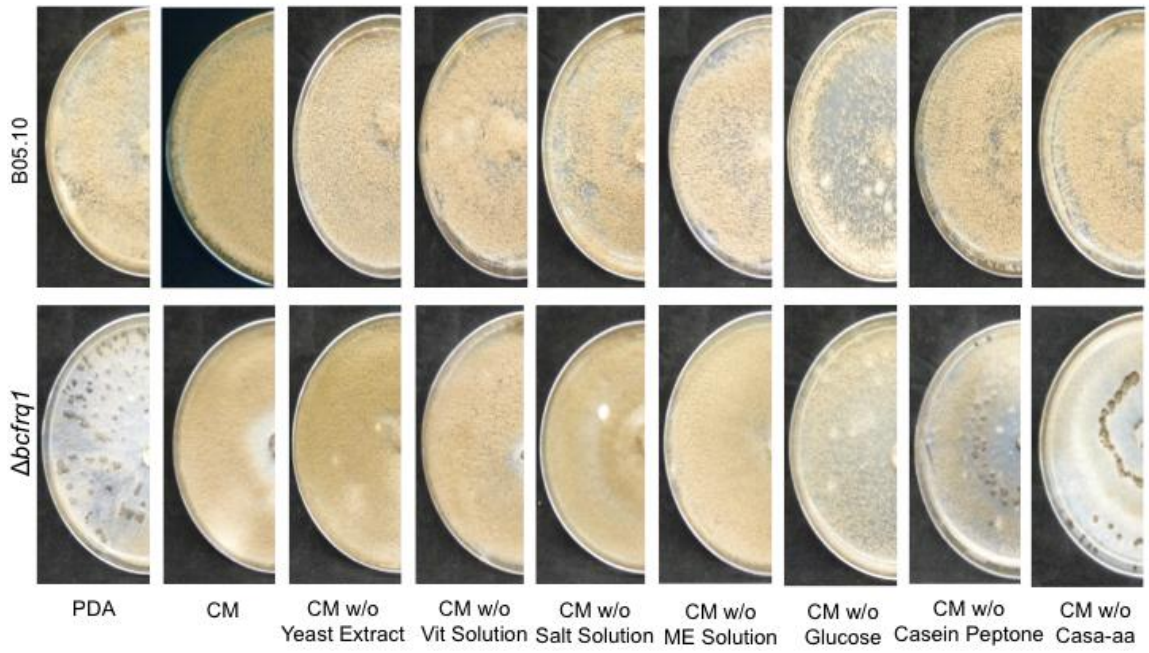

Figure 22. The Δ*bcfrq1* strain needs nitrogen sources in order to sporulate. Phenotypes of B05.10 WT and Δ*bcfrq1* strain grown in CM and CM modified, lacking any of the original components. Pictures are representative of two independent assays. Plates were grown for 14 days under LD. PDA altered phenotype as control. Vit, vitamin; ME, microelement.

4.2.5 BcFRQ1 is dispensable to cope with osmotic and oxidative stress

Since the osmolarity of the medium and changes in the intracellular ROS levels affects developmental processes in *B. cinerea* (Segmuller et al., 2007, Segmuller et al., 2008, Roca et al., 2012), we tested the effect of hyperosmotic conditions as well as oxidative stress in the Δ*bcfrq1* strain. For this purpose, we used as control the MAPK mutant Δ*bcsak1*, which is blocked in conidia formation, shows increased sclerotia development (as Δ*bcfrq1*) and is sensitive to osmotic and oxidative stress (Segmuller et al., 2007). On the other hand, the assays were done in PDA and CM due to the different phenotypes that Δ*bcfrq1*presents (Figure 20 and 21). The B05.10, Δ*bcfrq1* and Δ*bcsak1* strains were grown in the presence of 1.0 M and 1.5 M NaCl and 1.6 M Sorbitol. As observed in Figure 23A, the Δ*bcfrq1* mutant is not sensitive to osmotic stress -compared with B05.10- while Δ*bcsak1* is significantly more osmosensitive than the two first strains. Additionally, both mutants and the B05.10 strain were tested for sensitivity to oxidative stress based on the growth in the presence of 5 mM and 10 mM H_2O_2 as well as 250 μM and 500 μM menadione. As previously described (Segmuller et al., 2007), the growth rate was significantly reduced in Δ*bcsak1* when exposed to 5 mM and 10 mM H_2O_2, but B05.10 and Δ*bcfrq1* strains were not sensitive to this stressor agent (Figure 23B). On the other hand, sensitivity to menadione (at 250 and 500 μM) seemed to be unchanged in the three strains. In conclusion, deletion of *bcfrq1* does not influence osmotic and oxidative stress resistance.

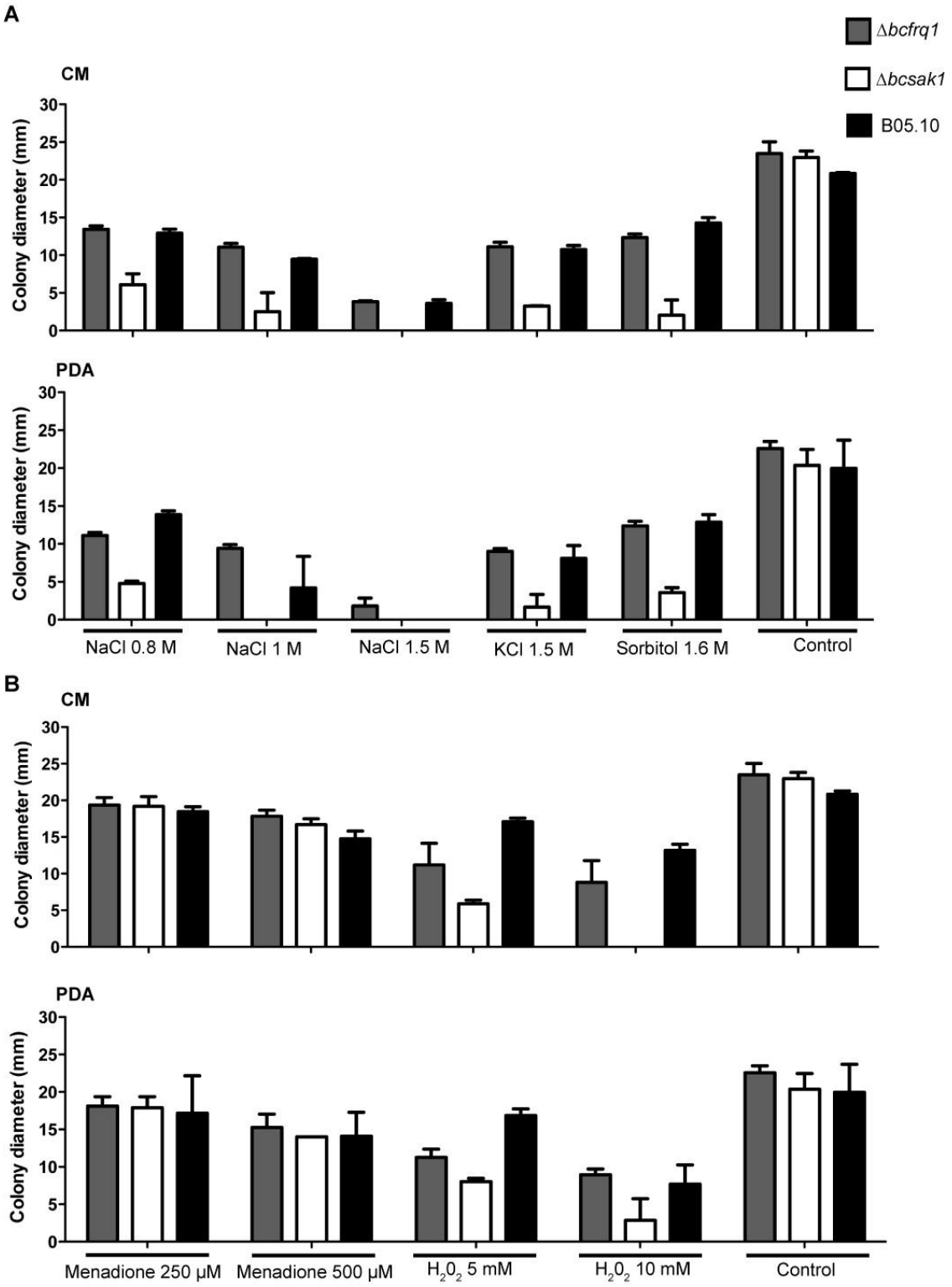

Figure 23. BcFRQ1 is not necessary to cope with osmotic and oxidative stress. B05.10, Δ*bcfrq1* and Δ*bcsak1* strains were grown on CM or PDA with different osmotic **(A)** and oxidative **(B)** stressor agents. Colony diameter was measured 2 days post inoculation on Petri dishes using and external calibrator scale and the ImageJ program.

4.2.6 Δ*bcfrq1* strain displays impaired virulence associated with microconidia production

As mentioned above, when we grew Δ*bcfrq1* strain on PDA, Gamborg B5 or Malt, it produces microconidia. Based on this result, it is possible to hypothesize that Δ*bcfrq1* should present a significantly reduced virulence since microconidia of *B. cinerea* develop a short germinal tube that is not able to infect (Jarvis, 1977, Urbasch, 1985). To unravel this question, leaves of *A. thaliana* Col-0 plants were infected with a microconidia suspension of the Δ*bcfrq1* strain. As expected, a totally impaired infection process was observed for all Δ*bcfrq1* deletions mutants, exhibiting near 98% reduction in the lesion area when compared to the B05.10 strain (Figure 24A and C). In order to assess whether the altered infection phenotype remains under circadian conditions, the virulence assay was performed under FRC, observing the same outcome. Trypan blue staining that allow the detection of dead plant cells as well as invasively growing hyphae revealed significant differences between the spreading lesions provoked by B05.10 and Δ*bcfrq1* strains (Figure 24B).

There is some evidence that conidia and mycelia of the same knockout strains may have different capabilities of penetration. Hence, mutants of the BcCRZ1 TF and the MAP kinase BMP3 are able to infect the plant when conidial suspensions are used, but no when the mycelia of these strains are used (Rui, 2007, Schumacher et al., 2008b). This could be explained by the different infection structures: appressoria or infection cushions that are formed by germ tubes and hyphae, respectively. Moreover, when the infected host tissue is wounded prior conidia or mycelia inoculations, the capability of the mutants to infect is better, which reflects a role in promoting the penetration process

(Rui, 2007, Schumacher et al., 2008b). So, due to the lack of macroconidia production by the Δ*bcfrq1* mutant (when grown in PDA plates), mycelia plugs were used to infect French bean (*P. vulgaris*) leaves, which is a highly susceptible host of *B. cinerea*. As shown in Figure 25A and B, when the infection was carried out on intact unwounded tissue, only the leaves infected with mycelia from B05.10 -and not Δ*bcfrq1* strain- showed signs of infection after 3 dpi under LD culture conditions. Nonetheless, the Δ*bcfrq1* deletion mutant was able to infect wounded tissue, although the lesion formation was significantly smaller than that of the B05.10 WT strain. These results suggest that the infection cushions that are formed by Δ*bcfrq1* hypha are impaired in the penetration of intact plant tissue. Interestingly, when we followed the bean infection process for 3, 4 and 5 days, we observed that after 96 hpi the microconidia from Δ*bcfrq1* can form small lesions, which also suggest a problem or delay in penetration (Figure 25C). Nevertheless, we can not rule out that the latter observation could be due to small amounts of macroconidia that could be present in the Δ*bcfrq1* inoculum and that since they are underrepresented in the sample, they may take a long time to start the infection process.

Finally, we wanted to assess the pathogenic capability of Δ*bcfrq1* when is grown in CM, because –as previously shown in Figure 21- in these medium composition it is capable to generate macroconidia. Figure 26 shows that the macroconidia of the deletion mutant are capable of producing regular lesions, which are actually statistically larger than those from the B05.10 strain when infecting *A. thaliana* (Figure 26A and B) and beans plants (Figure 26C).

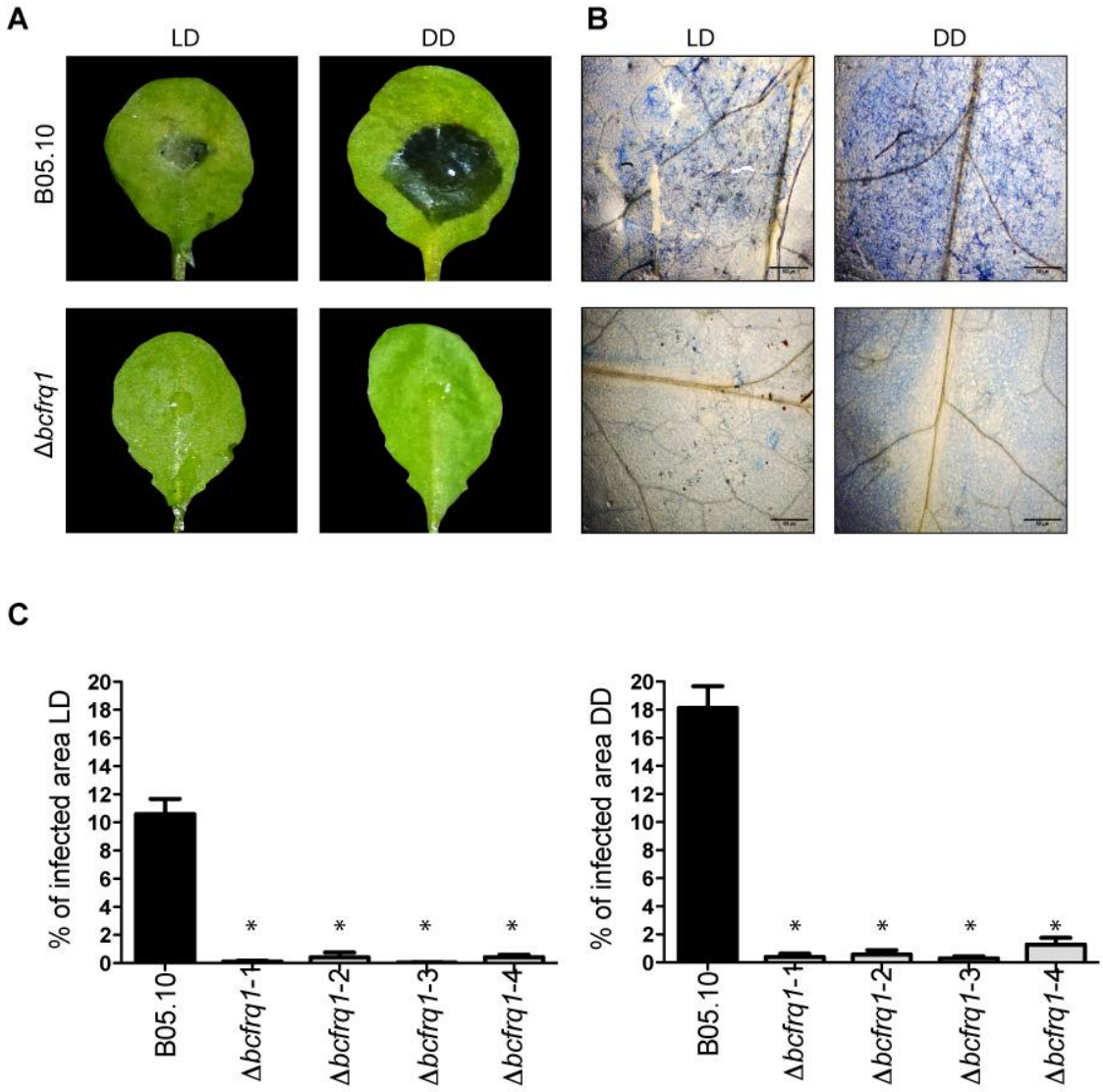

Figure 24. Microconidia from Δ*bcfrq1* strain present an altered infection phenotype. (A) Conidia ($2x10^5$/ml, 7µl) from the B05.10 wild-type (top) and a representative Δ*bcfrq1* mutant (bottom) strain inoculated on approximately 1 month old *A. thaliana* Col-0 plants, grown at 20 °C under LD (12:12 h) conditions. Spores were inoculated at dawn and then plants were grown for 3 days under LD or DD conditions. Pictures were acquired after 3 dpi. Representative leaves for each culture condition are shown. **(B)** Trypan blue staining showing fungal growth in plants at 3 dpi, which is visible as thread-like stained structures (black scale bars represent 500 µm). **(C)** Quantification of the lesion area, obtained from four independent virulence assays and four different Δ*bcfrq1* mutants. Bars represent the mean ± SEM. Significant differences in comparison with the lesion observed for the B05.10 wild-type strain are indicated with asterisks (Kruskal-Wallis test; $p<0.05$).

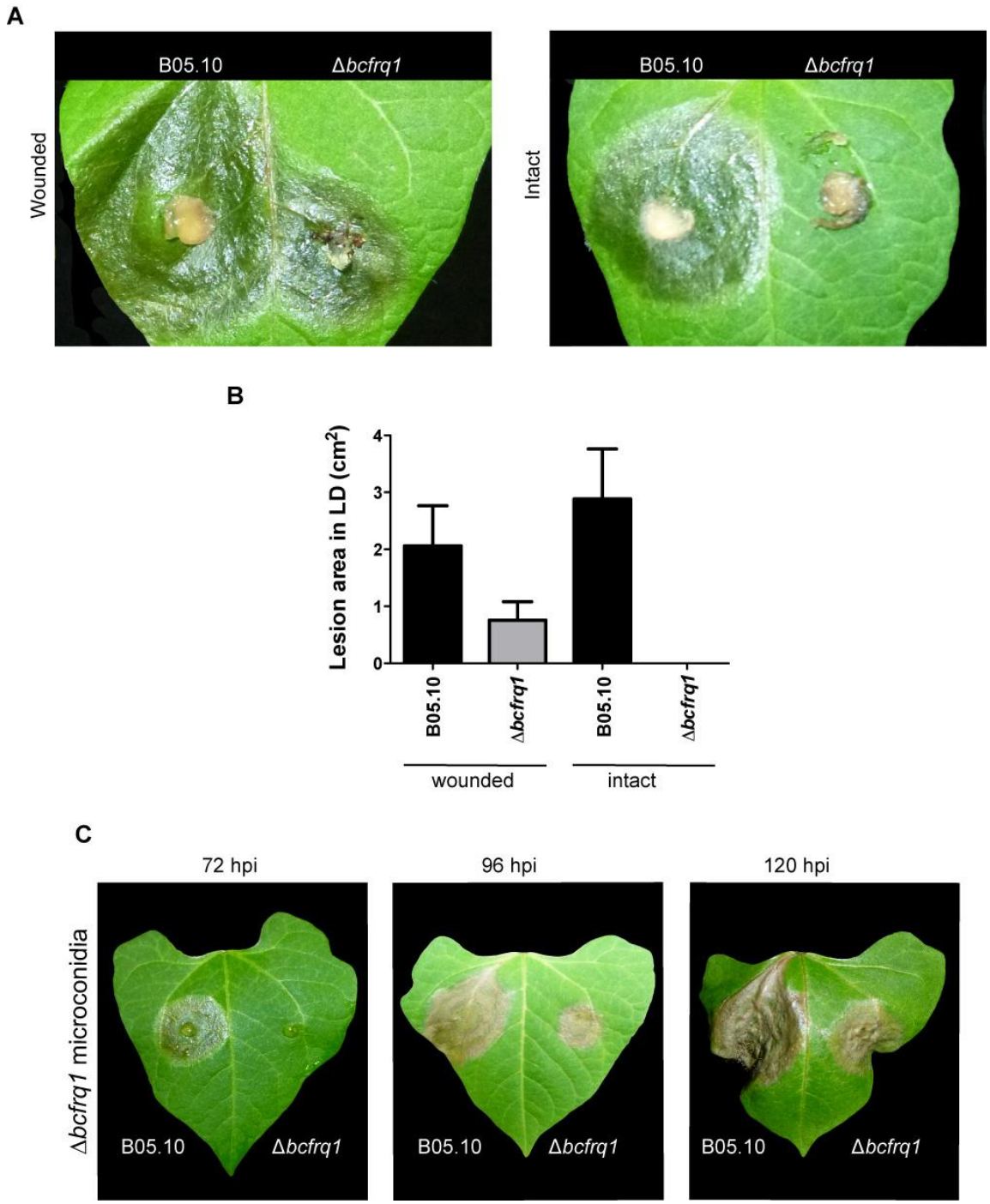
A
B05.10
Δbcfrq1
Wounded
B05.10
Δbcfrq1
Intact
B
Lesion area in LD (cm²)
0
1
2
3
4
B05.10
Δbcfrq1
B05.10
Δbcfrq1
wounded
intact
C
72 hpi
96 hpi
120 hpi
Δbcfrq1 microconidia
B05.10
Δbcfrq1
B05.10
Δbcfrq1
B05.10
Δbcfrq1

Figure 25. The Δ*bcfrq1* knockout strain is able to infect wounded French leaves and presents a delay in lesion formation. (A) Intact and wounded 14 days old plants were inoculated with mycelia plugs containing the B05.10 and Δ*bcfrq1* strains. Representative pictures were acquired 3 dpi under LD conditions. **(B)** Mean values ±SEM of lesion diameters were calculated. **(C)** Conidia ($2x10^5$ /ml, 7µl) from the B05.10 and Δ*bcfrq1* strain were used to infect 14 days old *P. vulgaris* plants. The infection process was follow during 5 days. Pictures were acquired at 72, 96 and 120 hpi. In the two virulence assays, inoculation was done at dawn and the plants and the fungus come from 12:12 photocycle.

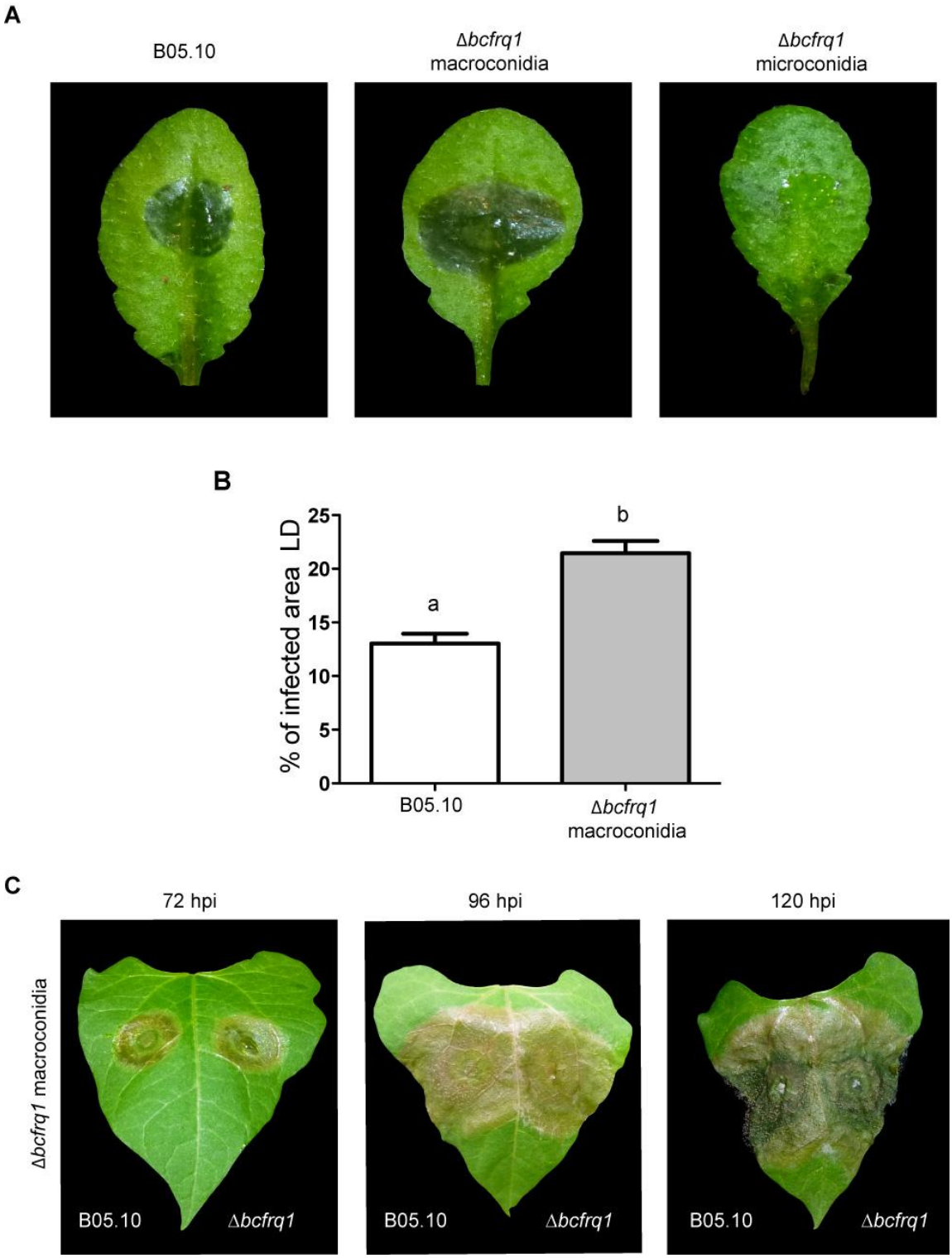
A
B05.10
Δbcfrq1
macroconidia
Δbcfrq1
microconidia
B
% of infected area LD
25
20
15
10
5
0
a
b
B05.10
Δbcfrq1
macroconidia
C
72 hpi
96 hpi
120 hpi
Δbcfrq1 macroconidia
B05.10
Δbcfrq1
B05.10
Δbcfrq1
B05.10
Δbcfrq1

Figure 26. Macroconidia obtained from the Δ*bcfrq1* strain grown in CM are capable to infect. (A) Conidia ($2x10^5$ /ml, 7µl) from the B05.10 WT strain and macro and microconidia from Δ*bcfrq1* strain were used to infect 30 days old *A. thaliana* Col-0 plants. Pictures were acquired 72 hpi. **(B)** Quantification of the lesion area obtained from three independent virulent assays. Bars represent the mean ± SEM. Different letters indicate statistical differences (Mann-Whitney; $p<0.05$). **(C)** *P. vulgaris* plants were infected with macroconidia from B05.10 WT and Δ*bcfrq1* strain. For all virulence assays, inoculation was done at dawn and the plants and the fungus come from 12:12 photocycle.

4.2.7 Genetic complementation with the *bcfrq1* gene restores macroconidia production and full-virulence in the Δ*bcfrq1* strain

The Δ*bcfrq1* mutant 1 was arbitrary chosen for genetic complementation. For this purpose, the *bcfrq1* gene was targeted to the endogenous locus by homologous recombination, yielding Δ*bcfrq1*+*bcfrq1* strain. Nourseothricin-resistant colonies were isolated and analyzed for complete integration of the genetic construct (Figure 27). For phenotypic characterization, three independent transformants containing the wild-type *bcfrq1* gene were analyzed. As expected, the expression of *bcfrq1* in the Δ*bcfrq1* genetic background restored the wild-type phenotype. Thus, the complemented strains stopped the production of abundant sclerotia (Figure 28A) and regained the ability to produce macroconidia in LD conditions (Figure 28A and B), while spores produced in PDA plates are able to efficiently infect *A. thaliana* Col-0 plants as the B05.10 wild-type strain (Figure 28C and D). In summary, deletion and genetic complementation analyses confirmed an unexpected key role of BcFRQ1 in development and virulence.

A

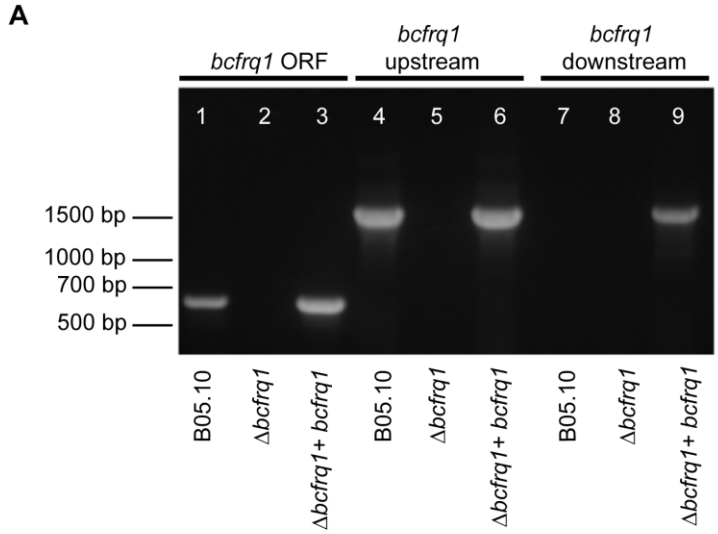

B

Amplicon	Primer pair	Sequence (5´-3´)	Expected size (bp)
downstream integration,at *bcfrq1* locus	oL686 oL585	AGCATGGGGATCAACTCTTG GGTACTGCCCCACTTAGTGGCAGCTCGCG	1,508
upstream integration, at the *bcfrq1* locus	oligoF1_new oL167	CGTTGATTGGAACAATGCAG TCGCAGGTGACCCGCCATACT	1,659
bcfrq1	frqFW_inner frqRC_inner	TCGCAGGTGACCCGCCATACT TCTAGACGCCGAACAACCATCCTT	627

Figure 27. Generation of the complemented Δ*bcfrq1* strain (Δ*bcfrq1*+*bcfrq1*). (A) Diagnostic PCRs of the complemented Δ*bcfrq1* strain (Δ*bcfrq1*+*bcfrq1*) showing the amplification of a fragment of *bcfrq1* (lane 3) inserted at the endogenous locus (lanes 6 and 9). Please note that oligonucleotide oL585 anneals at the nourseothricin resistance cassette. **(B)** Primer pairs used in diagnostic PCRs (with respect to the gene transcriptional orientation). For more information see Table 7.

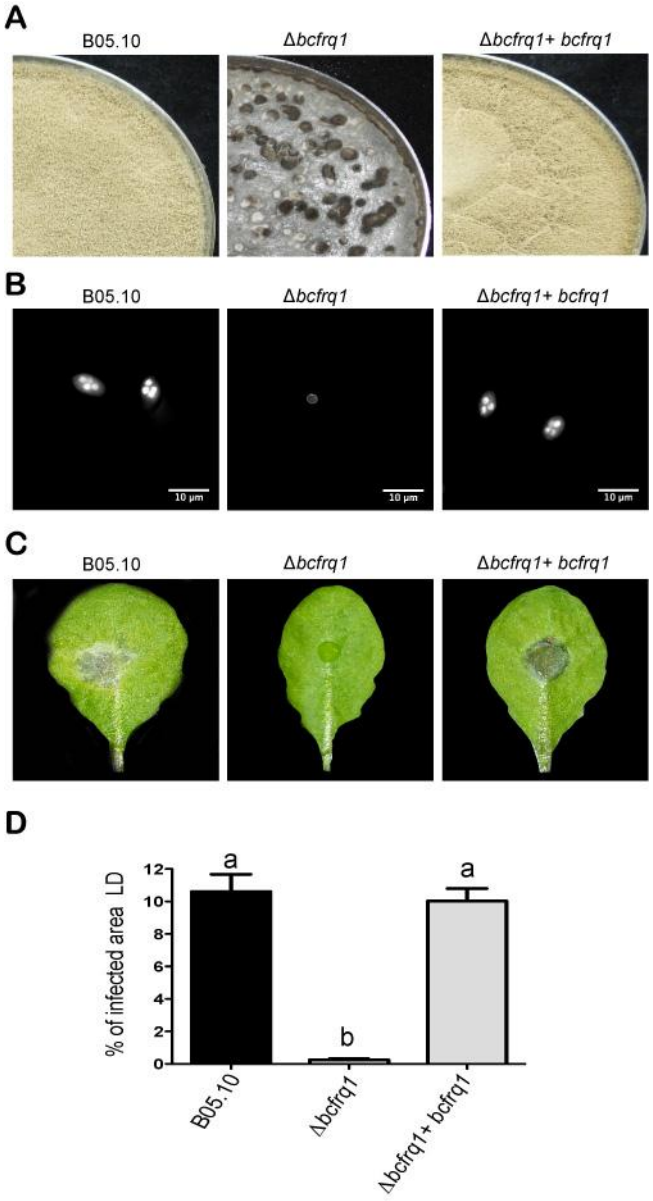

Figure 28. Genetic complementation of the Δ*bcfrq1* strain allows recovering wild-type phenotype. (A) B05.10, Δ*bcfrq1* and Δ*bcfrq1+bcfrq1* strains were incubated on PDA plates for 14 days under LD. **(B)** Hoechst-stained spores of B05.10 and one representative Δ*bcfrq1* and Δ*bcfrq1+bcfrq1* strain visualized by fluorescence microscopy using a Cytation 3 Cell Imaging Multi-Mode Reader **(C)** Lesion spreading of B05.10, Δ*bcfrq1* and Δ*bcfrq1+bcfrq1* strains on *A. thaliana* Col-0 plants incubated under LD conditions for three days. Inoculation was done at dawn and the plants and the fungus come from 12:12 photocycle. **(D)** Quantification of the lesion area produced by B05.10 and one representative Δ*bcfrq1* and Δ*bcfrq1+bcfrq1* mutant at 3 dpi. Bars represent mean values ± SEM (Kruskal-Wallis $p<0.05$).

4.2.7 Overexpression of *bcfrq1* strain leads to arrhythmicity and to decreased virulence

Since the Δ*bcfrq1* deletion mutant has different macro and microconidia phenotypes that depend on media composition, leading to two drastically opposed degrees of virulence (Figure 20, 21, 24 and 26), we decided to generate a *B. cinerea* strain in which, in addition to the endogenous *bcfrq1*, a new copy of this gene is added at a different locus and overexpressed under a strong promoter (OE::*bcfrq1*) (Figure 29). This strategy should abrogate rhythms in endogenous *bcfrq1* expression by constantly closing the negative feedback loop and leading to arrhythmicity, as it has been described in *N. crassa* (Aronson et al., 1994b). As expected, *bcfrq1* mRNA levels derived from the endogenous locus in the OE::*bcfrq1* strain (*bcfrq1* endo OE) are low, while the total *bcfrq1* transcript levels (total *bcfrq1* OE) are high. Both type of mRNA (individuals and total) are arrhythmic under DD conditions, contrasting to the rhythmic behavior of *bcfrq1* levels in a B05.10 wild-type strain in the same conditions (Figure 30).

Although the OE::*bcfrq1* strain displays a molecular circadian phenotype, it displays normal developmental characteristics such as production of macroconidia under any culture conditions (Figure 31A and B). Nonetheless, the mutant strain loses the ability to complete an efficient virulent process, producing significantly smaller lesions, while also failing to form secondary spreading lesions *in A. thaliana* and *P. vulgaris* hosts, even after 14 days post- infection (Figure 32A, B and C).

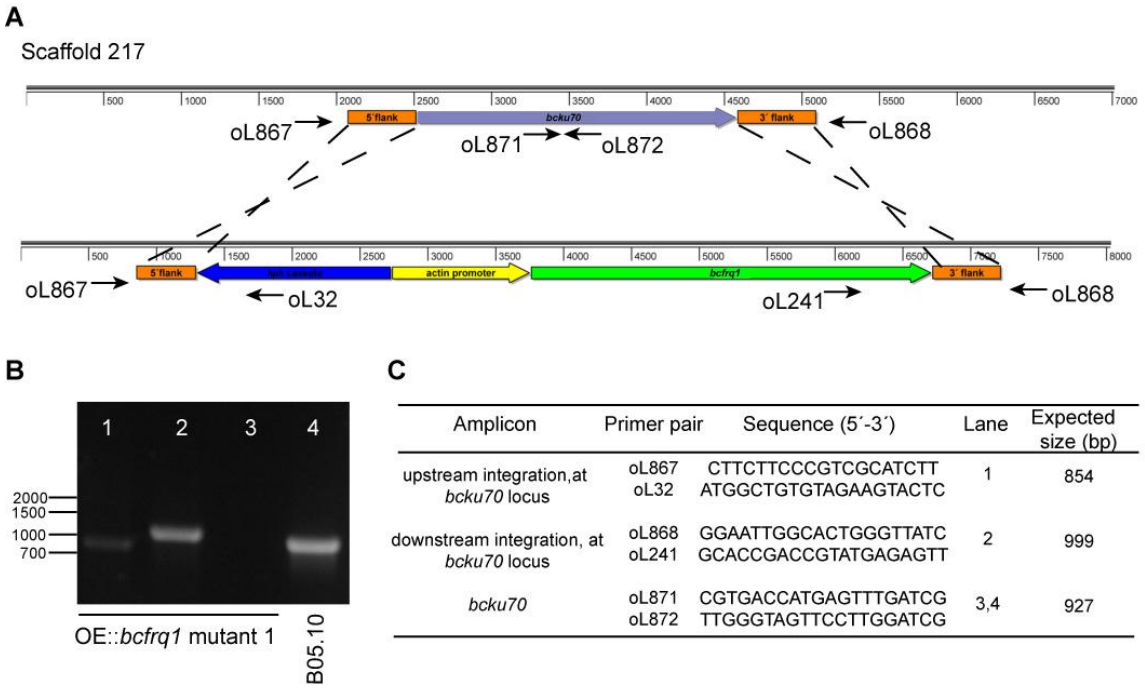

C

Amplicon	Primer pair	Sequence (5´-3´)	Lane	Expected size (bp)
upstream integration,at *bcku70* locus	oL867 oL32	CTTCTTCCCGTCGCATCTT ATGGCTGTGTAGAAGTACTC	1	854
downstream integration, at *bcku70* locus	oL868 oL241	GGAATTGGCACTGGGTTATC GCACCGACCGTATGAGAGTT	2	999
bcku70	oL871 oL872	CGTGACCATGAGTTTGATCG TTGGGTAGTTCCTTGGATCG	3,4	927

Figure 29. Generation of OE::*bcfrq1* strain. (A) Replacement strategy scheme showing the expected *in-locus* insertion of the replacement construct, as well as the replacement cassette (bottom) employed in this work. Schematic representation of a 7 kb genomic region of the *bcku70* locus, located in Supercontig 217 of the B05.10 strain genome database. The *bcku70* gene and its transcriptional orientation (2,063 bp; Bc1G_ 16015, genomic coordinates 15622-17684) are represented as a purple arrow. The position of the genomic regions employed for the homologous recombination (orange boxes) are shown (to scale) next to *bcku70*. Black arrows show primers used for diagnostic PCRs, indicating their respective position and orientation. **(B)** Diagnostic PCRs showing *in-locus* integration. Homologous integration at the upstream (lane 1) and downstream- *bcku70* locus (lanes 2) are shown for the OE::*bcfrq1* mutant. No wild-type locus was observed for the OE::*bcfrq1* strain after single-spore isolation (lane 3) in comparison with the B05.10 wild-type strain (lane 4). **(C)** Primer pairs used in diagnostic PCRs (with respect to the gene transcriptional orientation). For detailed information see Table 8.

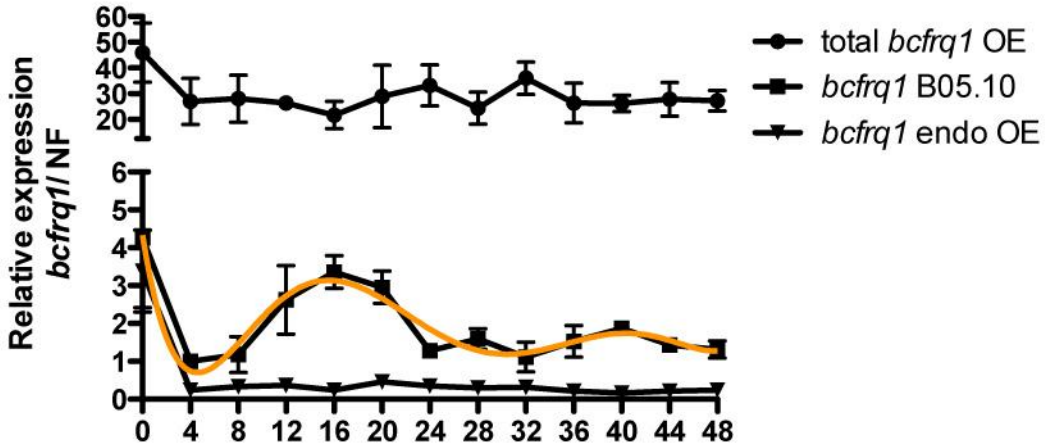

Figure 30. *bcfrq1* transcript levels become elevated and arrhythmic in the OE::*bcfrq1* genetic background. Total and endogenous *bcfrq1* transcript amounts were determined by RT-qPCR in the OE::*bcfrq1* strain and compared to *bcfrq1* transcript levels in the B05.10 strain. Transcript levels are normalized in reference to the culture grown 4 h in the dark determined for the B05.10 strain (1=DD4) and all the plots represent three biological replicates. Each point, in black, represents mean values ± SEM, while a trend line is depicted in orange. Primer pairs employed for RT-qPCR amplification are indicated in Table 3.

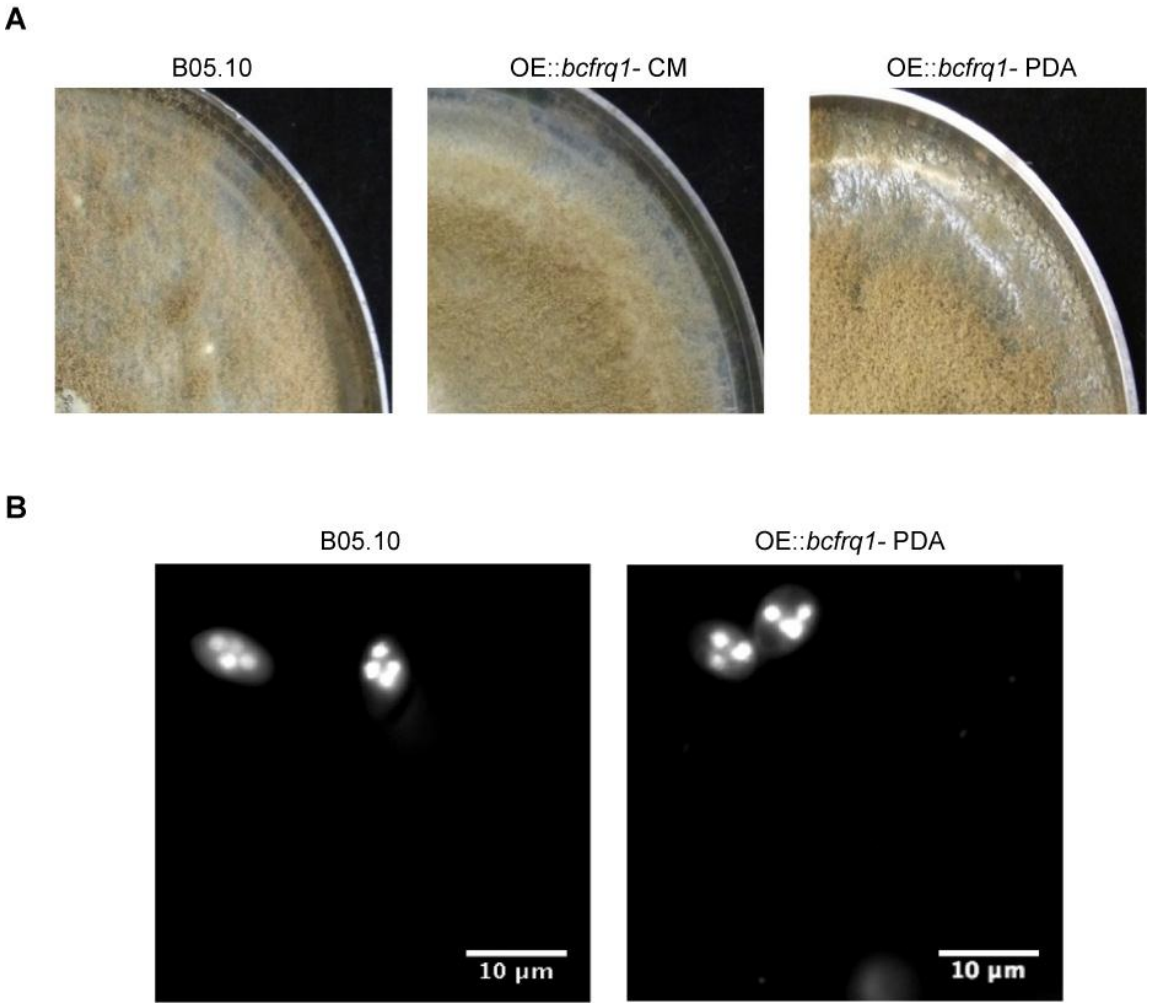

Figure 31. The OE::*bcfrq1* strain has normal developmental phenotypes. (A) B05.10 and OE::*bcfrq1* strains were incubated on CM and PDA for 14 days under LD culture conditions. **(B)** Fluorescence microscopy of 14 days old B05.10 and OE::*bcfrq1* strains grown in PDA plates. Conidia were staining with the nuclear dye Hoechst and visualized using a Cytation 3 Cell Imaging Multi-Mode Reader.

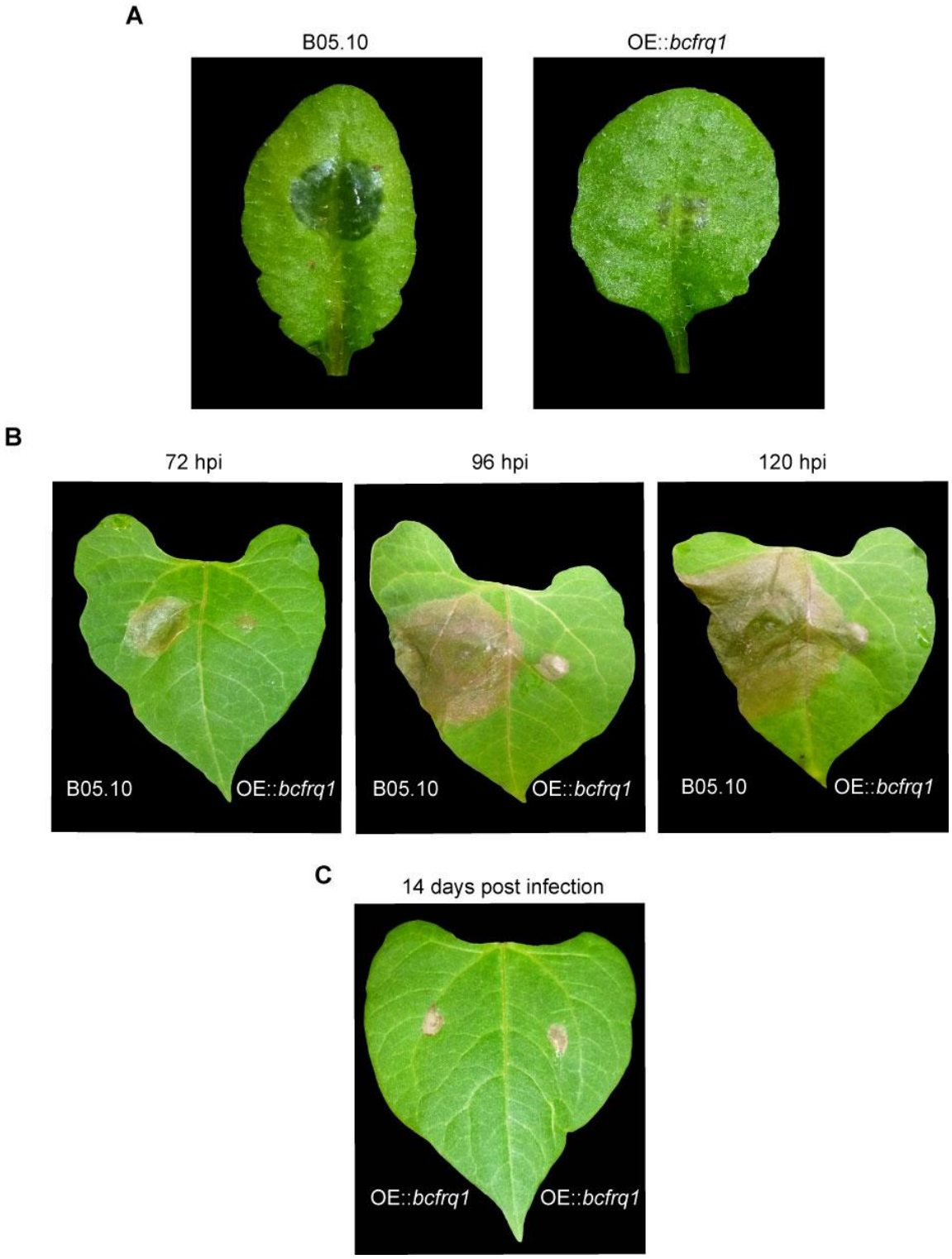
A
B05.10
OE::bcfrq1
B
72 hpi
96 hpi
120 hpi
B05.10
OE::bcfrq1
B05.10
OE::bcfrq1
B05.10
OE::bcfrq1
C
14 days post infection
OE::bcfrq1
OE::bcfrq1

Figura 32. The OE::*bcfrq1* strain presents an altered virulent process. (A) Lesion spreading of B05.10 wild-type and OE::*bcfrq1* strain on *A. thaliana* Col-0 plants, inoculated with a conidial suspension ($2x10^5$ /ml, 7µl). Pictures were acquired 72 hpi. **(B)** Lesion spreading of B05.10 and OE::*bcfrq1* strains on *P. vulgaris* plants, inoculated with a conidial suspension ($2x10^5$/ml, 7µl). Pictures were acquired after 72, 96 and 120 hpi. **(C)** Representative picture of an impaired lesion caused by OE::*bcfrq1* strain on *P. vulgaris* plant. Picture was acquired after 14 dpi. Virulence assays were done at dawn and the plants and the fungus come from 12:12 photocycle.

4.2.9 The outcome of the Botrytis-Arabidopsis interaction presents a time of infection dependent variation phenotype

As previously described, the *A. thaliana* circadian clock allows the plant to anticipate the infection process at the time of the day when pathogen attack is most likely to happen (as learnt by employing biotrophic oomycetes, virulent bacteria and insects) (Wang et al., 2011, Bhardwaj et al., 2011, Shin et al., 2012, Goodspeed et al., 2012, Zhang et al., 2013, Sharma and Bhatt, 2014). With this in mind, we decided to analyze what happens when a clock-containing pathogen like *B. cinerea* is assessed as the attacking organism.

Since we have observed that our *B. cinerea* clock mutant (Δ*bcfrq1* strain) has different developmental phenotypes that are depending on the culture media composition (PDA versus CM media), we decided to evaluate infection behavior of the B05.10 WT strain grown in both above-mentioned media. The results depicted in Figure 33 reveal that when both plant and fungus are grown in LD culture conditions, the outcome of the *B. cinerea* and *A. thaliana* interaction presents significant differences depending on the time of the day at which the first interaction between them occurs. Thus, when the initial physical contact of both organisms occurs at dawn, a significantly smaller lesion area is observed, in comparison when the infection takes place at dusk. On average, the percentage of leave-infected area was 6.1 and 16.8% at dawn and dusk, when the B.0510 strain was grown on PDA media. On the other hand, when the WT fungus comes from CM plates, the percentage of infected area was 12.8 and 18.7% between dawn and dusk. Nevertheless, from these results we cannot rule out if the differences are explained by a cyclical behavior -driven by the environment- in each

organism (or in both), or -if instead- it is being endogenously (circadianly) controlled. Consequently, we proceeded to define the contribution of each circadian system in this temporal regulation of the pathogenic outcome.

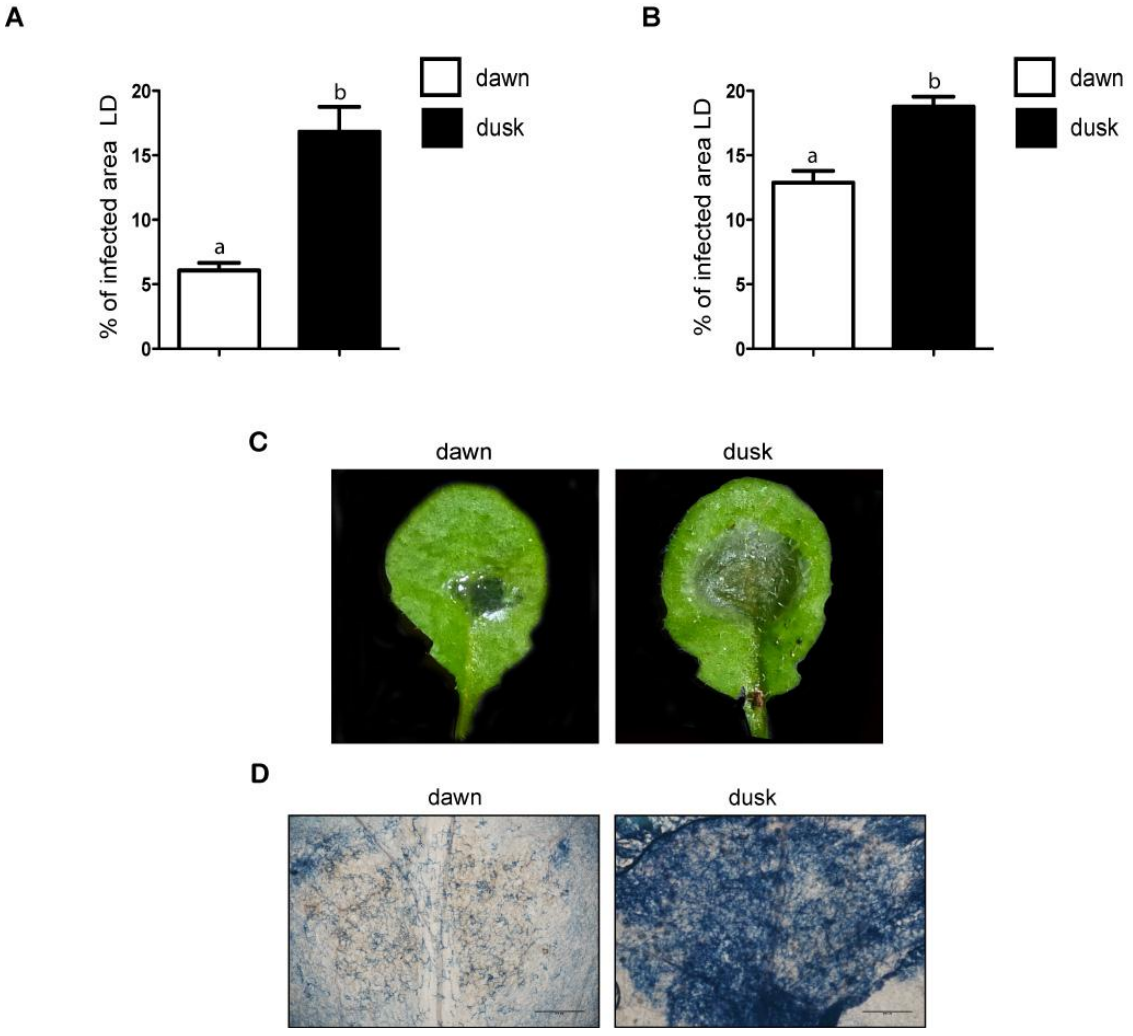

Figure 33. The outcome of the *B. cinerea*-plant interaction differs with the time of day. *A. thaliana* plants were infected at dawn or dusk with conidia from B05.10 wild-type strain obtained from PDA **(A)** and CM **(B)** plates. Quantification of lesion spreading were obtained from three independent virulence assays after 72 hpi under LD conditions. Bars represent the mean ±SEM. Different letters indicate significant difference among the samples; Mann- Whitney ($p < 0,05$). **(C)** Representative picture showing the differences in the infection process between dawn and dusk in *A. thaliana* plants infected with WT conidia obtain from PDA plates. **(D)** Trypan blue staining showing fungal growth at 3 dpi under LD, conidia for infection were obtain from PDA plates (black scale bars represent 500 μm).

4.2.10 An endogenous circadian clock controls the infection process of *B. cinerea* on *A. thaliana*

To evaluate the contribution of the *B. cinerea* circadian system in virulence, three Botrytis clock mutant strains were used. The Δ*bcwcl1* deletion mutant (Canessa et al., 2013) and the OE::*bcfrq1* strain were chosen, since *bcfrq1* mRNA levels are extremely low and flat in the first strain, while the second presents high and arrhythmic expression of *bcfrq1* mRNA (Figure 16 and 30). The third strain corresponds to Δ*bcfrq1* grown on CM plates, since macroconidia of this clock-null strain can be obtained from such condition. On the other hand, the *A. thaliana* CCA1-overexpressing line (CCA1ox) (Wang and Tobin, 1998, Bhardwaj et al., 2011) and the triple mutant *prr9 prr7 prr5* (*d975*) (Nakamichi et al., 2005, Nakamichi et al., 2009) that are arrhythmic with respect to circadian outputs in LL, DD and LD, were also employed.

In order to test the role of the circadian clock and to eliminate effects driven by the environment cycles (LD), infection experiments were first performed under FRC. As described in materials and methods, prior to inoculation Col-0 and CCA1ox *A. thaliana* plants were grown for two weeks under a 12:12 photoperiod, while the WT and mutant *B. cinerea* strains were also grown under the same conditions. Plants were inoculated with Botrytis either at dawn or dusk, to then be transferred to constant darkness for 72 h. Three dpi, the result of the plant-fungus interaction was evaluated. As shown in Figure 34A, the outcome of the *B. cinerea*/*A. thaliana* interaction significantly differed depending of the time of the day at which the presentation of the fungus occurred, while maintaining both organisms under FRC in constant darkness, during the development of the infection process. Thus, when B05.10 interacts with Col-0 Arabidopsis plants, a

bigger percentage of infected area was observed at dusk (14.8 and 19.6% at dawn and dusk, respectively). To unravel if these differences are explained by a temporal regulation commanded by the Arabidopsis' clock, the Botrytis´ clock or both, CCA1ox arrhytmic plants were challenged with the same WT strain. As shown in Figure 34A and 35, a bigger percentage of lesion area was still observed when the WT strain infected this arrhythmic Arabidopsis plant at dusk (20.7 and 26.8% at dawn and dusk, respectively). Importantly, the basal level of infection was higher in the CCA1ox genetic background. The fact that there is a time-of-the-day difference or temporal regulation even when an *A. thaliana* clock-deficient mutant is used, powerfully suggests that the fungal clock is playing a key role in the interaction outcome. In agreement with this hypothesis, the arrhythmic Δ*bcwcl1* strain is unable to produce a significantly bigger lesion area at dusk in the rhythmic Col-0 and arrhythmic CCA1ox plant (Figure 34A and 35), and, as a matter of fact, no statistically significant differences were observed between the two times of infection analyzed.

In order to exclude the possibility that the loss of temporal variation seen for the infections with Δ*bcwcl1* in DD resulted from defects in the blue light signaling pathway rather than by the absence of a functional circadian clock, the OE::*bcfrq1* mutant was used. As shown in Figure 34B and 35, the B05.10 WT strain has increased virulence at dusk when infecting Col-0 and CCA1ox plants (15.4 and 21.3% at dawn and dusk for Col-0; 22.8 and 28.8% at dawn and dusk for CCA1ox). Notably, OE::*bcfrq1* displayed, as also seen for the other arrhythmic *B. cinerea´*s strain (Δ*bcwcl1*), a loss of the circadian effect on virulence, being unable to achieve better infection at night in both Col-0 (6.5 and 4.8% at dawn and dusk, respectively) and CCA1ox (5.3 and 5.0% at

dawn and dusk, respectively) *A. thaliana* plants.

Finally, Δ*bcfrq1* macroconidia gave us the opportunity to confirm the influence of the fungal clock in the plant-pathogen circadian phenotype under study. Consistent with the previous observations, WT Botrytis showed the ability to infect strongly at night (14.78 and 23.3% at dawn and dusk for Col-0; 21.7 and 30.7% at dawn and dusk for CCA1ox), while infection with the Δ*bcfrq1* clock deficient strain resulted in the loss of temporal regulation, with no statistically significant differences in the percentage of leave infected area when inoculation was performed at dawn or at dusk in both rhythmic (23.3 and 26.2 % at dawn and dusk, respectively) and arrhythmic (31.4 and 30.3 % at dawn and dusk, respectively) plants (Figure 34C and 35). The fact that the temporal regulation in the outcome of the interaction is present even when the WT fungus infects the arrhythmic *A. thaliana* ecotype, but that is not observed when the arrhythmic fungus infects the rhythmic Col-0 plant, strongly indicates that the outcome of the *B. cinerea*/*A. thaliana* interaction is influenced by the fungal circadian clock, leading the pathogen to achieve differential infection levels at night versus day.

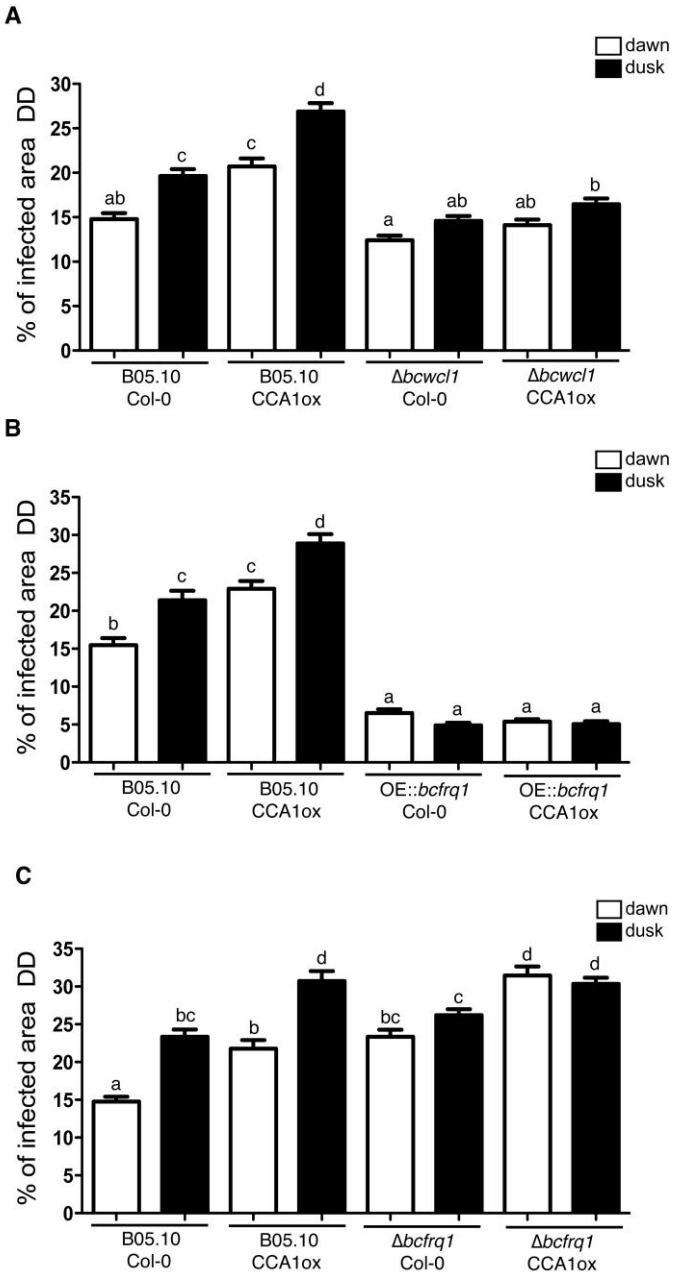

Figure 34. The infection process of *B. cinerea* on *A. thaliana* is controlled by an endogenous circadian clock. Measurements of lesion spreading of B05.10 WT, Δ*bcwcl1* **(A)**, OE::*bcfrq1* **(B)** and Δ*bcfrq1* **(C)** strain on *A. thaliana* Col-0 and CCA1ox plants inoculated with a conidial suspension ($2x10^5$ /ml, 7µl) at dawn or dusk under FRC (DD). The results were obtained from four independent virulence assays. Bars represent the mean ±SEM. Different letters indicate significant difference among the samples; three-way analysis of variance and Tukey´s HSD ($p<0,05$).

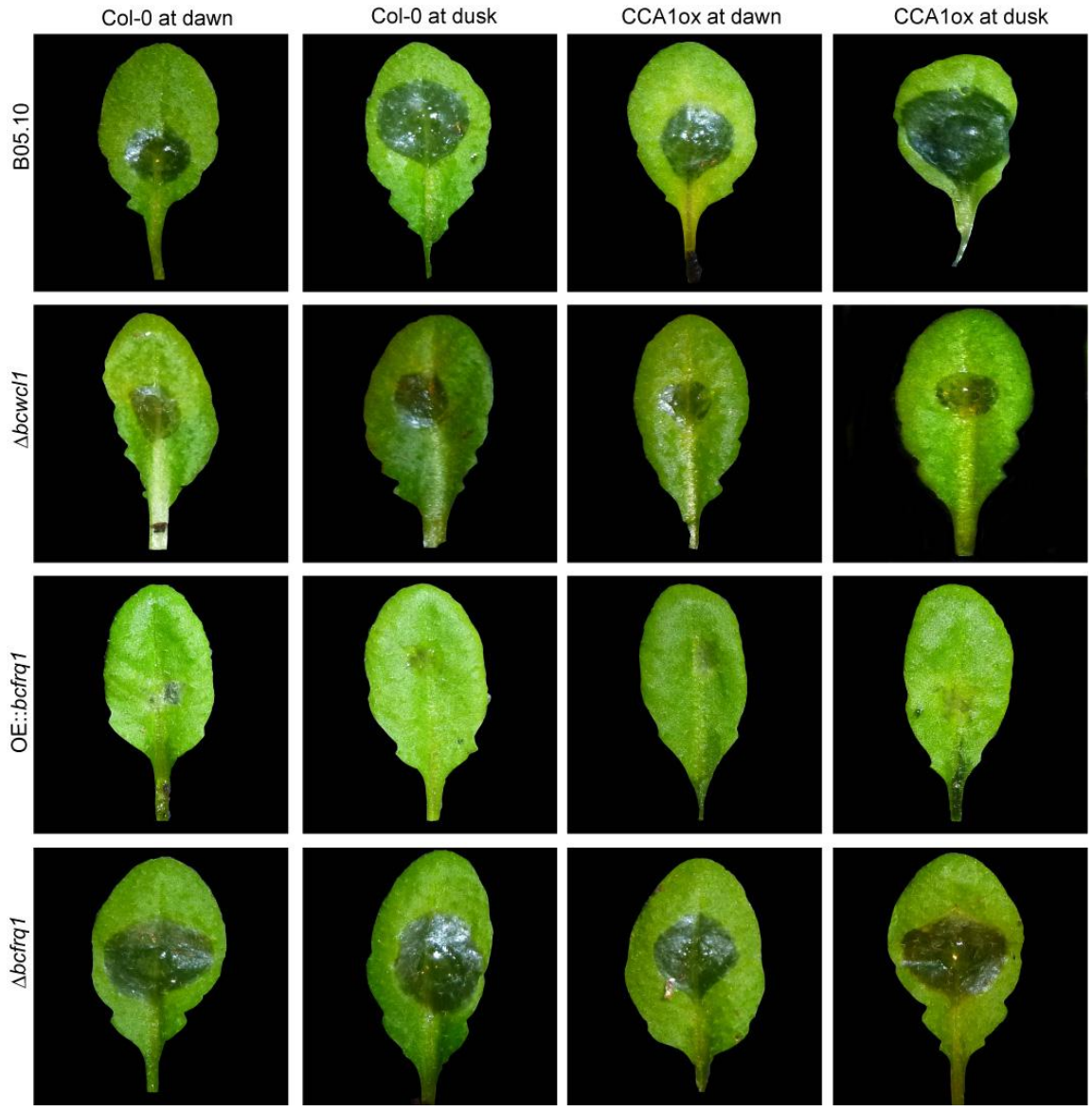

Figure 35. *B. cinerea* has better ability to infect at night in rhythmic and clock-null Arabidopsis plants. Representative pictures of lesion spreading of B05.10 wild-type, Δ*bcwcl1*, OE::*bcfrq1* and Δ*bcfrq1* strain on *A. thaliana* Col-0 and CCA1ox plants inoculated with a conidial suspension ($2x10^5$ /ml, 7µl) at dawn or dusk under FRC (DD).

4.2.11 Light-dark cycles confirm the importance of the *B. cinerea* circadian clock in regulating virulence under environmental relevant conditions

To obtain further proof highlighting the importance of fungal versus plant clock in mediating the interaction, infection assays were performed under LD culture conditions, in order to mimic a natural environment in which plants and pathogens meet daily. Figure 36A and 36B depicts that meanwhile the B05.10 WT strain displays significant differences in its infection capability between dawn and dusk when inoculated on Col-0 and CCA1ox plants, the *B. cinerea´s* clock mutants were unable to produce bigger lesion area at dusk, which reflects and confirms that the differences in the infection behavior observed between dawn and dusk for the *B. cinerea* WT strain under both DD and LD culture conditions are due to the control of its circadian clock rather than driven by environmental cues. Thus, these results are consistent with a scenario in which the fungal clock, rather than an environmental driven behavior or the plant clock, is largely responsible for the outcome of the interaction.

4.2.12 Under constant light the *A. thaliana* clock acquires a dominant role

Additional assays were performed under FRC, but this time under constant light (LL). As reported, this setting allows the plant's clock to free-run (McClung, 2001), while the *B. cinerea* clock does not (Figure 16C). As shown in Figure 36C and as observed in the previous experiments, inoculation of Col-0 plants at dusk with the B05.10 WT strain (which does not have a clock under LL) showed a bigger significant percentage of infected area (3.0 and 4.5% at dawn and dusk, respectively), but notably, no significant differences were observed between dawn or dusk (5.6 and 5.2%,

respectively), when the CCA1ox plants were challenged with the B05.10 strain, demonstrating that under LL conditions – and in contrast to what is seen in LD and DD- the *A. thaliana* circadian clock acquires a preponderant role.

4.2.13 Additional plant arrhythmic mutants and inverted-cycle infection further confirm the relevance of the fungal clock under FRC

To provide additional lines of evidence supporting the importance of the fungal versus the plant clock under FRC (DD), we tested the behavior of WT *B. cinerea* on the *prr9 prr7 prr5* (*d975*) arrhythmic Arabidopsis mutant (Nakamichi et al., 2005, Nakamichi et al., 2009). Once again, we observed that despite the absence of a functional clock in the plant, the WT *B. cinerea* strain is capable of producing differential lesions with larger ones at night (16.9 and 23.2% at dawn and dusk for Col-0; 23.6 and 28.3%at dawn and dusk for *d975*), and that moreover, this arrhythmic triple Arabidopsis mutant is –as also observed for CCA1ox- more sensitive to this pathogen (Figure 36D)

Finally, we proceeded to work with inverted cycles in order to determine in a different manner the relevance of both clocks. Thus, the fungus was entrained in an inverted light-dark cycle (12-h out-of-phase) to the one under which the plants were grown. Then we proceeded to infect the plants at dawn or dusk with *B. cinerea* that had the same internal time or that had the opposite time than the plants, maintaining them thereafter in FRC (DD) for 72 h. Plants inoculated with the fungus that had been under the same LD entrainment recapitulated the type of results already shown (Figure 34). Notably, in the inverted cycle experiment, we observed that plants challenged at dawn

showed larger lesions when the fungus that was inoculated on them had dusk-time, while plants inoculated at dusk with fungus that had dawn-time displayed smaller lesions (Figure 36E). In the aggregate, these experiments provide additional and compelling evidence supporting the importance of the *B. cinerea* clock in controlling its pathogenic potential.

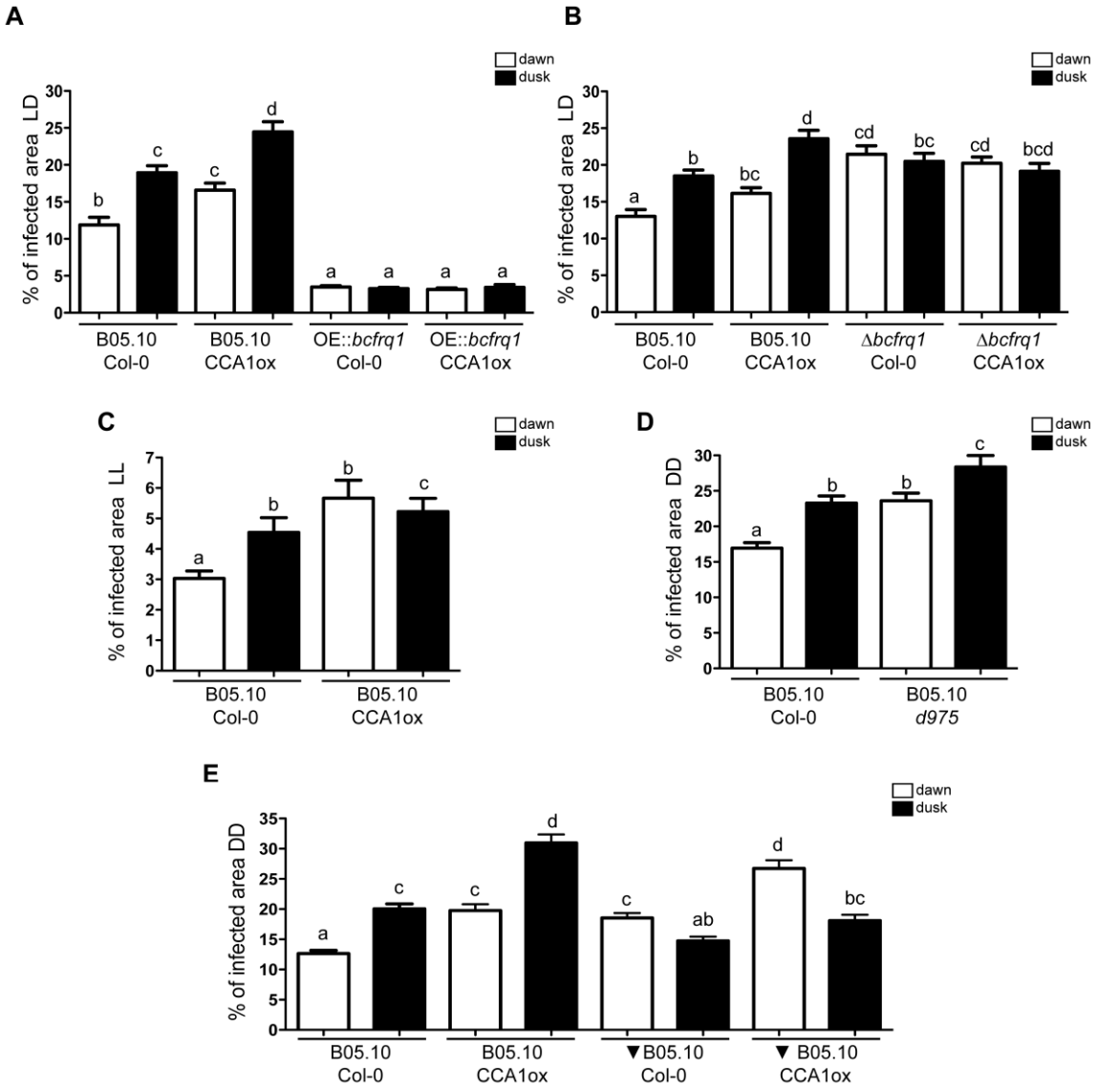
A
B
C
D
E
dawn
dusk
% of infected area LD
% of infected area LL
% of infected area DD
B05.10 Col-0
B05.10 CCA1ox
OE::bcfrq1 Col-0
OE::bcfrq1 CCA1ox
ΔbcfrQ1 Col-0
ΔbcfrQ1 CCA1ox
B05.10 d975
▼B05.10 Col-0
▼ B05.10 CCA1ox

Figure 36. The *B. cinerea* circadian clock influences the outcome of the interaction under 12:12 photocycles as well as under constant darkness conditions. (A) Disruption of the clock by *bcfrq1* overexpression (OE::*bcfrq1*) affects temporal variation of virulence in LD. **(B)** There are no differences in the infection behavior observed between dawn and dusk for the Δ*bcfrq1* strain in LD. **(C)** Under LL, the Arabidopsis clock- but not the Botrytis clock- provides a time-of the-day effect on susceptibility. **(D)** The B05.10 strain has the ability to produce bigger lesions at dusk in both Col-0 and *d975* arrhythmic mutant plants. **(E)** The relative magnitude of lesions achieved at dawn or dusk follows the time sensed by the fungus and not the plant. WT B05.10 strain was grown under the same LD cycle or 12 hours out of phase (represented as a black inverted triangle) than the plants. Arabidopsis were inoculated at dawn or dusk with *B. cinerea* grown in the same phase or having opposite times. In all graphs, after macroconidia inoculations, WT (Col-0) and mutant plants were kept under the specified LD, LL or DD regimes. Lesion area measurements were performed 3 dpi, obtained from three independent virulence assays. Bars represent mean ± SEM. Different letters indicate significant difference among the samples; three-way analysis of variance and Tukey´s HSD ($p<0,05$) for panel A, B and E; two-way analysis of variance and Tukey´s HSD ($p<0,05$) for panel C and D.

5. DISCUSSION

5.1 Shedding light on the *B. cinerea* light responses

For over a century, it has been known that light represents a key environmental cue for the plant pathogenic fungus *B. cinerea*. Old studies had already underlined the importance of light on the biology of this fungus: tropic responses of conidiophores, conidial germ tubes and fruiting bodies (Robinson, 1914, Godfrey, 1923, Gettkandt, 1952, Jaffe and Etzold, 1962, Jarvis, 1972), while others described light impact on fungal morphogenesis, promoting conidiation and suppressing sclerotia development (Peltier, 1912, Brierley, 1918). Until the development of this thesis, no molecular approaches had been undertaken to address these phenomena and the impact that light could have on *B. cinerea´s* virulence, neither how the ability to anticipate cyclic environmental changes could modify its pathogenic potential. So, we decided to initiate molecular studies to explore light perception in *B. cinerea*, focusing on the putative TF/blue-light photoreceptor BcWCL1, while also advancing the dissection of *B. cinerea´s* circadian system.

As previously indicated, the WCC is formed by two GATA-type TFs, in which WC-1 acts as the blue light-sensing domain that exerts a central and conserved role in fungal light regulation, as seen in *N. crassa* (He et al., 2002, Froehlich et al., 2002). The WCC has also been described in other ascomycetes like *A. nidulans* LreA/ LreB (Purschwitz et al., 2008), *T. atroviride* BLR-1/ BLR-2 (Casas-Flores et al., 2004), zygomycetes (*P. blakesleeanus* MadA/ MadB (Idnurm et al., 2006, Sanz et al., 2009) and basidiomycetes (*C. neoformans*) BCW1/ BCW2 (Idnurm and Heitman, 2005). Nonetheless, it is noteworthy that only in *N. crassa* it has been demonstrated that WC-1

is a real blue light photoreceptor, since it is associated with stoichiometric amounts of the chromophore flavin and, moreover, when the LOV domain is removed, light responses are eliminated (He et al., 2002). As shown here, the *B. cinerea* genome encodes for homologues of the TFs WC-1 and WC-2. Both proteins exhibit characteristic conserved regions, including the WC-1 LOV domain necessary to sense light and the WC-1/WC-2 PAS domains that can mediate the interaction of both TFs in nuclei of *B. cinerea*, as recently observed by BIFC analyses (Schumacher, 2012).

B. cinerea responds to white light, producing an increase in expression for genes encoding photoreceptors as well as TFs when dark-grown developmentally mycelia were exposed to light (Figure 3 and 7). Remarkably, although in *N. crassa* it has been established that the increase in transcript levels of all analyzed light-responsive genes is based on the action of the WCC, our study revealed that the *B. cinerea* orthologous for some of these genes maintained light responsiveness even in the absence of *bcwcl1* (Figure 7), indicating that the function of BcWCL1 to drive gene expression in response to light is only partially conserved in *B. cinerea* and suggesting that other photoreceptors are participating in the responses to light. Among the shared WCC targets in *B. cinerea* and *N. crassa* that were analyzed in this thesis are genes encoding for heme biosynthesis, for proteins that are part of the circadian clock (also characterized in this work), for putative blue light photoreceptors including *bcvvd1* and *bccry1*, a putative green light photoreceptor (*bop1*) and for several putative TFs (*bctlf1*, *bccsp1*, *bcsah1*, *bcadv1* and *bcvad3*). While light induction of the expression of the genes encoding for the TFs *csp-1*, *sub- 1* and *sah-1* directly depends on the WCC in *N. crassa*, only *bccsp1* expression loses light responsiveness in a Δ*bcwcl1* background. In contrast, *bcltf1* (*sub-1*

in *N. crassa*) and *bcsah1* were still expressed in a light-dependent manner in the mutant. In contrast, *bcvad3* or *bcadv1* levels are not increased by light, although the expression of the *N. crassa* orthologues has been shown to respond to the light stimuli (Smith et al., 2010). In aggregate, these results suggest that targets of WCC in *N. crassa* are not totally conserved in *B. cinerea*, opening up interesting questions related to the evolution of transcriptional networks and underlying physiology changes that are triggered upon light stimulation in this plant pathogen.

Divergence of downstream signaling events may reflect that light differentially affects the lifestyles of different fungi, even those of closely relates species. Thus, for example, light strongly favors conidiation in *A. nidulans* (Mooney et al., 1990), minimally affects this process in *A. fumigatus* (Fuller et al., 2013), while in *A. oryzae* conidiation is repressed by light (Hatakeyama et al., 2007). Also, interesting differences related to sexual and sclerotial development are observed in response to light and its absence, respectively, in various Aspergilli (Dyer and O'Gorman, 2012). In the genus *Trichoderma*, White Collar homologues have also been shown to regulate light responses, showing strong evidence for genes under a negative regulation in response to this environmental cue (Carreras-Villasenor et al., 2012). Similarly, while several genes are positively regulated by light in *C. neoformans*, other processes as mating (cell fusion) are negatively affected by this environmental signal (Idnurm and Heitman, 2005). Remarkably, sclerotial development is differentially regulated by light in the closely related species *B. cinerea* and *S. sclerotiorum*.

Despite the fact that several filamentous fungi employ light as an environmental cue that provides information on the whereabouts (spilled in the soil, inside the host,

exposed to the air), they have to cope like most organisms with the detrimental effects of light. Considering that *B. cinerea* is adapted to natural light conditions, the B05.10 WT strain exhibits comparable growth rates in LD and DD under laboratory conditions (Figure 2C and 6A). However, excessive illumination (LL) significantly impairs growth of the B05.10 strain and even more in the case of the Δ*bcwcl1* mutants (Figure 6). The toxic effect of light can be enhanced and reversed by applying additional oxidative stress (H_2O_2) or antioxidants (ascorbate), respectively, indicating that light causes oxidative stress and that the BcWCL1 is mediating the adaptation to this condition (Figure 9). Thus, it is possible to hypothesize that among the blue light/ WCC target genes are those encoding enzymes involved in ROS detoxification and/ or DNA repair.

In *N. crassa*, the increase of ROS (by addition of menadione, or deletion of *sod-1*) allows to visualize the rhythmic output of the circadian clock on the control of conidiation (Belden et al., 2007). Therefore, it is tempting to speculate that the enhanced ‘‘banding’’ phenotype observed under 12:12 LD photocycles for the Δ*bcwcl1* mutant may be because of differences in the intracellular ROS levels, since the knockout strain has problems to cope with ROS. Indeed, these bands are eliminated when race tubes are filled with an antioxidant (Figure 10). Nonetheless, the Δ*bcwcl1* knockout strain also presents a hyper conidiation phenotype (under LD, LL and DD, data not shown), which can contribute to the exacerbated rhythmic conidiation pattern. It is possible to hypothesize that BcWCL1 is acting as a repressor agent of conidiation, since *bcsha1* transcript levels (which is involved in the asexual reproduction in *N. crassa*) are elevated in the absence of BcWCL1 and even under DD conditions.

One of the important findings obtained during this thesis is the observation that lighting conditions can dramatically change virulence of the *B. cinerea* B05.10 wild-type strain. Thus, we observed that in the presence of constant light virulence is dramatically decreased and lesions reach in average 28% of the size they develop in the presence of constant darkness. Although we detected constant light reduced growth rate (27% of the growth observed in DD) (Figure 6), this decline can not be responsible of the decrease of pathogenic potential. Now we know that in LL conditions, *B. cinerea* has a dysfunctional circadian clock, which in some way is affecting the virulence process. Therefore, it can be stated that light conditions negatively affect virulence in *B. cinerea*. Another interpretation could be that plant defenses are positively affected by light. In this regard, studies performed in *A. thaliana* have reported on the capacity of light to elevate the H_2O_2 production, with the concomitant increased of callose formation (Luna et al., 2011), which could subsequently hamper the fungal ability to colonize the plant tissue. So, the use of blind *B. cinerea* mutants can contribute to underscore the importance of light during the fungal-plant interaction, but from the fungal perspective.

Thus, herein we demonstrated a function for the putative TF/blue light photoreceptor BcWCL1 during plant infection in the presence of light, as lesion size are further reduced in Δ*bcwcl1* (Figure 12), compared to the wild-type strain. Importantly, and in agreement with BcWCL1 role in light perception, this effect on virulence is more dramatic under constant light conditions, compared to photo cycles, while it is inexistent in constant darkness (Figure 12). Although we observed that there is a decrease in the Δ*bcwcl1* growth rate in LL and LD, this diminution can not explain the decline in the infection process: for example, under LL the Δ*bcwcl1* presents a 25% of reduction in its

growth rate in comparison with the B05.10 strain (Figure 6), while the reduction in virulence for Δ*bcwcl1* is 67% compared with the wild-type strain (Figure 12). Since excessive light impairs the growth of the mutant by generating ROS, the Δ*bcwcl1* deletion mutant may have problems to cope with ROS that are produced by the plant within the extent of an oxidative burst as part of the host defense mechanisms.

5.2 Timing in the *B. cinerea*- *A. thaliana* interaction

Circadian clocks allow organisms to organize their inner physiology in a temporal way, providing adaptation to the environment. It is well known that clocks confers selective advantages in mammals, plants and cyanobacteria (Ouyang et al., 1998, Dodd et al., 2005, Yerushalmi and Green, 2009, Lowrey and Takahashi, 2011), but the process is poorly understood in pathogens and the limited available data is only at a phenotypical level (Goodspeed et al., 2012, Mideo et al., 2013). The latter is mainly because there are no molecular studies addressing the presence of circadian clocks in any infectious organism. The study presented here, provides the first molecular evidence of the existence of a circadian oscillator in fungi other than Neurospora in general, and in particular in a fungal plant pathogen (or in any pathogenic organism!), providing compelling evidence that circadian regulation can underpin the regulation of fungal virulence.

Conidia is considered the main dispersed inoculum of *B. cinerea* (Holz et al., 2004) and it has been shown that at least for a biotrophic pathogen, sporulation occurs at night and spores are disseminated at dawn because enhanced humidity optimizes germination and colonization (Slusarenko and Schlaich, 2003), which suggest that the

sporulation process could be under circadian control, driven by an endogenous clock. In order to test this hypothesis, we examined if the conidiation rhythm observed in *B. cinerea* under a LD photoperiod (Figure 2D and Figure 6C) was also observed under DD conditions (that is if it was controlled by an endogenous clock, and was not just a driven environmental response). Interestingly, no circadian regulation of conidiation was observed in *B. cinerea* under FRC (Figure 15), which differs from what has been described for *N. crassa*, in which asexual sporulation is under circadian control (Sargent et al., 1966). Nevertheless, for this latter organism, this observation could be explained since the Neurospora strain used for decades for circadian laboratory studies possesses a mutation in the *ras-1* gene that allows a clear visualization of circadian rhythms in conidiation (Belden et al., 2007). Although the "real" wild-type *N. crassa* strain shows this circadian conidiation behavior when race tubes are filled with culture media supplemented with H_2O_2 or menadione, these ROS-stimuli were not able to promote the appearance of overt rhythms in conidiation in dark grown *B. cinerea* (data not shown).

Despite the absence of phonotypical data, we were able to establish the existence of an endogenous circadian clock through molecular assays (Figure 16, 18 and 30). *bcfrq1* mRNA levels oscillate under light-dark cycles and also under FRC. Importantly, they are lost in a Δ*bcwcl1* strain and under LL conditions (Figure 16). This is consistent with the notion that in *N. crassa frq* transcript levels oscillate under a cyclical environment (Dunlap, 1999) and also in constant darkness (Aronson et al., 1994b). Likewise, in Neurospora a dysfunctional circadian clock is evidenced under LL -due to high *frq* expression levels- (Crosthwaite et al., 1995) and also in a Δ*wc-1* strain (Lee et al., 2003). This last observation is also consistent with the fast light responsiveness of

bcfrq1 mRNA upon light stimulation, which depends on *bcwcl1* (Figure 7) (Canessa et al., 2013).

In addition, by overexpressing an extra copy of *bcfrq1* under a constitutive promoter, we demonstrated that *bcfrq1* expression levels at the endogenous locus become low and arrhythmic (Figure 30), recapitulating the iconic experiment performed by Aronson and coworkers (Aronson et al., 1994b) in *N. crassa*, which provided solid evidence for the central role of negative feedback loop in circadian core-mechanisms. Additionally, we showed that BcFRQ1 protein levels not only oscillate under DD culture conditions, but that also anticipate changes in temperature cycles and that can be entrained by cycles of different T (Figure 18). Together, these data demonstrate the presence of a functional circadian oscillator in *B. cinerea,* closing the gap in knowledge regarding clock mechanisms in fungi other than Neurospora. Although there have been attempts to describe circadian rhythms (output) in Aspergillus (Greene et al., 2003) or yeast (Eelderink-Chen et al., 2010), and that more recently the importance of circadian bioluminescence in a mushroom was described (Oliveira et al., 2015), in all cases the molecular bases of the underlying oscillators remain obscure. Importantly, our data demonstrate the presence of a circadian machinery in *B. cinerea* and confirm that the absence of an observable developmental rhythm is not evidence of lack of circadian control in this organism.

Remarkably, the Δ*bcfrq1* strain has a strong impact on sexual/ asexual reproduction that is dependent on the culture condition used (Figure 20 and 21). The latter clearly differs with what has been reported for the *frq* knockout strain (frq^{10}) of *N. crassa*, which shows no phenotypic alterations related to the production of conidia

(Aronson et al., 1994a). When cultivated on rich undefined PDA media, Gamborg B5 or Malt media, Δ*bcfrq1* forms sclerotia and produces microconidia and because of the lack of macroconidiation it is unable to infect (Jarvis, 1977, Urbasch, 1985) (Figure 24). Nonetheless, by employing a complete defined media (CM), we were able to cease the production of sclerotia under LD and to recover the generation of macroconidia, capable of infection (Figure 26). The fact that secondary nitrogen sources in the complete medium are responsible of reverting the phenotype of Δ*bcfrq1* (Figure 22) suggest that a relationship exists between nitrogen metabolism and the pathways controlled by BcFRQ1 outside the core circadian oscillator, which reflect that this protein has novel extra circadian functions that are either absent or not previously described in *N. crassa*. Moreover, the developmental phenotype of Δ*bcfrq1* (sclerotia and microconidia production) is observed even under conditions where the fungal clock is already disrupted by a constant environmental cue (LL; data not shown), and also because in the absence of BcWCL1 (where the clock is also broken) multinucleated conidia capable of infection are easily produced (Figure 12). With respect to the latter, we noticed that the phenotypes of Δ*bcwcl1* and Δ*bcfrq1* strains are quite different, even though one of the molecular consequences of BcWCL1 absence is low level of *bcfrq1* transcripts (Figure 7). Therefore, in the Δ*bcwcl1* strain part of the phenotypes should overlap with the ones in Δ*bcfrq1,* nevertheless, this does not occur. A plausible explanation resides in the known ability of FRQ to modify WCC activity. Thus, in Neurospora, the absence of FRQ leads to hyperactivity of WC-1 and its destabilization due to transcription-associated turnover (Shi et al., 2010). So, defects in signaling connected with BcWCL1 and other associated proteins involved in light signaling and development (i.e. BcVEL1

(Schumacher et al., 2012, Schumacher et al., 2015)) could be impacted by the absence of BcFRQ1.

Sclerotia are melanin pigments structures involve in stress responses, which functions as sugar reserves for dormancy periods of the sexual spores (Schumacher and Tudzynski, 2012). The latter suggest that BcFRQ1 could also be participating in tolerance to different stressors, due to the particular sclerotia phenotype that Δ*bcfrq1* strain presents under any light condition tested (Figure 20 and 21). Indeed, the MAPK mutant Δ*bcsak1* presents the same phenotypes of microconidia and sclerotia production of that of Δ*bcfrq1* strain and is not able to cope with oxidative and osmotic stress (Segmuller et al., 2007). Nonetheless, although BcFRQ1 is involved in differentiation programs, the protein is not necessary to cope, at least, with osmotic and stress responses (Figure 23), supporting the idea that a nutritional stress may be responsible for the switch between asexual/ sexual cycle in the knockout strain (Figure 22).

Recently, clock-mediated regulation in plants indicates that these organisms can anticipate biotic stimuli such as oomycete/bacterial pathogens and herbivore attacks (Sharma and Bhatt, 2014). Wang (Wang et al., 2011) demonstrated that the Arabidopsis central component CIRCADIAN CLOCK ASSOCIATED 1 (CCA1) acts as a positive integrator between the clock and defense pathways in resistance against the oomycete pathogen *Hyaloperonospora arabidopsidis* (*Hpa*), activating the expression of defense gene near dawn, when *CCA1* expression is high. *cca1* loss of function mutant has reduced resistance and overexpression of CCA1 would be increasing the defense response. Nevertheless, *lhy* mutants (LHY, a closely related MYB TF from CCA1) do not show decrement in disease resistance, although it displays a similar shortening of

circadian period to that seen in *cca1* mutants (McClung, 2006). Thus, it was not clear whether the circadian clock is regulating the plant immunity or if CCA1 is acting also on an output pathway non-regulated by the clock, rather than through the central clock mechanism (McClung, 2011). Thereby, Bhardwaj (Bhardwaj et al., 2011) found that under LL conditions, CCA1ox and *elf-3* (EARLY FLOWERING LOCUS) *A. thaliana* arrhythmic plants show loss of morning temporal regulation and altered susceptibility to infiltrated *Pseudomonas syringae* pv *tomato* (Pst) DC3000. On the other hand, Zhang (Zhang et al., 2013) reinforced and extended the study of Bhardwaj (Bhardwaj et al., 2011) of the involvement of the circadian clock in plant innate immunity, by showing that CCA1ox plants lost the temporal regulation in defense response and have enhanced susceptibility to *P. syringae* spray- infection in both LL and LD and that *cca1-1lhy-20* and *LHYox* plants presents the same susceptibility to *P. syringae* strains under LD, which can be explain since CCA1 and LHY are gating the stomatal defense response to dark. From these data we can ask two things: Why CCA1ox plants have different susceptibility to different pathogens and why plants present different temporal regulation in it defense mechanism? Altough Bhardwaj (Bhardwaj et al., 2011) and Zhang (Zhang et al., 2013) showed that CCA1ox has enhanced susceptibility to *P. syringae*, the latter author also observed that this arrhythmic plant has enhanced resistance to *Hyaloperonospora arabidopsidis* (*Hpa*), which is in agreement with the results published by Wang (Wang et al., 2011). So, the differences in response to these two different organisms suggest that there are distinct mechanisms that the plants use to defend themselves against different pathogens. In this way, is extremely important to define and use the same virulent/attacking organism in the studies in order to interpret

the results in a correctly manner. By answering the second question, Zhang (Zhang et al., 2013) demonstrated that different modes of infection resulted in different outcomes: Col-0 plants demonstrated higher resistance when infiltrated with *P. syringae* at dawn than at night, however, with spray-infection the plants were more resistant at night than in the morning. This result is explain since spray infection could mimic the mode of bacterial infection in nature, where stomata (which are open at dawn and close at dusk) provide a barrier to restrict pathogen entry, while in case of bacterial infiltration, the success of infection largely depends on the basal level defense of the host. Therefore, it is necessary to use appropriate infection methods in determining the outcome of a plant-pathogen interaction.

In this study, we demonstrated for the first time that the outcome of the interaction between a necrotrophic pathogen and its host differs with the time of the day, being the infection process more aggressive at dusk. Using the WT fungus and the CCA1ox and *d975* arrhythmic plants, we find that there is still a temporal regulation in the final product of the interaction between dawn and dusk, suggesting that the attacking organism clock is providing a clear control of the process. By using three *B. cinerea* strains with a dysfunctional circadian clock (Δ*bcwcl1*, OE::*bcfrq1* and Δ*bcfrq1*) under circadian DD and natural environmental LD conditions and the B05.10 wild-type strain entrained out-of-phase with the plant, we further confirmed that the circadian clock of *B. cinerea* impacts it fitness and is required to support and optimize maximal virulence at dusk (Figure 34, 35, 36). Nonetheless, in LL, a condition known to reduce *B. cinerea* basal infection levels (Figure 12) (Canessa et al., 2013), the environmental disruption of the fungal clock does not dramatically change the time-dependent outcome of the

interaction, while in return the plant clock seems to adopt an important role as revealed by the data in the CCA1ox mutant (Figure 36C), results that are aligned to what has been previously described for bacterial and oomycetes pathogens (Bhardwaj et al., 2011, Wang et al., 2011, Zhang et al., 2013).

Intriguingly, once we compensate Δ*bcfrq1* failure to produce microconida -by manipulating media composition- we observed that its macroconidia have a bigger infection capability than the B05.10 WT strain. However, the temporal difference to infect better at night is lost (Fig. 34C and 36B). It is intriguing that when removing a central clock component, such as BcFRQ1 (but not BcWCL1), the infection is significantly enhanced. Nonetheless -and as described above- similar results have been described for *A. thaliana*: Zhang and colleagues (Zhang et al., 2013) reported that arrhythmic CCA1ox plants have enhanced resistance to the oomycete pathogen *Hpa*, which is in agreement with the results published by Wang and colleagues (Wang et al., 2011). Nevertheless, Bhardwaj and colleagues (Bhardwaj et al., 2011) and Zhang et al., (Zhang et al., 2013) showed that the CCA1ox plants have enhanced susceptibility and loss of temporal regulation in defense to the virulent bacteria *P. syringae*. Thus, although one would intuitively predict that an arrhythmic plant is always more prone to infection (due to the loss of the adaptive advantage of the clock), some of the results in *A. thaliana* reveal the opposite. Thus, as it was described for the plant clock protein CCA1, BcFRQ1 could be acting on other output pathways not regulated by the circadian clock (McClung, 2011) further complicating the molecular dissection of clock regulation on virulence mechanisms.

In this fencing contest between these two organisms, the dominance of each clock is judge and the results presented here indicate that under DD and LD conditions, the *B. cinerea* clock plays an important role in the interaction, thus explaining part of the temporal variation of the infection process. The most important plant defense mechanism against necrotrophic infection is the jasmonic acid (JA) pathway (Browse, 2009). Interestingly, a circadian gating effect allows higher JA-signaling activity response during the morning (Goodspeed et al., 2012, Shin et al., 2012). Consequently, it is possible to hypothesize that the circadian clock of *B. cinerea* allows the fungus to anticipate the JA plant defense response, optimizing and generating its maximal virulence potential at dusk. Further studies will help us to elucidate the mechanisms by which the circadian clock is modulating the pathogenic potential of this hostile organism at different times of the day.

6. CONCLUSION

By addressing the main hypothesis of this thesis, we have provided molecular evidence that there is a light machinery in *B. cinerea*. In doing so, we have shown that in opposition to *N. crassa*, some WCC targets -but not all- depend on a WC-1 ortholog, revealing a complex underlying photobiology in this phytopathogen. Clear responses to light are enhanced in the absence of BcWCL1 revealing a more complex dialogue between this and other photoreceptors. Moreover, BcWCL1 is necessary to achieve full virulence in the presence of light, highlighting the role of light sensing in *B. cinerea* physiology and virulence.

On the other hand, this thesis represents a pioneer work in providing molecular evidence of the existence of a circadian clock in a pathogenic organism. Surprisingly, we unveiled extra-circadian functions for the core-clock component BcFRQ1, something unexpected based on what has been learnt for Neurospora FRQ over the last 25 years. By using *A. thaliana* as host model, we have shown daily differences in the pathogenic outcome of the Arabidopsis-Botrytis system. We observed that the lesions produced by this necrotrophic fungus on Arabidopsis leaves are smaller when the interaction between these two organisms occurs at dawn. Remarkably, this effect does not depend solely on the plant clock, but instead largely relays on the pathogen circadian system. Genetic disruption of the *B. cinerea* oscillator by mutation, overexpression of BcFRQ1, or by suppression of its rhythmicity by constant light, abrogates circadian regulation of fungal virulence. By conducting experiments with out-of-phase light-dark cycles, we confirmed that the outcome of the interaction depends on the time sensed by the fungus, providing

the first evidence of a microbial clock modulating and optimizing pathogenic traits at specific times of the day.

Finally, this work will contribute to the development and adoption of natural strategies to control *B. cinerea,* by applying concepts similar to chronotherapy or by using defined light conditions in greenhouses or in the post- harvest products that are stored/exported during long periods of time. Moreover, this study helps to strengthen the applied research in fungi, contributing to the general knowledge of light and circadian impact on the physiology of the organisms.

7. PUBLICATIONS

The following is a list of manuscripts published/submitted by the thesis author during the course of the doctorate.

1. Canessa P*, Schumacher J*, **Hevia MA**, Tudzynski P, Larrondo LF. Assessing the effects of light on differentiation and virulence of the plant pathogen *Botrytis cinerea*: characterization of the White Collar Complex. PLoS One. 2013 Dec 31;8(12):e84223. * *Both authors contributed equally*.

2. **Hevia MA*,** Canessa P*, Müller- Esparza H, Larrondo LF. When two clocks collide: a circadian oscillator in the fungus *Botrytis cinerea* regulates virulence when infecting *Arabidopsis thaliana*. P.N.A.S. In press. **Both authors contributed equally*.

8. REFERENCES

AMSELEM, J., CUOMO, C. A., VAN KAN, J. A., VIAUD, M., BENITO, E. P., COULOUX, A., COUTINHO, P. M., DE VRIES, R. P., DYER, P. S., FILLINGER, S., FOURNIER, E., GOUT, L., HAHN, M., KOHN, L., LAPALU, N., PLUMMER, K. M., PRADIER, J. M., QUEVILLON, E., SHARON, A., SIMON, A., TEN HAVE, A., TUDZYNSKI, B., TUDZYNSKI, P., WINCKER, P., ANDREW, M., ANTHOUARD, V., BEEVER, R. E., BEFFA, R., BENOIT, I., BOUZID, O., BRAULT, B., CHEN, Z., CHOQUER, M., COLLEMARE, J., COTTON, P., DANCHIN, E. G., DA SILVA, C., GAUTIER, A., GIRAUD, C., GIRAUD, T., GONZALEZ, C., GROSSETETE, S., GULDENER, U., HENRISSAT, B., HOWLETT, B. J., KODIRA, C., KRETSCHMER, M., LAPPARTIENT, A., LEROCH, M., LEVIS, C., MAUCELI, E., NEUVEGLISE, C., OESER, B., PEARSON, M., POULAIN, J., POUSSEREAU, N., QUESNEVILLE, H., RASCLE, C., SCHUMACHER, J., SEGURENS, B., SEXTON, A., SILVA, E., SIRVEN, C., SOANES, D. M., TALBOT, N. J., TEMPLETON, M., YANDAVA, C., YARDEN, O., ZENG, Q., ROLLINS, J. A., LEBRUN, M. H. & DICKMAN, M. 2011. Genomic analysis of the necrotrophic fungal pathogens Sclerotinia sclerotiorum and Botrytis cinerea. *PLoS Genet,* 7**,** e1002230.

ARONSON, B. D., JOHNSON, K. A. & DUNLAP, J. C. 1994a. Circadian clock locus frequency: protein encoded by a single open reading frame defines period length and temperature compensation. *Proc Natl Acad Sci U S A,* 91**,** 7683-7.

ARONSON, B. D., JOHNSON, K. A., LOROS, J. J. & DUNLAP, J. C. 1994b. Negative Feedback Defining a Circadian Clock - Autoregulation of the Clock Gene-Frequency. *Science,* 263**,** 1578-1584.

BAKER, C. L., KETTENBACH, A. N., LOROS, J. J., GERBER, S. A. & DUNLAP, J. C. 2009. Quantitative proteomics reveals a dynamic interactome and phase-specific phosphorylation in the Neurospora circadian clock. *Mol Cell,* 34**,** 354-63.

BAKER, C. L., LOROS, J. J. & DUNLAP, J. C. 2012. The circadian clock of Neurospora crassa. *FEMS Microbiol Rev,* 36**,** 95-110.

BALLARIO, P., VITTORIOSO, P., MAGRELLI, A., TALORA, C., CABIBBO, A. & MACINO, G. 1996. White collar-1, a central regulator of blue light responses in Neurospora, is a zinc finger protein. *EMBO J,* 15**,** 1650-7.

BAYRAM, O., BIESEMANN, C., KRAPPMANN, S., GALLAND, P. & BRAUS, G. H. 2008. More than a repair enzyme: Aspergillus nidulans photolyase-like CryA is a regulator of sexual development. *Mol Biol Cell,* 19**,** 3254-62.

BELDEN, W. J., LARRONDO, L. F., FROEHLICH, A. C., SHI, M., CHEN, C. H., LOROS, J. J. & DUNLAP, J. C. 2007. The band mutation in Neurospora crassa is a dominant allele of ras-1 implicating RAS signaling in circadian output. *Genes Dev,* 21**,** 1494-505.

BELL-PEDERSEN, D., CASSONE, V. M., EARNEST, D. J., GOLDEN, S. S., HARDIN, P. E., THOMAS, T. L. & ZORAN, M. J. 2005. Circadian rhythms from multiple oscillators: lessons from diverse organisms. *Nat Rev Genet,* 6**,** 544-56.

BELL-PEDERSEN, D., SHINOHARA, M. L., LOROS, J. J. & DUNLAP, J. C. 1996. Circadian clock-controlled genes isolated from Neurospora crassa are late night-to early morning-specific. *Proc Natl Acad Sci U S A,* 93**,** 13096-101.

BHARDWAJ, V., MEIER, S., PETERSEN, L. N., INGLE, R. A. & RODEN, L. C. 2011. Defence responses of Arabidopsis thaliana to infection by Pseudomonas syringae are regulated by the circadian clock. *PLoS ONE,* 6**,** e26968.

BLUHM, B. H., BURNHAM, A. M. & DUNKLE, L. D. 2010. A circadian rhythm regulating hyphal melanization in Cercospora kikuchii. *Mycologia,* 102**,** 1221-8.

BLUMENSTEIN, A., VIENKEN, K., TASLER, R., PURSCHWITZ, J., VEITH, D., FRANKENBERG-DINKEL, N. & FISCHER, R. 2005. The Aspergillus nidulans phytochrome FphA represses sexual development in red light. *Curr Biol,* 15**,** 1833-8.

BOLTON, M. D., THOMMA, B. P. & NELSON, B. D. 2006. Pathogen profile - Sclerotinia sclerotiorum (Lib.) de Bary: biology and molecular traits of a cosmopolitan pathogen. *Molecular Plant Pathology***,** 1-16.

BOURRET, J. A., LINCOLN, R. G. & CARPENTER, B. H. 1969. Fungal endogenous rhythms expressed by spiral figures. *Science,* 166**,** 763-4.

BREEN, D. P., VUONO, R., NAWARATHNA, U., FISHER, K., SHNEERSON, J. M., REDDY, A. B. & BARKER, R. A. 2014. Sleep and circadian rhythm regulation in early Parkinson disease. *JAMA Neurol,* 71**,** 589-95.

BRIERLEY, W. B. 1918. The microconidia of Botrytis cinerea. Studies from the pathological Laboratory VII. *Bulletin of Miscellaneous Information (Royal Gardens, Kew)***,** 129–146.

BROOKS, C. C., JS 1917. Temperature relations of apple-rot fungi. *Journal of Agricultural Research,* 8**,** 139-164.

BROWSE, J. 2009. Jasmonate passes muster: a receptor and targets for the defense hormone. *Annu Rev Plant Biol,* 60**,** 183-205.

BUTTNER, P., KOCH, F., VOIGT, K., QUIDDE, T., RISCH, S., BLAICH, R., BRUCKNER, B. & TUDZYNSKI, P. 1994. Variations in ploidy among isolates of Botrytis cinerea: implications for genetic and molecular analyses. *Curr Genet,* 25**,** 445-50.

CANESSA, P., SCHUMACHER, J., HEVIA, M. A., TUDZYNSKI, P. & LARRONDO, L. F. 2013. Assessing the effects of light on differentiation and virulence of the plant pathogen Botrytis cinerea: characterization of the White Collar Complex. *PLoS One,* 8**,** e84223.

CARRERAS-VILLASENOR, N., SANCHEZ-ARREGUIN, J. A. & HERRERA-ESTRELLA, A. H. 2012. Trichoderma: sensing the environment for survival and dispersal. *Microbiology,* 158**,** 3-16.

CARVALHO, L. C., SANTOS, S., VILELA, B. J. & AMANCIO, S. 2008. Solanum lycopersicon Mill. and Nicotiana benthamiana L. under high light show distinct responses to anti-oxidative stress. *J Plant Physiol,* 165**,** 1300-12.

CASAS-FLORES, S., RIOS-MOMBERG, M., BIBBINS, M., PONCE-NOYOLA, P. & HERRERA-ESTRELLA, A. 2004. BLR-1 and BLR-2, key regulatory elements of photoconidiation and mycelial growth in Trichoderma atroviride. *Microbiology,* 150**,** 3561-9.

CENIS, J. L. 1992. Rapid extraction of fungal DNA for PCR amplification. *Nucleic*

Acids Res, 20**,** 2380.
CERRUDO, I., KELLER, M. M., CARGNEL, M. D., DEMKURA, P. V., DE WIT, M., PATITUCCI, M. S., PIERIK, R., PIETERSE, C. M. & BALLARE, C. L. 2012. Low red/far-red ratios reduce Arabidopsis resistance to Botrytis cinerea and jasmonate responses via a COI1-JAZ10-dependent, salicylic acid-independent mechanism. *Plant Physiol,* 158**,** 2042-52.
CHANDRA-SHEKARA, A. C., GUPTE, M., NAVARRE, D., RAINA, S., RAINA, R., KLESSIG, D. & KACHROO, P. 2006. Light-dependent hypersensitive response and resistance signaling against Turnip Crinkle Virus in Arabidopsis. *Plant J,* 45**,** 320-34.
CHEN, C. H., DUNLAP, J. C. & LOROS, J. J. 2010. Neurospora illuminates fungal photoreception. *Fungal Genet Biol,* 47**,** 922-9.
CHEN, C. H., RINGELBERG, C. S., GROSS, R. H., DUNLAP, J. C. & LOROS, J. J. 2009. Genome-wide analysis of light-inducible responses reveals hierarchical light signalling in Neurospora. *EMBO J,* 28**,** 1029-42.
CHENG, P., HE, Q., HE, Q., WANG, L. & LIU, Y. 2005. Regulation of the Neurospora circadian clock by an RNA helicase. *Genes Dev,* 19**,** 234-41.
CHOQUER, M., ROBIN, G., LE PECHEUR, P., GIRAUD, C., LEVIS, C. & VIAUD, M. 2008. Ku70 or Ku80 deficiencies in the fungus Botrytis cinerea facilitate targeting of genes that are hard to knock out in a wild-type context. *FEMS Microbiol Lett,* 289**,** 225-32.
CHRISTIANSON, T. W., SIKORSKI, R. S., DANTE, M., SHERO, J. H. & HIETER, P. 1992. Multifunctional yeast high-copy-number shuttle vectors. *Gene,* 110**,** 119-22.
CHUNG, D. W., GREENWALD, C., UPADHYAY, S., DING, S., WILKINSON, H. H., EBBOLE, D. J. & SHAW, B. D. 2011. acon-3, the Neurospora crassa ortholog of the developmental modifier, medA, complements the conidiation defect of the Aspergillus nidulans mutant. *Fungal Genet Biol,* 48**,** 370-6.
COLLADO, I. G., SANCHEZ, A. J. & HANSON, J. R. 2007. Fungal terpene metabolites: biosynthetic relationships and the control of the phytopathogenic fungus Botrytis cinerea. *Nat Prod Rep,* 24**,** 674-86.
COLOT, H. V., PARK, G., TURNER, G. E., RINGELBERG, C., CREW, C. M., LITVINKOVA, L., WEISS, R. L., BORKOVICH, K. A. & DUNLAP, J. C. 2006. A high-throughput gene knockout procedure for Neurospora reveals functions for multiple transcription factors. *Proc Natl Acad Sci U S A,* 103**,** 10352-7.
CORREA, A., LEWIS, Z. A., GREENE, A. V., MARCH, I. J., GOMER, R. H. & BELL-PEDERSEN, D. 2003. Multiple oscillators regulate circadian gene expression in Neurospora. *Proc Natl Acad Sci U S A,* 100**,** 13597-602.
CORROCHANO, L. M. 2011. Fungal photobiology: a synopsis. *IMA Fungus,* 2**,** 25-8.
CROSTHWAITE, S. K., DUNLAP, J. C. & LOROS, J. J. 1997. Neurospora wc-1 and wc-2: transcription, photoresponses, and the origins of circadian rhythmicity. *Science,* 276**,** 763-9.
CROSTHWAITE, S. K., LOROS, J. J. & DUNLAP, J. C. 1995. Light-induced resetting of a circadian clock is mediated by a rapid increase in frequency transcript. *Cell,* 81**,** 1003-12.

CURTIS, A. M., BELLET, M. M., SASSONE-CORSI, P. & O'NEILL, L. A. 2014. Circadian clock proteins and immunity. *Immunity,* 40**,** 178-86.

DALMAIS, B., SCHUMACHER, J., MORAGA, J., P, L. E. P., TUDZYNSKI, B., COLLADO, I. G. & VIAUD, M. 2011. The Botrytis cinerea phytotoxin botcinic acid requires two polyketide synthases for production and has a redundant role in virulence with botrydial. *Mol Plant Pathol,* 12**,** 564-79.

DE WIT, M., SPOEL, S. H., SANCHEZ-PEREZ, G. F., GOMMERS, C. M., PIETERSE, C. M., VOESENEK, L. A. & PIERIK, R. 2013. Perception of low red:far-red ratio compromises both salicylic acid- and jasmonic acid-dependent pathogen defences in Arabidopsis. *Plant J,* 75**,** 90-103.

DEAN, R., VAN KAN, J. A., PRETORIUS, Z. A., HAMMOND-KOSACK, K. E., DI PIETRO, A., SPANU, P. D., RUDD, J. J., DICKMAN, M., KAHMANN, R., ELLIS, J. & FOSTER, G. D. 2012. The Top 10 fungal pathogens in molecular plant pathology. *Mol Plant Pathol,* 13**,** 414-30.

DEMKURA, P. V. & BALLARE, C. L. 2012. UVR8 mediates UV-B-induced Arabidopsis defense responses against Botrytis cinerea by controlling sinapate accumulation. *Mol Plant,* 5**,** 642-52.

DIOLEZ, A., MARCHES, F., FORTINI, D. & BRYGOO, Y. 1995. Boty, a long-terminal-repeat retroelement in the phytopathogenic fungus Botrytis cinerea. *Appl Environ Microbiol,* 61**,** 103-8.

DODD, A. N., SALATHIA, N., HALL, A., KEVEI, E., TOTH, R., NAGY, F., HIBBERD, J. M., MILLAR, A. J. & WEBB, A. A. 2005. Plant circadian clocks increase photosynthesis, growth, survival, and competitive advantage. *Science,* 309**,** 630-3.

DOEHLEMANN, G., BERNDT, P. & HAHN, M. 2006. Different signalling pathways involving a Galpha protein, cAMP and a MAP kinase control germination of Botrytis cinerea conidia. *Mol Microbiol,* 59**,** 821-35.

DONG, G., KIM, Y. I. & GOLDEN, S. S. 2010. Simplicity and complexity in the cyanobacterial circadian clock mechanism. *Curr Opin Genet Dev,* 20**,** 619-25.

DUNLAP, J. C. 1999. Molecular bases for circadian clocks. *Cell,* 96**,** 271-90.

DUNLAP, J. C. & LOROS, J. J. 2004. The neurospora circadian system. *J Biol Rhythms,* 19**,** 414-24.

DUNLAP, J. C., LOROS, J. J., COLOT, H. V., MEHRA, A., BELDEN, W. J., SHI, M., HONG, C. I., LARRONDO, L. F., BAKER, C. L. & CHEN, C. H. 2007. A circadian clock in Neurospora: how genes and proteins cooperate to produce a sustained, entrainable, and compensated biological oscillator with a period of about a day. *Cold Spring Harbor Symposia on Quantitative Biology,* 72**,** 57-68.

DURGAN, D. J. & YOUNG, M. E. 2010. The cardiomyocyte circadian clock: emerging roles in health and disease. *Circ Res,* 106**,** 647-58.

DYER, P. S. & O'GORMAN, C. M. 2012. Sexual development and cryptic sexuality in fungi: insights from Aspergillus species. *FEMS Microbiol Rev,* 36**,** 165-92.

EDMUNDS, L. N., JR., APTER, R. I., ROSENTHAL, P. J., SHEN, W. K. & WOODWARD, J. R. 1979. Light effects in yeast: persisting oscillations in cell division activity and amino acid transport in cultures of Saccharomyces cerevisiae entrained by light-dark cycles. *Photochem Photobiol,* 30**,** 595-601.

EELDERINK-CHEN, Z., MAZZOTTA, G., STURRE, M., BOSMAN, J.,

ROENNEBERG, T. & MERROW, M. 2010. A circadian clock in Saccharomyces cerevisiae. *Proc Natl Acad Sci U S A,* 107**,** 2043-7.

ELAD, Y., WILLIAMSON, B., TUDZYNSKI, B. & DELEN, N. 2007. *Botrytis: Biology, Pathology and Control*, Springer.

ENGELMANN, W. & JOHNSSON, A. 1998. Rhythms in organ movement. *In:* LUMSDEN, P. J. & MILLAR, A. J. (eds.) *Biological Rhythms and Photoperiodism in Plants.* Oxford: BIOS Scientific Publishers.

ESTERIO, M. & AUGER, J. 2006. Implicancias de la variabilidad genética en el control de Botrytis cinerea en vides en Chile: Resistencia a fungicidas.*Revista Aconex,* 92**,** 17-24.

ESTERIO, M., MUÑOZ, G., RAMOS, C., COFRÉ, G., ESTÉVEZ, R., SALINAS, A. & AUGER, J. 2011. Characterization of Botrytis cinerea Isolates Present in Thompson Seedless Table Grapes in the Central Valley of Chile. *Plant Disease,* 95**,** 683-690.

FARETRA, F. 1987. Production of apothecia of Botryotinia fuckeliana (de Bary) Whetz. under controlled environmental conditions

. *Phytopathologia mediterranea,* 26**,** 29-35.

FELDMAN, J. F. 1982. Annual Review of Plant Physiology. *Genetic approaches to circadian clocks,* 33**,** 583-608.

FOURNIER, E., GIRAUD, T., ALBERTINI, C. & BRYGOO, Y. 2005. Partition of the Botrytis cinerea complex in France using multiple gene genealogies. *Mycologia,* 97**,** 1251-67.

FOURNIER, E., LEVIS, C., FORTINI, D., LEROUX, P., GIRAUD, T. & BRYGOO, Y. 2003. Characterization of Bc-hch, the Botrytis cinerea homolog of the Neurospora crassahet-c vegetative incompatibility locus, and its use as a population marker. *Mycologia,* 95**,** 251-61.

FROEHLICH, A. C., LIU, Y., LOROS, J. J. & DUNLAP, J. C. 2002. White Collar-1, a circadian blue light photoreceptor, binding to the frequency promoter. *Science,* 297**,** 815-9.

FROEHLICH, A. C., LOROS, J. J. & DUNLAP, J. C. 2003. Rhythmic binding of a WHITE COLLAR-containing complex to the frequency promoter is inhibited by FREQUENCY. *Proc Natl Acad Sci U S A,* 100**,** 5914-9.

FROEHLICH, A. C., NOH, B., VIERSTRA, R. D., LOROS, J. & DUNLAP, J. C. 2005. Genetic and molecular analysis of phytochromes from the filamentous fungus Neurospora crassa. *Eukaryot Cell,* 4**,** 2140-52.

FULLER, K. K., RINGELBERG, C. S., LOROS, J. J. & DUNLAP, J. C. 2013. The fungal pathogen Aspergillus fumigatus regulates growth, metabolism, and stress resistance in response to light. *MBio,* 4.

GALLEGO, M. & VIRSHUP, D. M. 2007. Post-translational modifications regulate the ticking of the circadian clock. *Nat Rev Mol Cell Biol,* 8**,** 139-48.

GENOUD, T., BUCHALA, A. J., CHUA, N. H. & METRAUX, J. P. 2002. Phytochrome signalling modulates the SA-perceptive pathway in Arabidopsis. *Plant J,* 31**,** 87-95.

GETTKANDT, G. 1952. Zur kenntnis des phototropismus der keimmyzelien einiger parasitischer Pilze.

GIESBERT, S., SIEGMUND, U., SCHUMACHER, J., KOKKELINK, L. & TUDZYNSKI, P. 2014. Functional analysis of BcBem1 and its interaction

partners in Botrytis cinerea: impact on differentiation and virulence. *PLoS One*, 9**,** e95172.
GIOTI, A., SIMON, A., LE PECHEUR, P., GIRAUD, C., PRADIER, J. M., VIAUD, M. & LEVIS, C. 2006. Expression profiling of Botrytis cinerea genes identifies three patterns of up-regulation in planta and an FKBP12 protein affecting pathogenicity. *J Mol Biol,* 358**,** 372-86.
GIRAUD, T., FORTINI, D., LEVIS, C., LAMARQUE, C., LEROUX, P., LOBUGLIO, K. & BRYGOO, Y. 1999. Two Sibling Species of the Botrytis cinerea Complex, transposa and vacuma, Are Found in Sympatry on Numerous Host Plants. *Phytopathology,* 89**,** 967-73.
GIRAUD, T., FORTINI, D., LEVIS, C., LEROUX, P. & BRYGOO, Y. 1997. RFLP markers show genetic recombination in Botryotinia fuckeliana (Botrytis cinerea) and transposable elements reveal two sympatric species. *Mol Biol Evol,* 14**,** 1177-85.
GODFREY, G. H. 1923. Gray mold of castor bean. *Journal of agricultural research,* XXIII**,** 679–716.
GONZALEZ, R. 2014. The relationship between bipolar disorder and biological rhythms. *J Clin Psychiatry,* 75**,** e323-31.
GOOCH, V. D., MEHRA, A., LARRONDO, L. F., FOX, J., TOUROUTOUTOUDIS, M., LOROS, J. J. & DUNLAP, J. C. 2008. Fully codon-optimized luciferase uncovers novel temperature characteristics of the Neurospora clock. *Eukaryot Cell,* 7**,** 28-37.
GOODSPEED, D., CHEHAB, E. W., COVINGTON, M. F. & BRAAM, J. 2013. Circadian control of jasmonates and salicylates: the clock role in plant defense. *Plant Signal Behav,* 8**,** e23123.
GOODSPEED, D., CHEHAB, E. W., MIN-VENDITTI, A., BRAAM, J. & COVINGTON, M. F. 2012. Arabidopsis synchronizes jasmonate-mediated defense with insect circadian behavior. *Proc Natl Acad Sci U S A,* 109**,** 4674-7.
GREENE, A. V., KELLER, N., HAAS, H. & BELL-PEDERSEN, D. 2003a. A Circadian Oscillator in Aspergillus spp. Regulates Daily Development and Gene Expression. *Eukaryotic Cell,* 2**,** 231-237.
GREENE, A. V., KELLER, N., HAAS, H. & BELL-PEDERSEN, D. 2003b. A circadian oscillator in Aspergillus spp. regulates daily development and gene expression. *Eukaryot Cell,* 2**,** 231-7.
GRIEBEL, T. & ZEIER, J. 2008. Light regulation and daytime dependency of inducible plant defenses in Arabidopsis: phytochrome signaling controls systemic acquired resistance rather than local defense. *Plant Physiol,* 147**,** 790-801.
GRONOVER, C. S., KASULKE, D., TUDZYNSKI, P. & TUDZYNSKI, B. 2001. The role of G protein alpha subunits in the infection process of the gray mold fungus Botrytis cinerea. *Mol Plant Microbe Interact,* 14**,** 1293-302.
GUO, A., REIMERS, P. J. & LEACH, J. E. 1993. Effect of light on incompatible interactions between Xanthomonas oryzae pv oryzae and rice. *Physiological and Molecular Plant Pathology***,** 413-425.
HARMER, S. L. 2009. The circadian system in higher plants. *Annu Rev Plant Biol,* 60**,** 357-77.
HATAKEYAMA, R., NAKAHAMA, T., HIGUCHI, Y. & KITAMOTO, K. 2007. Light

represses conidiation in koji mold Aspergillus oryzae. *Biosci Biotechnol Biochem,* 71**,** 1844-9.
HE, Q., CHENG, P., YANG, Y., WANG, L., GARDNER, K. H. & LIU, Y. 2002. White collar-1, a DNA binding transcription factor and a light sensor. *Science,* 297**,** 840-3.
HEINTZEN, C. & LIU, Y. 2007. The Neurospora crassa Circadian Clock. 58**,** 25-66.
HEINTZEN, C., LOROS, J. J. & DUNLAP, J. C. 2001. The PAS protein VIVID defines a clock-associated feedback loop that represses light input, modulates gating, and regulates clock resetting. *Cell,* 104**,** 453-64.
HERRERA-ESTRELLA, A. & HORWITZ, B. A. 2007. Looking through the eyes of fungi: molecular genetics of photoreception. *Mol Microbiol,* 64**,** 5-15.
HOLZ, G., COERTZE, S. & WILLIAMSON, B. 2004. The ecology of Botrytis on plant surfaces. *In:* ELAD, Y., WILLIAMSON, B., TUDZYNSKI, P. & DELEN, N. (eds.) *Botrytis: Biology, Pathology and Control.* Dordrecht, the Netherlands: Kluwer Academic Publishers.
HONDA, Y. & YUNOKI, T. 1978. Action spectrum for photosporogenesis in Botrytis cinerea Pers. ex Fr. *Plant Physiology,* 61**,** 711-713.
HOWE, G. A. 2004. Jasmonates as signals in the wound response. *Journal of Plant Growth Regulation,* 23**,** 223-237.
HUNT, S. M., THOMPSON, S., ELVIN, M. & HEINTZEN, C. 2010. VIVID interacts with the WHITE COLLAR complex and FREQUENCY-interacting RNA helicase to alter light and clock responses in Neurospora. *Proc Natl Acad Sci U S A,* 107**,** 16709-14.
HURLEY, J. M., DASGUPTA, A., EMERSON, J. M., ZHOU, X., RINGELBERG, C. S., KNABE, N., LIPZEN, A. M., LINDQUIST, E. A., DAUM, C. G., BARRY, K. W., GRIGORIEV, I. V., SMITH, K. M., GALAGAN, J. E., BELL-PEDERSEN, D., FREITAG, M., CHENG, C., LOROS, J. J. & DUNLAP, J. C. 2014. Analysis of clock-regulated genes in Neurospora reveals widespread posttranscriptional control of metabolic potential. *Proc Natl Acad Sci U S A,* 111**,** 16995-7002.
IDNURM, A. & CROSSON, S. 2009. The photobiology of microbial pathogenesis. *PLoS Pathog,* 5**,** e1000470.
IDNURM, A. & HEITMAN, J. 2005. Light controls growth and development via a conserved pathway in the fungal kingdom. *PLoS Biol,* 3**,** e95.
IDNURM, A. & HEITMAN, J. 2010. Ferrochelatase is a conserved downstream target of the blue light-sensing White collar complex in fungi. *Microbiology,* 156**,** 2393-407.
IDNURM, A., RODRIGUEZ-ROMERO, J., CORROCHANO, L. M., SANZ, C., ITURRIAGA, E. A., ESLAVA, A. P. & HEITMAN, J. 2006. The Phycomyces madA gene encodes a blue-light photoreceptor for phototropism and other light responses. *Proc Natl Acad Sci U S A,* 103**,** 4546-51.
IDNURM, A., VERMA, S. & CORROCHANO, L. M. 2010. A glimpse into the basis of vision in the kingdom Mycota. *Fungal Genet Biol,* 47**,** 881-92.
ISLAM, S. Z., BABADOOST, M. & HONDA, Y. 2002. Effect of red light treatment of seedlings of pepper, pumpkin, and tomato on the occurrence of Phytophthora damping-off. *Hortscience,* 37**,** 678–681.

ISLAM, S. Z., HONDA, Y. & ARASE, S. 1998. Light-induced resistance of broad bean against Botrytis cinerea. *Journal of Phytopathology,* 146**,** 479–485.

JAFFE, L. & ETZOLD, H. 1962. Orientation and locus of tropic photoreceptor molecules in spores of Botrytis and Osmunda. *The Journal of Cell Biology,* 13**,** 13-31.

JARVIS, W. R. 1972. Phototropism in Botrytis cinerea. *Transactions of the British Mycological Society* 58**,** 526-IN516.

JARVIS, W. R. 1977. *Botryotinia and Botrytis Species. Taxonomy and Pathogenicity.,* Canada, Ottawa : Research Branch, Canada Department of Agriculture.

JENSEN, C. & LYSEK, G. 1983. Differences in the mycelial growth rhythms in a population ofSclerotinia fructigena *Experientia*.

KAHRSTROM, C. T. 2012. Host response: Phagocytosis runs like clockwork. *Nat Rev Microbiol,* 10**,** 162.

KARS, I., KROOSHOF, G. H., WAGEMAKERS, L., JOOSTEN, R., BENEN, J. A. & VAN KAN, J. A. 2005a. Necrotizing activity of five Botrytis cinerea endopolygalacturonases produced in Pichia pastoris. *Plant J,* 43**,** 213-25.

KARS, I., MCCALMAN, M., WAGEMAKERS, L. & JA, V. A. N. K. 2005b. Functional analysis of Botrytis cinerea pectin methylesterase genes by PCR-based targeted mutagenesis: Bcpme1 and Bcpme2 are dispensable for virulence of strain B05.10. *Mol Plant Pathol,* 6**,** 641-52.

KIM, H., RIDENOUR, J. B., DUNKLE, L. D. & BLUHM, B. H. 2011a. Regulation of stomatal tropism and infection by light in *Cercospora zeae-maydis:* evidence for coordinated host/pathogen responses to photoperiod? *PLoS Pathog,* 7**,** e1002113.

KIM, S., SINGH, P., PARK, J., PARK, S., FRIEDMAN, A., ZHENG, T., LEE, Y. H. & LEE, K. 2011b. Genetic and molecular characterization of a blue light photoreceptor MGWC-1 in Magnaporth oryzae. *Fungal Genet Biol,* 48**,** 400-7.

KIPPERT, F. 1989. Circadian control of heat tolerance in stationary phase cultures of Schizosaccharomyces pombe. *Arch Microbiol,* 151**,** 177-9.

KIPPERT, F., NINNEMANN, H. & ENGELMANN, W. 1991. Photosynchronization of the circadian clock of Schizosaccharomyces pombe: Mitochondrial cytochrome b is an essential component. *Current Genetics*.

KLIMPEL, A., GRONOVER, C. S., WILLIAMSON, B., STEWART, J. A. & TUDZYNSKI, B. 2002. The adenylate cyclase (BAC) in Botrytis cinerea is required for full pathogenicity. *Mol Plant Pathol,* 3**,** 439-50.

KOTZABASIS, K., NAVAKOUDIS, E. & VAKALOUNAKIS, D. 2008. Photobiological control of crop production and plant diseases. *Zeitschrift für Naturforschung,* 63**,** 113-123.

LAKIN-THOMAS, P. L., BELL-PEDERSEN, D. & BRODY, S. 2011. The genetics of circadian rhythms in Neurospora. *Adv Genet,* 74**,** 55-103.

LAMBREGHTS, R., SHI, M., BELDEN, W. J., DECAPRIO, D., PARK, D., HENN, M. R., GALAGAN, J. E., BASTURKMEN, M., BIRREN, B. W., SACHS, M. S., DUNLAP, J. C. & LOROS, J. J. 2009. A high-density single nucleotide polymorphism map for Neurospora crassa. *Genetics,* 181**,** 767-81.

LARRONDO, L. F., COLOT, H. V., BAKER, C. L., LOROS, J. J. & DUNLAP, J. C. 2009. Fungal functional genomics: tunable knockout-knock-in expression and tagging strategies. *Eukaryot Cell,* 8**,** 800-4.

LARRONDO, L. F., LOROS, J. J. & DUNLAP, J. C. 2012. High-resolution spatiotemporal analysis of gene expression in real time: in vivo analysis of circadian rhythms in Neurospora crassa using a FREQUENCY-luciferase translational reporter. *Fungal Genet Biol,* 49**,** 681-3.

LARRONDO, L. F., OLIVARES-YANEZ, C., BAKER, C. L., LOROS, J. J. & DUNLAP, J. C. 2015. Circadian rhythms. Decoupling circadian clock protein turnover from circadian period determination. *Science,* 347**,** 1257277.

LATORRE, B., RIOJA, M. & LILLO, C. 2002. Efecto de la temperatura en el desarrollo de la infección-producida por Botrytis cinerea en flores y bayas de uva de mesa. *Revista Enología,* 1.

LATORRE, B. & RIOJA, M. 2002. Efecto de la Temperatura y de la Humedad Relativa Sobre la Germinación de Conidias de Botrytis Cinerea. . *Ciencia e investigación agraria: revista latinoamericana de ciencias de la agricultura,* 29**,** 66-72

LEACH, C. M. 1962. Sporulation of diverse species of fungi under near-ultraviolet radiation. *Canadian Journal of Botany,* 40**,** 151-161.

LEE, J. E. & EDERY, I. 2008. Circadian regulation in the ability of Drosophila to combat pathogenic infections. *Curr Biol,* 18**,** 195-9.

LEE, K., DUNLAP, J. C. & LOROS, J. J. 2003. Roles for WHITE COLLAR-1 in circadian and general photoperception in Neurospora crassa. *Genetics,* 163**,** 103-14.

LEROCH, M., KLEBER, A., SILVA, E., COENEN, T., KOPPENHOFER, D., SHMARYAHU, A., VALENZUELA, P. D. T. & HAHN, M. 2013. Transcriptome Profiling of Botrytis cinerea Conidial Germination Reveals Upregulation of Infection-Related Genes during the Prepenetration Stage. *Eukaryotic Cell,* 12**,** 614-626.

LEROCH, M., MERNKE, D., KOPPENHOEFER, D., SCHNEIDER, P., MOSBACH, A., DOEHLEMANN, G. & HAHN, M. 2011. Living colors in the gray mold pathogen Botrytis cinerea: codon-optimized genes encoding green fluorescent protein and mCherry, which exhibit bright fluorescence. *Appl Environ Microbiol,* 77**,** 2887-97.

LEVIS, C., FORTINI, D. & BRYGOO, Y. 1997. Flipper, a mobile Fot1-like transposable element in Botrytis cinerea. *Mol Gen Genet,* 254**,** 674-80.

LINDEN, H., BALLARIO, P. & MACINO, G. 1997. Blue light regulation in Neurospora crassa. *Fungal Genet Biol,* 22**,** 141-50.

LOWREY, P. L. & TAKAHASHI, J. S. 2011. Genetics of circadian rhythms in Mammalian model organisms. *Adv Genet,* 74**,** 175-230.

LUNA, E., PASTOR, V., ROBERT, J., FLORS, V., MAUCH-MANI, B. & TON, J. 2011. Callose deposition: a multifaceted plant defense response. *Mol Plant Microbe Interact,* 24**,** 183-93.

MALZAHN, E., CIPRIANIDIS, S., KALDI, K., SCHAFMEIER, T. & BRUNNER, M. 2010. Photoadaptation in Neurospora by competitive interaction of activating and inhibitory LOV domains. *Cell,* 142**,** 762-72.

MCCLUNG, C. 2006. Plant circadian rhythms. *Plant Cell,* 18**,** 792-803.

MCCLUNG, C. R. 2001. CIRCADIAN RHYTHMS IN PLANTS. *Annu Rev Plant Physiol Plant Mol Biol,* 52**,** 139-162.

MCCLUNG, C. R. 2011. Plant biology: defence at dawn. *Nature* 570**,** 44-45.

MCCLUNG, C. R., FOX, B. A. & DUNLAP, J. C. 1989. The Neurospora clock gene frequency shares a sequence element with the Drosophila clock gene period. *Nature,* 339**,** 558-62.

MEHRA, A., BAKER, C. L., LOROS, J. J. & DUNLAP, J. C. 2009. Post-translational modifications in circadian rhythms. *Trends Biochem Sci,* 34**,** 483-90.

MIDEO, N., REECE, S. E., SMITH, A. L. & METCALF, C. J. 2013. The Cinderella syndrome: why do malaria-infected cells burst at midnight? *Trends Parasitol,* 29**,** 10-6.

MOLINA, G. 2006. Selección de hongos antagonistas para el control biológico de Botrytis cinerea en viveros forestales en Chile. *Bosque,* 27**,** 126-134.

MONTENEGRO-MONTERO, A. & LARRONDO, L. F. 2013. The Neurospora Circadian System: From Genes to Proteins and Back in Less Than 24 hours. *In:* KASBEKAR, D. & MCCLUSKEY, K. (eds.) *Neurospora. Genomics and Molecular Biology*. Norfolk, UK: Caister Academic Press.

MOONEY, J. L., HASSETT, D. E. & YAGER, L. N. 1990. Genetic analysis of suppressors of the veA1 mutation in Aspergillus nidulans. *Genetics,* 126**,** 869-74.

NAFISI, M., STRANNE, M., ZHANG, L., VAN KAN, J. A. & SAKURAGI, Y. 2014. The endo-arabinanase BcAra1 is a novel host-specific virulence factor of the necrotic fungal phytopathogen Botrytis cinerea. *Mol Plant Microbe Interact,* 27**,** 781-92.

NAKAMICHI, N., KITA, M., ITO, S., YAMASHINO, T. & MIZUNO, T. 2005. PSEUDO-RESPONSE REGULATORS, PRR9, PRR7 and PRR5, together play essential roles close to the circadian clock of Arabidopsis thaliana. *Plant Cell Physiol,* 46**,** 686-98.

NAKAMICHI, N., KUSANO, M., FUKUSHIMA, A., KITA, M., ITO, S., YAMASHINO, T., SAITO, K., SAKAKIBARA, H. & MIZUNO, T. 2009. Transcript profiling of an Arabidopsis PSEUDO RESPONSE REGULATOR arrhythmic triple mutant reveals a role for the circadian clock in cold stress response. *Plant Cell Physiol,* 50**,** 447-62.

NAKAMURA, Y., ISHIMARU, K., TAHARA, Y., SHIBATA, S. & NAKAO, A. 2014. Disruption of the suprachiasmatic nucleus blunts a time of day-dependent variation in systemic anaphylactic reaction in mice. *J Immunol Res,* 2014**,** 474217.

NOWROUSIAN, M., DUFFIELD, G. E., LOROS, J. J. & DUNLAP, J. C. 2003. The frequency gene is required for temperature-dependent regulation of many clock-controlled genes in Neurospora crassa. *Genetics,* 164**,** 923-933.

OLDENBURG, K. R., VO, K. T., MICHAELIS, S. & PADDON, C. 1997. Recombination-mediated PCR-directed plasmid construction in vivo in yeast. *Nucleic Acids Res,* 25**,** 451-2.

OLIVEIRA, A. G., STEVANI, C. V., WALDENMAIER, H. E., VIVIANI, V., EMERSON, J. M., LOROS, J. J. & DUNLAP, J. C. 2015. Circadian control sheds light on fungal bioluminescence. *Curr Biol,* 25**,** 964-8.

OUYANG, Y., ANDERSSON, C. R., KONDO, T., GOLDEN, S. S. & JOHNSON, C. H. 1998. Resonating circadian clocks enhance fitness in cyanobacteria. *Proc Natl Acad Sci U S A,* 95**,** 8660-4.

PATEL, R. M., HENEGHAN, M. N., VAN KAN, J. A., BAILEY, A. M. & FOSTER,

G. D. 2008. The pOT and pLOB vector systems: improving ease of transgene expression in Botrytis cinerea. *J Gen Appl Microbiol,* 54**,** 367-76.

PAUL TUDZYNSKI, V. S. 2004. Approaches to molecular genetics and genomics of Botrytis. *In:* ELAD Y, W. B., TUDZYNSKI P & DELEN NEDS (ed.) *Botrytis: Biology, Pathology and Control*

PELTIER, G. L. 1912. A consideration of the physiology and life history of a parasitic Botrytis on pepper and lettuce. . *Missouri Botanical Garden Annual Report***,** 41–74.

PINEDO, C., WANG, C. M., PRADIER, J. M., DALMAIS, B., CHOQUER, M., LE PECHEUR, P., MORGANT, G., COLLADO, I. G., CANE, D. E. & VIAUD, M. 2008. Sesquiterpene synthase from the botrydial biosynthetic gene cluster of the phytopathogen Botrytis cinerea. *ACS Chem Biol,* 3**,** 791-801.

PONTECORVO, G., ROPER, J. A., HEMMONS, L. M., MACDONALD, K. D. & BUFTON, A. W. 1953. The genetics of Aspergillus nidulans. *Adv Genet,* 5**,** 141-238.

PREGUEIRO, A. M., PRICE-LLOYD, N., BELL-PEDERSEN, D., HEINTZEN, C., LOROS, J. J. & DUNLAP, J. C. 2005. Assignment of an essential role for the Neurospora frequency gene in circadian entrainment to temperature cycles. *Proc Natl Acad Sci U S A,* 102**,** 2210-5.

PURSCHWITZ, J., MULLER, S., KASTNER, C. & FISCHER, R. 2006. Seeing the rainbow: light sensing in fungi. *Curr Opin Microbiol,* 9**,** 566-71.

PURSCHWITZ, J., MULLER, S., KASTNER, C., SCHOSER, M., HAAS, H., ESPESO, E. A., ATOUI, A., CALVO, A. M. & FISCHER, R. 2008. Functional and physical interaction of blue- and red-light sensors in Aspergillus nidulans. *Curr Biol,* 18**,** 255-9.

QUIDDE, T., OSBOURN, A. E. & TUDZYNSKI, P. 1998. Detoxification of OE6-tomatine by Botrytis cinerea. *Current Genetics,* 25**,** 445-450.

RAHMAN, M. Z., HONDA, Y. & ARASE, S. 2003. Red-light-induced resistance in broad bean (Vicia faba L.) to leaf spot disease caused by Alternaria tenuissima. *Journal of Phytopathology,* 151**,** 86–91.

REINO, J. H.-G., R; DURAN-PATRON, R; COLLADO, IG 2004. Virulence-toxin production relationship in isolates of the plant pathogenic fungus Botrytis cinerea. *Journal of Phytopathology,* 152**,** 563-566.

ROBERTSON, F. C., SKEFFINGTON, A. W., GARDNER, M. J. & WEBB, A. A. 2009. Interactions between circadian and hormonal signalling in plants. *Plant Mol Biol,* 69**,** 419-27.

ROBINSON, I. & REDDY, A. 2014. Molecular mechanisms of the circadian clock work in mammals. *FEBS Letters,* 588**,** 2477-2483.

ROBINSON, W. 1914. Some experiments on the effect of external stimuli on the sporidia of Puccinia malvacearum. *Annals of Botany,* 28**,** 331-340.

ROCA, M. G., WEICHERT, M., SIEGMUND, U., TUDZYNSKI, P. & FLEISSNER, A. 2012. Germling fusion via conidial anastomosis tubes in the grey mould Botrytis cinerea requires NADPH oxidase activity. *Fungal Biol,* 116**,** 379-87.

RODEN, L. C. & INGLE, R. A. 2009. Lights, rhythms, infection: the role of light and the circadian clock in determining the outcome of plant-pathogen interactions. *Plant Cell,* 21**,** 2546-52.

RODRIGUEZ-ROMERO, J., HEDTKE, M., KASTNER, C., MULLER, S. & FISCHER, R. 2010. Fungi, hidden in soil or up in the air: light makes a difference. *Annu Rev Microbiol,* 64**,** 585-610.

ROHRIG, J., KASTNER, C. & FISCHER, R. 2013. Light inhibits spore germination through phytochrome in Aspergillus nidulans. *Curr Genet,* 59**,** 55-62.

ROLKE Y, L. S., QUIDDE T, WILLIAMSON B, SCHOUTEN A, WELTRING KM, SIEWERS V, TENBERGE KB, TUDZYNSKI B ANDTUDZYNSKI P 2004. Functional analysis of H2O2-generating systems in Botrytis cinerea: the major Cu–Zn-superoxide dismutase (BCSOD1) contributes to virulence on French bean, whereas a glucose oxidase (BCGOD1) is dispensable. *Molecular Plant Pathology,* 5**,** 17-27.

ROLLAND, S., JOBIC, C., FEVRE, M. & BRUEL, C. 2003. Agrobacterium-mediated transformation of Botrytis cinerea, simple purification of monokaryotic transformants and rapid conidia-based identification of the transfer-DNA host genomic DNA flanking sequences. *Curr Genet,* 44**,** 164-71.

RUI, O. H. M. 2007. The Sit 2-type MAP kinase Bmp3 of Botrytis cinerea is required for normal saprotrophic growth, conidiation, plant surface sensing and host tissue colonization. *Molecular Plant Pathology,* 8**,** 173-184.

RUIZ-ROLDAN, M. C., GARRE, V., GUARRO, J., MARINE, M. & RONCERO, M. I. 2008. Role of the white collar 1 photoreceptor in carotenogenesis, UV resistance, hydrophobicity, and virulence of Fusarium oxysporum. *Eukaryot Cell,* 7**,** 1227-30.

SANCAR, C., SANCAR, G., HA, N., CESBRON, F. & BRUNNER, M. 2015. Dawn- and dusk-phased circadian transcription rhythms coordinate anabolic and catabolic functions in Neurospora. *BMC Biol,* 13**,** 17.

SANCAR, G., SANCAR, C., BRUGGER, B., HA, N., SACHSENHEIMER, T., GIN, E., WDOWIK, S., LOHMANN, I., WIELAND, F., HOFER, T., DIERNFELLNER, A. & BRUNNER, M. 2011. A global circadian repressor controls antiphasic expression of metabolic genes in Neurospora. *Mol Cell,* 44**,** 687-97.

SANCHEZ, S. E., CAGNOLA, J. I., CREPY, M., YANOVSKY, M. J. & CASAL, J. J. 2011. Balancing forces in the photoperiodic control of flowering. *Photochem Photobiol Sci,* 10**,** 451-60.

SANZ, C., RODRIGUEZ-ROMERO, J., IDNURM, A., CHRISTIE, J. M., HEITMAN, J., CORROCHANO, L. M. & ESLAVA, A. P. 2009. Phycomyces MADB interacts with MADA to form the primary photoreceptor complex for fungal phototropism. *Proc Natl Acad Sci U S A,* 106**,** 7095-100.

SARGENT, M. L., BRIGGS, W. R. & WOODWARD, D. O. 1966. Circadian nature of a rhythm expressed by an invertaseless strain of Neurospora crassa. *Plant Physiol,* 41**,** 1343-9.

SCHEIERMANN, C., KUNISAKI, Y. & FRENETTE, P. S. 2013. Circadian control of the immune system. *Nat Rev Immunol,* 13**,** 190-8.

SCHOONBEEK, H., DEL SORBO, G. & DE WAARD, M. A. 2001. The ABC transporter BcatrB affects the sensitivity of Botrytis cinerea to the phytoalexin resveratrol and the fungicide fenpiclonil. *Mol Plant Microbe Interact,* 14**,** 562-71.

SCHUMACHER, J. 2012. Tools for Botrytis cinerea: New expression vectors make the gray mold fungus more accessible to cell biology approaches. *Fungal Genet Biol,* 49**,** 483-97.

SCHUMACHER, J., DE LARRINOA, I. F. & TUDZYNSKI, B. 2008a. Calcineurin-responsive zinc finger transcription factor CRZ1 of Botrytis cinerea is required for growth, development, and full virulence on bean plants. *Eukaryot Cell,* 7**,** 584-601.

SCHUMACHER, J., KOKKELINK, L., HUESMANN, C., JIMENEZ-TEJA, D., COLLADO, I. G., BARAKAT, R., TUDZYNSKI, P. & TUDZYNSKI, B. 2008b. The cAMP-dependent signaling pathway and its role in conidial germination, growth, and virulence of the gray mold Botrytis cinerea. *Mol Plant Microbe Interact,* 21**,** 1443-59.

SCHUMACHER, J., PRADIER, J. M., SIMON, A., TRAEGER, S., MORAGA, J., COLLADO, I. G., VIAUD, M. & TUDZYNSKI, B. 2012. Natural variation in the VELVET gene bcvel1 affects virulence and light-dependent differentiation in Botrytis cinerea. *PLoS One,* 7**,** e47840.

SCHUMACHER, J., SIMON, A., COHRS, K. C., TRAEGER, S., PORQUIER, A., DALMAIS, B., VIAUD, M. & TUDZYNSKI, B. 2015. The VELVET complex in the gray mold fungus Botrytis cinerea: impact of BcLAE1 on differentiation, secondary metabolism and virulence. *Mol Plant Microbe Interact*.

SCHUMACHER, J., SIMON, A., COHRS, K. C., VIAUD, M. & TUDZYNSKI, P. 2014. The transcription factor BcLTF1 regulates virulence and light responses in the necrotrophic plant pathogen Botrytis cinerea. *PLoS Genet,* 10**,** e1004040.

SCHUMACHER, J. & TUDZYNSKI, P. 2012. Morphogenesis and Infection in Botrytis cinerea. 22**,** 225-241.

SEGMULLER, N., ELLENDORF, U., TUDZYNSKI, B. & TUDZYNSKI, P. 2007. BcSAK1, a stress-activated mitogen-activated protein kinase, is involved in vegetative differentiation and pathogenicity in Botrytis cinerea. *Eukaryot Cell,* 6**,** 211-21.

SEGMULLER, N., KOKKELINK, L., GIESBERT, S., ODINIUS, D., VAN KAN, J. & TUDZYNSKI, P. 2008. NADPH oxidases are involved in differentiation and pathogenicity in Botrytis cinerea. *Mol Plant Microbe Interact,* 21**,** 808-19.

SHARMA, M. & BHATT, D. 2014. The circadian clock and defence signalling in plants. *Mol Plant Pathol*.

SHI, M., COLLETT, M., LOROS, J. J. & DUNLAP, J. C. 2010. FRQ-interacting RNA helicase mediates negative and positive feedback in the Neurospora circadian clock. *Genetics,* 184**,** 351-61.

SHIN, J., HEIDRICH, K., SANCHEZ-VILLARREAL, A., PARKER, J. E. & DAVIS, S. J. 2012. TIME FOR COFFEE represses accumulation of the MYC2 transcription factor to provide time-of-day regulation of jasmonate signaling in Arabidopsis. *Plant Cell,* 24**,** 2470-82.

SIEWERS, V., VIAUD, M., JIMENEZ-TEJA, D., COLLADO, I. G., GRONOVER, C. S., PRADIER, J. M., TUDZYNSKI, B. & TUDZYNSKI, P. 2005. Functional analysis of the cytochrome P450 monooxygenase gene bcbot1 of Botrytis cinerea indicates that botrydial is a strain-specific virulence factor. *Mol Plant Microbe Interact,* 18**,** 602-12.

SLUSARENKO, A. J. & SCHLAICH, N. L. 2003. Downy mildew of Arabidopsis thaliana caused by Hyaloperonospora parasitica (formerly Peronospora parasitica). *Mol Plant Pathol,* 4**,** 159-70.

SMITH, K. M., SANCAR, G., DEKHANG, R., SULLIVAN, C. M., LI, S., TAG, A. G., SANCAR, C., BREDEWEG, E. L., PRIEST, H. D., MCCORMICK, R. F., THOMAS, T. L., CARRINGTON, J. C., STAJICH, J. E., BELL-PEDERSEN, D., BRUNNER, M. & FREITAG, M. 2010. Transcription factors in light and circadian clock signaling networks revealed by genomewide mapping of direct targets for neurospora white collar complex. *Eukaryot Cell,* 9**,** 1549-56.

STAATS, M., VAN BAARLEN, P. & VAN KAN, J. A. 2005. Molecular phylogeny of the plant pathogenic genus Botrytis and the evolution of host specificity. *Mol Biol Evol,* 22**,** 333-46.

STABEN, C., JENSEN, B., SINGER, M., POLLOCK, J. & SCHECHTMAN, M. 1989. Use of a bacterial hygromycin B resistance gene as a dominant selectable marker in Neurospora crassa transformation. *Fungal Genetics and Biology,* 36**,** 79-81.

STEFANATO, F. L., ABOU-MANSOUR, E., BUCHALA, A., KRETSCHMER, M., MOSBACH, A., HAHN, M., BOCHET, C. G., METRAUX, J. P. & SCHOONBEEK, H. J. 2009. The ABC transporter BcatrB from Botrytis cinerea exports camalexin and is a virulence factor on Arabidopsis thaliana. *Plant J,* 58**,** 499-510.

SUMMA, K. C. & TUREK, F. W. 2014. Chronobiology and obesity: Interactions between circadian rhythms and energy regulation. *Adv Nutr,* 5**,** 312s-9s.

SUZUKI, Y., KUMAGAI, T. & ODA, Y. 1977. Locus of blue and near ultraviolet reversible photoreaction in the stages of conidial development in Botrytis cinerea. *Journal of general microbiology,* 98**,** 199-204.

SUZUKI, Y. & ODA, Y. 1979. Inhibitory loci of both blue and near ultraviolet lights on lateral-type sclerotial development in Botrytis cinerea. *Annals of the Phytopathological Society of Japan,* 45**,** 54-61.

SWEENEY, B. M. 1976. Circadian rhythms, definition and general characterization. In The molecular basis of circadian rhythms *The molecular basis of circadian rhythms.* Abakon-Verlagsgesellschaft, Berlin.

TAKAHASHI, J. S., HONG, H. K., KO, C. H. & MCDEARMON, E. L. 2008. The genetics of mammalian circadian order and disorder: implications for physiology and disease. *Nat Rev Genet,* 9**,** 764-75.

TAN, K. K. 1974. Blue-light inhibition of sporulation in Botrytis cinerea. *Journal of General Microbiology,* 82**,** 191-200.

TAN, K. K. 1975a. Interaction of near-ultraviolet, blue, red, and far-red light in sporulation of Botrytis cinerea. . *Transactions of the British Mycological Society* 64**,** 215-222.

TAN, K. K. 1975b. Recovery from the blue-light inhibition of sporulation in Botrytis cinerea. *Transactions of the British Mycological Society,* 64**,** 223-228.

TAN, K. K. & EPTON, H. 1973. Effect of light on the growth and sporulation of Botrytis cinerea. *Transactions of the British Mycological Society,* 67**,** 147-157.

TAN, K. K. & EPTON, H. 1974. Further studies on light and sporulation in Botrytis cinerea. *Transactions of the British Mycological Society,* 62.

TANG, C. T., LI, S., LONG, C., CHA, J., HUANG, G., LI, L., CHEN, S. & LIU, Y.

2009. Setting the pace of the Neurospora circadian clock by multiple independent FRQ phosphorylation events. *Proc Natl Acad Sci U S A,* 106**,** 10722-7.

TANI, H., KOSHINO, H., SAKUNO, E., CUTLER, H. G. & NAKAJIMA, H. 2006. Botcinins E and F and Botcinolide from Botrytis cinerea and structural revision of botcinolides. *J Nat Prod,* 69**,** 722-5.

TANI, H., KOSHINO, H., SAKUNO, E. & NAKAJIMA, H. 2005. Botcinins A, B, C, and D, metabolites produced by Botrytis cinerea, and their antifungal activity against Magnaporthe grisea, a pathogen of rice blast disease. *J Nat Prod,* 68**,** 1768-72.

TEN HAVE, A., MULDER, W., VISSER, J. & VAN KAN, J. A. 1998. The endopolygalacturonase gene Bcpg1 is required for full virulence of Botrytis cinerea. *Mol Plant Microbe Interact,* 11**,** 1009-16.

THANING, C. & NILSSON, H. E. 2000. A narrow range of wavelengths active in regulating apothecial development in Sclerotinia sclerotiorum. *Annals of the Phytopathological Society of Japan,* 45**,** 54-61.

TUDZYNSKI, P. K., L 2009. Botrytis cinerea: molecular aspects of a necrotrophic life style. *The Mycota V: Plant Relationships.*

URBASCH, I. 1985. Ultrastructural Studies on the Microconidia of Botrytis cinerea Pers. and their phialoconidial development. *Journal of Phytopathology,* 112**,** 229-237.

VALETTE-COLLET, O., CIMERMAN, A., REIGNAULT, P., LEVIS, C. & BOCCARA, M. 2003. Disruption of Botrytis cinerea pectin methylesterase gene Bcpme1 reduces virulence on several host plants. *Mol Plant Microbe Interact,* 16**,** 360-7.

VAN KAN, J. A. 2006. Licensed to kill: the lifestyle of a necrotrophic plant pathogen. *Trends Plant Sci,* 11**,** 247-53.

VANDESOMPELE, J., DE PRETER, K., PATTYN, F., POPPE, B., VAN ROY, N., DE PAEPE, A. & SPELEMAN, F. 2002. Accurate normalization of real-time quantitative RT-PCR data by geometric averaging of multiple internal control genes. *Genome Biol,* 3**,** RESEARCH0034.

VITALINI, M. W., DE PAULA, R. M., PARK, W. D. & BELL-PEDERSEN, D. 2006. The rhythms of life: circadian output pathways in Neurospora. *J Biol Rhythms,* 21**,** 432-44.

WANG, H., JIANG, Y. P., YU, H. J., XIA, X. J., SHI, K., ZHOU, Y. H. & YU, J. Q. 2010. Light quality affects incidence of powdery mildew, expression of defence-related genes and associated metabolism in cucumber plants. *European Journal of Plant Pathology,* 127**,** 125-135.

WANG, W., BARNABY, J. Y., TADA, Y., LI, H., TOR, M., CALDELARI, D., LEE, D. U., FU, X. D. & DONG, X. 2011. Timing of plant immune responses by a central circadian regulator. *Nature,* 470**,** 110-4.

WANG, Z. Y. & TOBIN, E. M. 1998. Constitutive expression of the CIRCADIAN CLOCK ASSOCIATED 1 (CCA1) gene disrupts circadian rhythms and suppresses its own expression. *Cell,* 93**,** 1207-17.

WILLIAMSON, B. 1994. Latency and quiescence in survival and success of fungal plant pathogens. *In:* B, B. J. A. W. (ed.) *Ecology of Plant Pathogens.*

WINSTON, F., DOLLARD, C. & RICUPERO-HOVASSE, S. L. 1995. Construction of a set of convenient Saccharomyces cerevisiae strains that are isogenic to S288C. *Yeast,* 11**,** 53-5.

Y., E. 1997. Responses of plants to infection by Botrytis cinerea and novel means involved in reducing their susceptibility to infection. *Biological Reviews* 72**,** 381-422.

YERUSHALMI, S. & GREEN, R. M. 2009. Evidence for the adaptive significance of circadian rhythms. *Ecol Lett,* 12**,** 970-81.

YOSHIDA, Y. & HASUNUMA, K. 2004. Reactive oxygen species affect photomorphogenesis in Neurospora crassa. *J Biol Chem,* 279**,** 6986-93.

YOSHIDA, Y., IIGUSA, H., WANG, N. & HASUNUMA, K. 2011. Cross-talk between the cellular redox state and the circadian system in Neurospora. *PLoS One,* 6**,** e28227.

ZEIER, J., PINK, B., MUELLER, M. J. & BERGER, S. 2004. Light conditions influence specific defence responses in incompatible plant-pathogen interactions: uncoupling systemic resistance from salicylic acid and PR-1 accumulation. *Planta,* 219**,** 673-83.

ZHANG, C., XIE, Q., ANDERSON, R. G., NG, G., SEITZ, N. C., PETERSON, T., MCCLUNG, C. R., MCDOWELL, J. M., KONG, D., KWAK, J. M. & LU, H. 2013. Crosstalk between the circadian clock and innate immunity in Arabidopsis. *PLoS Pathog,* 9**,** e1003370.

ZHANG, Z., QIN, G., LI, B. & TIAN, S. 2014. Knocking out Bcsas1 in Botrytis cinerea impacts growth, development, and secretion of extracellular proteins, which decreases virulence. *Mol Plant Microbe Interact,* 27**,** 590-600.

ZHENG, L., CAMPBELL, M., MURPHY, J., LAM, S. & XU, J. R. 2000. The BMP1 gene is essential for pathogenicity in the gray mold fungus Botrytis cinerea. *Mol Plant Microbe Interact,* 13**,** 724-32.

ZHU, H., NOWROUSIAN, M., KUPFER, D., COLOT, H. V., BERROCAL-TITO, G., LAI, H., BELL-PEDERSEN, D., ROE, B. A., LOROS, J. J. & DUNLAP, J. C. 2001. Analysis of expressed sequence tags from two starvation, time-of-day-specific libraries of Neurospora crassa reveals novel clock-controlled genes. *Genetics,* 157**,** 1057-65.